Local Galaxies

Jenny Greene

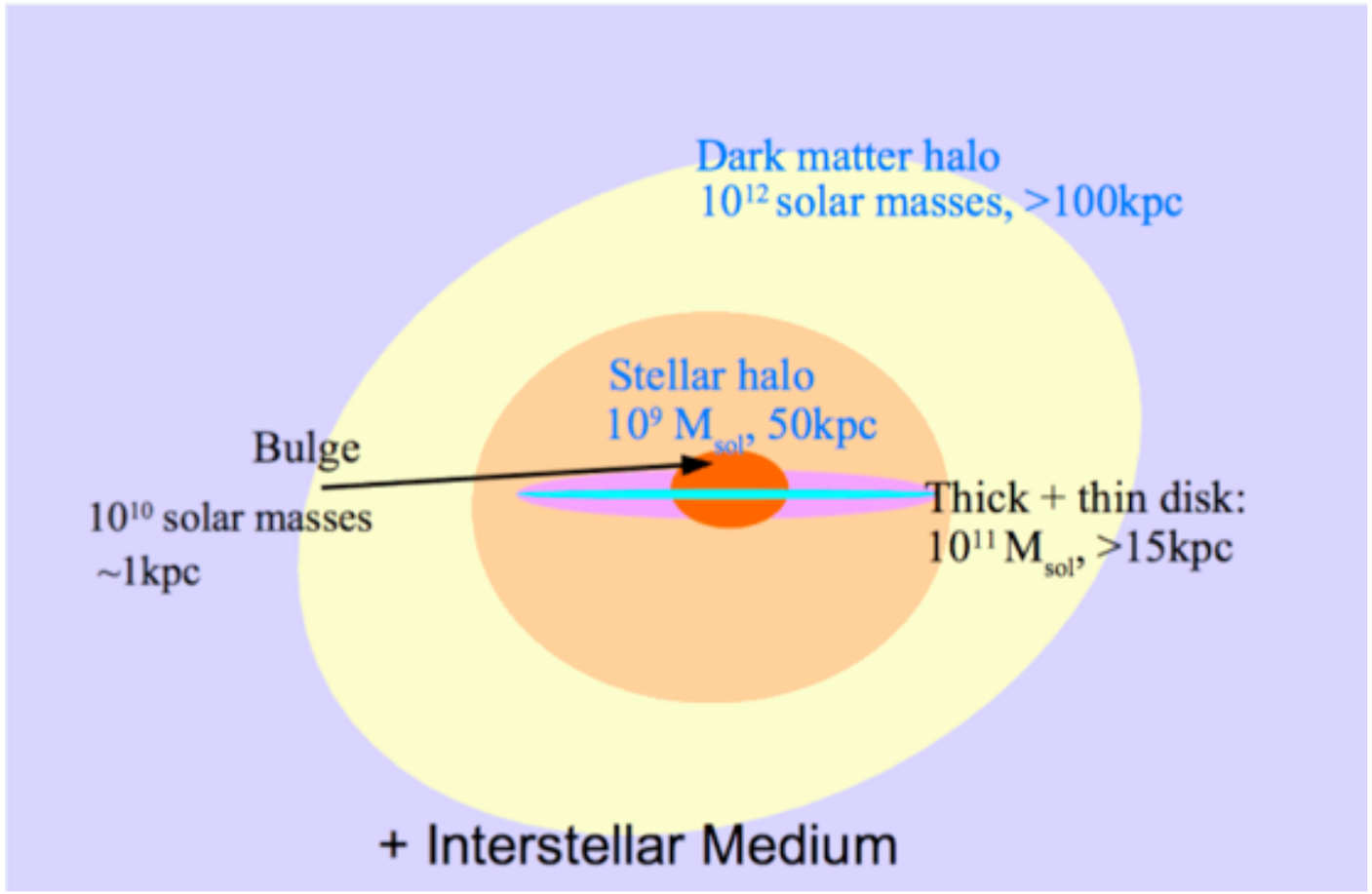

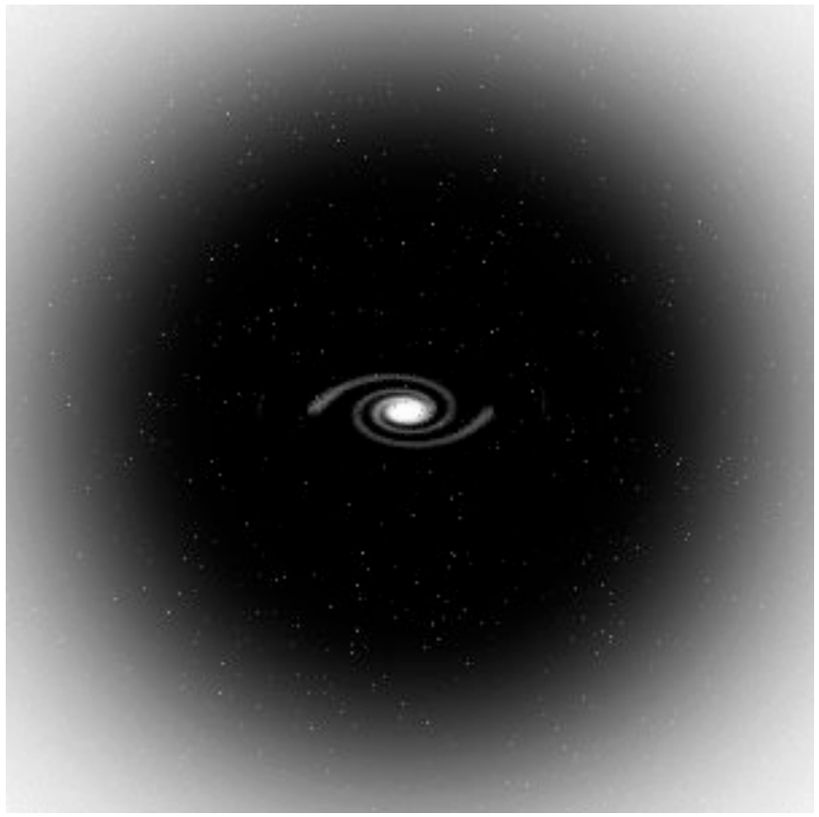

Galaxy relative to halo; Whittle lectures

Galaxies are composed of stars, gas, DM.
DM dominates on large scales, but baryons dominate in the luminous centers of galaxies.

Nucleus: dense; star formation; supermassive black hole
Bulge: spheroidal; mixed ages; kinematically "hot" & little rotation
Disk: gas & stars; younger; star formation; spiral arms; kinematically "cold" & rotates
Halo: low density; GCs present; old; Dark Matter dominates

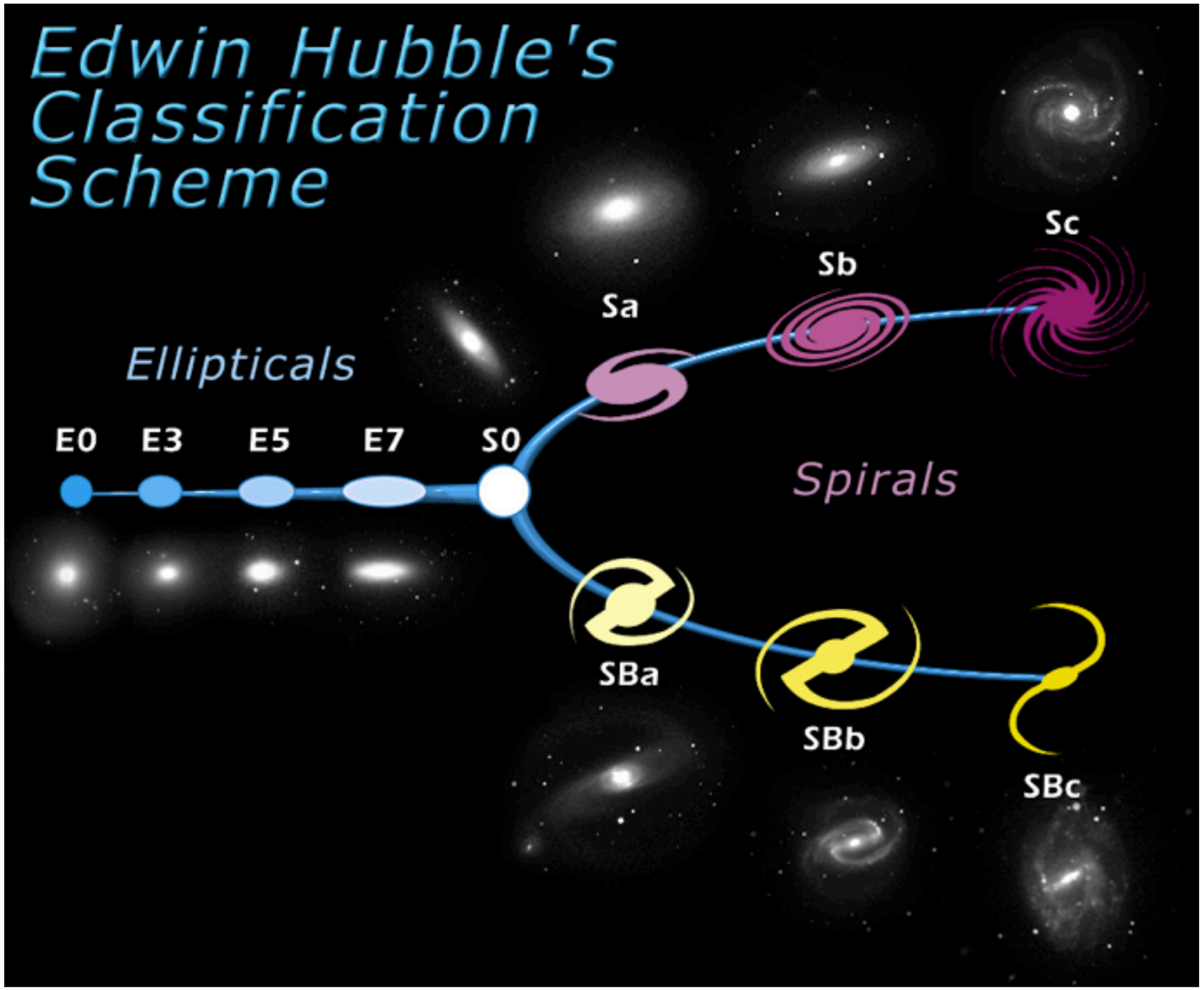

Primary separation between E and S type galaxies.

Classification criteria: From Sa → Sb → Sc :

1. fractional contribution of the bulge decreases;
2. spiral arm pitch angle increases;
3. degree of resolution into young stars and gas increases.

Types of Galaxies: Ellipticals

Elliptical isophotes

Supported predominantly by random motions: we think were formed via mergers

Old stars

No cold gas (typically)

These galaxies are compact/highly concentrated

Range in mass from ~10^8 $M_\odot$ to ~10^{12} $M_\odot$

M87

Types of Galaxies: Spiral

Spiral galaxies contain a disky (rotation-dominated) component, random component is small

There is a bulge (elliptical) component in the center

Gas rich, spiral structure

Two types: barred and unbarred

Disks are very spread out relative to elliptical galaxies, low concentration.

Our Milky Way is a typical spiral, intermediate between Sb and Sc. It has a weak bar.

Bulge = small elliptical

M51

disk

Basic points:

disks are flat

disks have spiral structure

orbits are almost in a single plane

- disks rotate
- random motions are small
- stars have a large range of ages

THE ASTROPHYSICAL JOURNAL, **302**:564–578, 1986 March 15

SYSTEMATICS OF BULGE-TO-DISK RATIOS

F. SIMIEN
Observatoire de Lyon

AND

G. DE VAUCOULEURS
Department of Astronomy and McDonald Observatory, University of Texas

Received 1985 February 15; accepted 1985 September 5

ABSTRACT

Decompositions of the blue-band luminosity profiles of 98 galaxies into spheroidal ($r^{1/4}$) and disk (exponential) components on a homogeneous system are used to study the systematics of bulge-to-disk ratios and related parameters. The mean dependences on morphological type of the fractional luminosity of the spheroid, of the effective radii and specific intensities, and of the mean absolute magnitudes of each component are established. The correlations between effective radius and specific intensity for ellipticals and the spheroidal components of lenticulars and spirals are compared.

The data neither support nor contradict the hypothesis that ellipticals are merely diskless lenticulars; although the spheroids of the latter are systematically smaller and denser than the former and, on average, are fainter in total absolute luminosity, both classes obey the same density-radius relation which differs from the similar relation for the spirals; on the average spiral bulges, particularly among late types, are fainter at constant effective radius.

The data do not support the following hypotheses: (i) that lenticulars form a "gas-poor" sequence parallel to the gas-rich spirals; the validity of their traditional placement between the elliptical and spiral classes is confirmed; (ii) that the absolute magnitude of the spheroid determines the stage T along the Hubble sequence; at each stage there is a large range of spheroid luminosities, and a wide overlap with adjacent stages. Instead the data confirm that the classification sequence is primarily one of decreasing bulge-to-disk ratios, as originally intended by Hubble.

Decomposition techniques, comparison with other methods of analysis, selection effects, systematic and accidental errors, and correlations with other parameters are discussed in several appendices.

B/T Correlates with Hubble Type

Bulge fraction

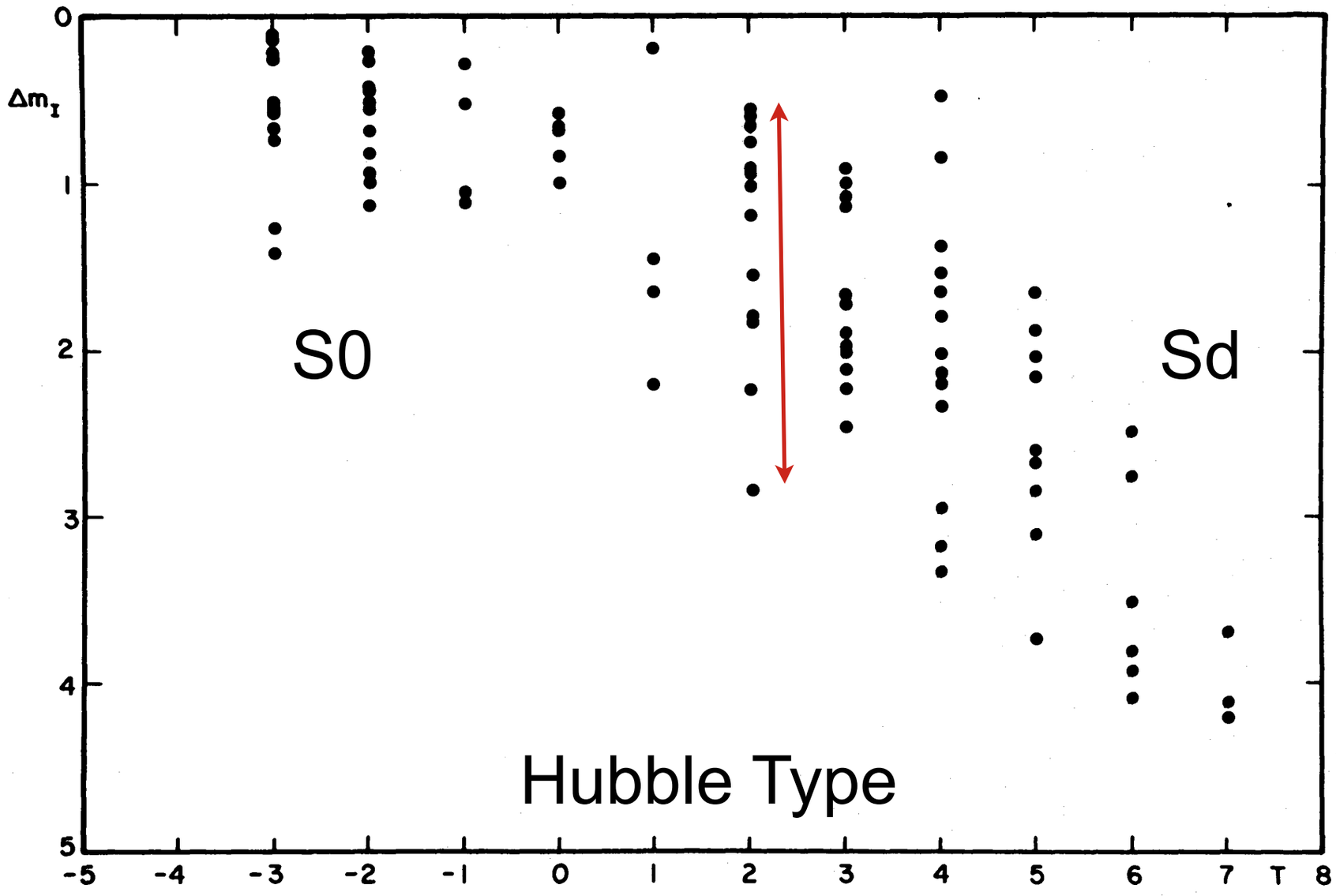

FIG. 2.—Fractional luminosity of spheroidal component expressed as magnitude difference $\langle \Delta m_1 \rangle$ between spheroid and galaxy as a whole. Individual values vs. morphological type T (stage along revised Hubble sequence). Most of the scatter ($\sigma \approx 0.7$ mag) is due to photometric and decomposition errors, with little contributions from classification errors or cosmic scatter.

Hubble Sequence Defined for Massive Galaxies

van den Bergh, S. 1998, Galaxy Morphology and Classification
(Cambridge: Cambridge Univ. Press)

From E — Sc,
the Hubble sequence
is roughly independent of
luminosity
and instead is a sequence
of other physical properties.

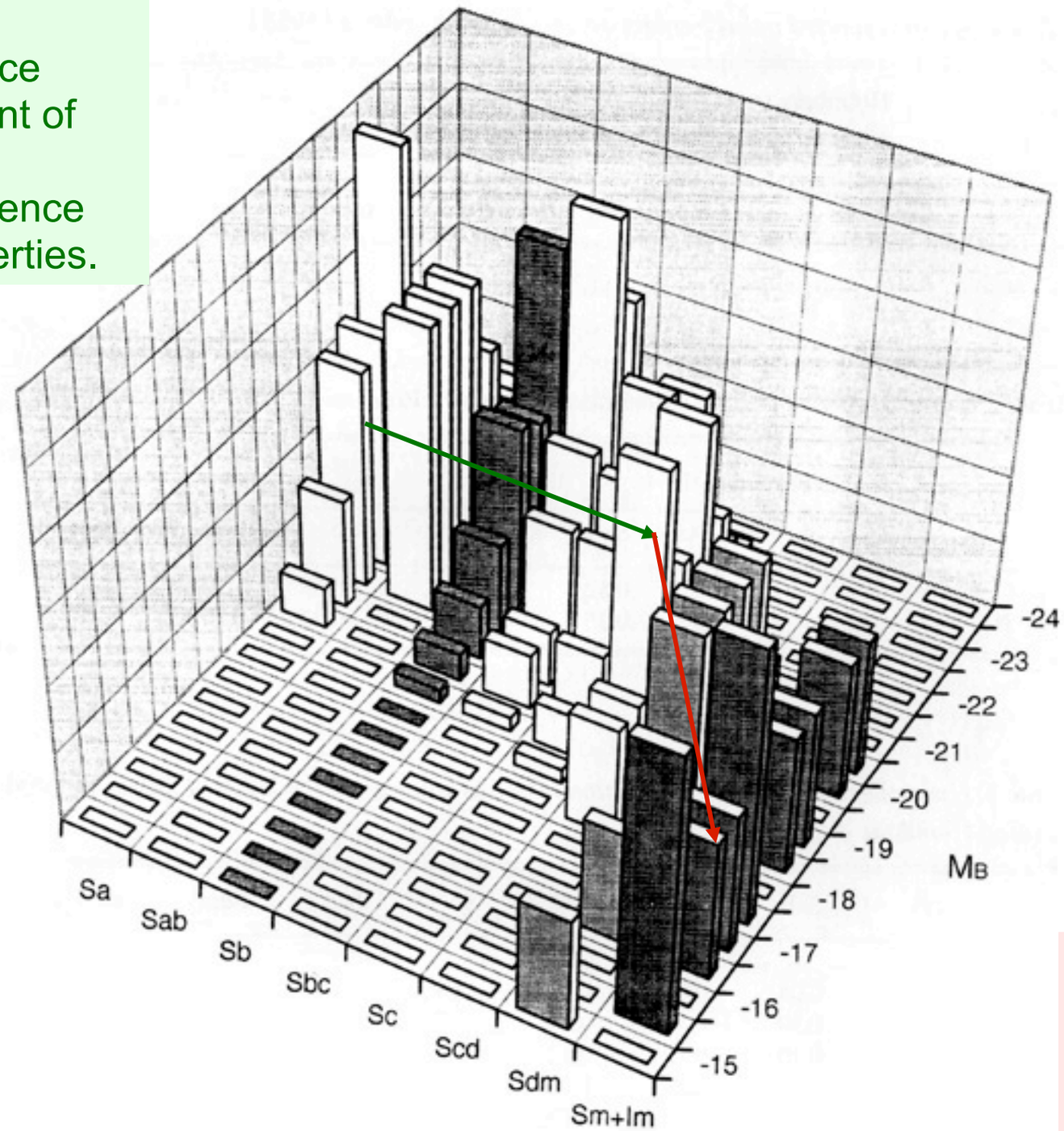

From Sc — Im, the
Hubble Sequence
is mainly a luminosity
sequence.

Fig. 1 Luminosity distributions for Shapley–Ames galaxies (Sandage & Tammann 1981) as a function of Hubble type. Objects of types Sd–Sm–Im are seen to be much less luminous than those with types Sa–Sb–Sc.

PHYSICAL PARAMETERS ALONG THE HUBBLE SEQUENCE

Annu. Rev. Astron. Astrophys. 1994. 32: 115–52

Morton S. Roberts

National Radio Astronomy Observatory,[1] Charlottesville, Virginia 22903

Martha P. Haynes

Center for Radiophysics and Space Research and National Astronomy and Ionosphere Center,[2] Cornell University, Ithaca, New York 14853, and National Radio Astronomy Observatory, Green Bank, West Virginia 24944

Focuses on RC3, the Uppsala General Catalog (low surface brightness galaxies) and an Arecibo survey for the HI measurements; Also considers a smaller volume-limited survey

radius

B-band luminosity

total mass

mass-to-light ratio

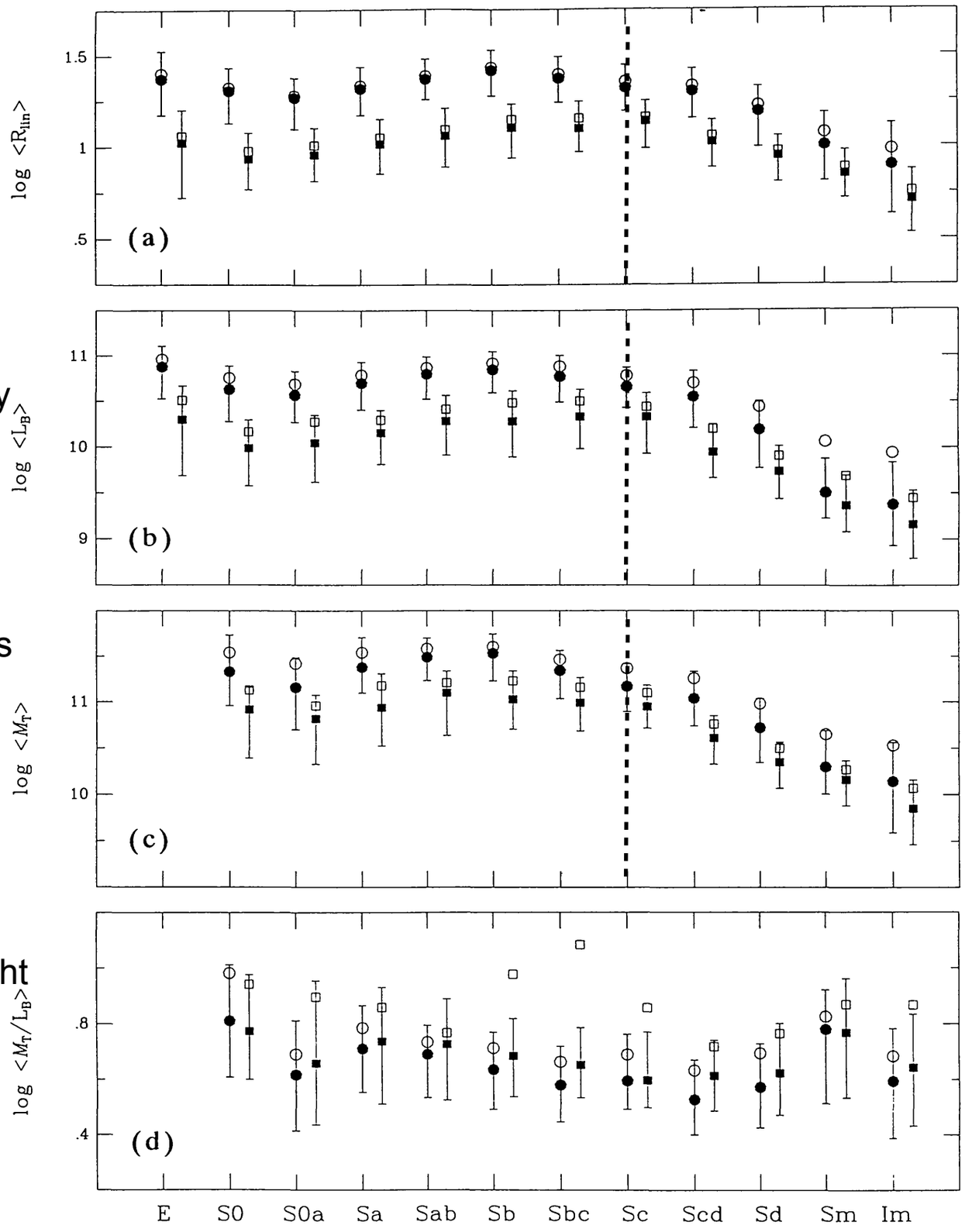

Figure 2 Global galaxy parameters vs morphological type. Circles represent the RC3-UGC sample; squares the RC3-LSc sample. Filled symbols are medians; open ones are mean values. The lower bar is the 25^{th} percentile; the upper the 75^{th} percentile. Their range measures half the sample. The sample size is given in Table 1. (*a*) log linear radius R_{lin}(kpc) to an isophote of 25 B mag/arcsec^2 , (*b*) log blue luminosity L_B in solar units, (*c*) log total mass M_T in solar units, (*d*) log total mass-to-luminosity ratio M_T/L_B.

What about 1 million galaxies?

Spectroscopic catalog	Class	N(total)	N(main)	N(SEGUE)
	All	1,640,960	1,374,080	266,880
	Galaxies	929,555	928,567	988
	Quasars (z <2.3)	104,740	103,121	1,619
	Quasars (z ≥2.3)	16,633	15,411	1,222
	M stars and later	84,047	76,125	7,922
	Other stars	380,214	150,748	229,466
	Sky spectra	97,398	75,209	22,189
	Unknown	28,383	24,767	3,616

640 spectra are observed simultaneously on one *plate*.
There are:

- 1802 Legacy ("main-survey") plates,
- 86 repeat observations ("extra plates") of 77 distinct Legacy plates,
- 676 observations of 660 distinct special plates, including
- 410 observations of 212 distinct special plates taken under SEGUE.

www.sdss.org/dr7

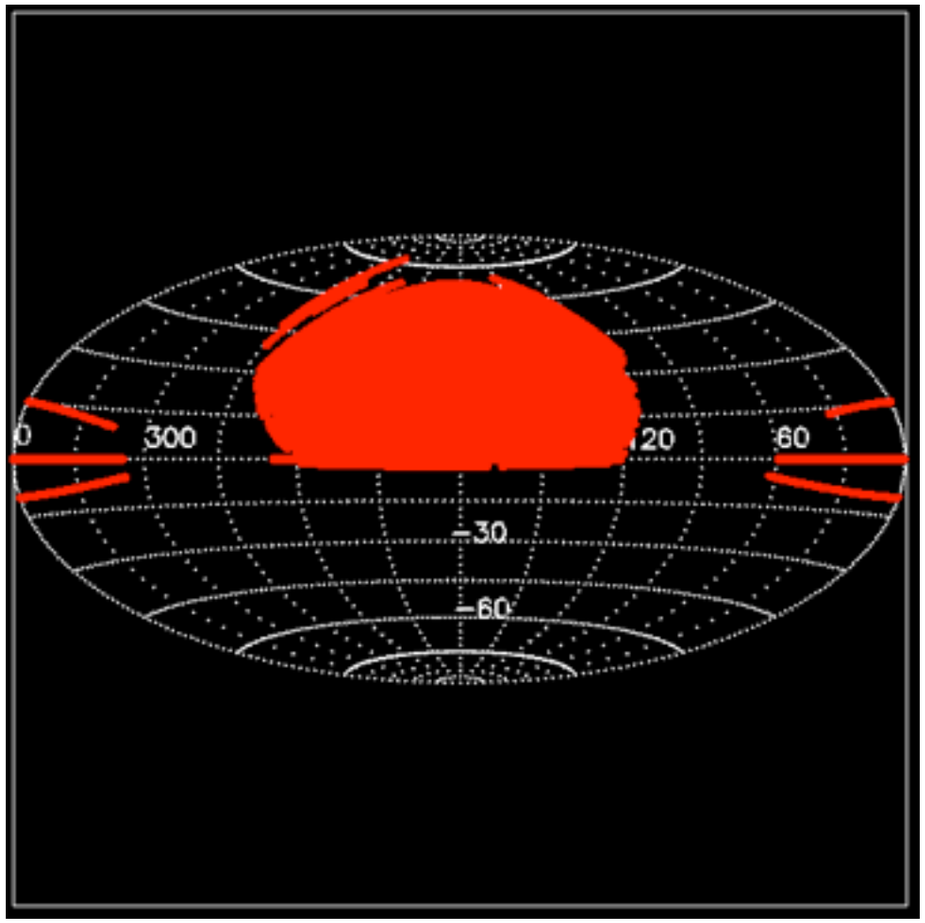

SDSS

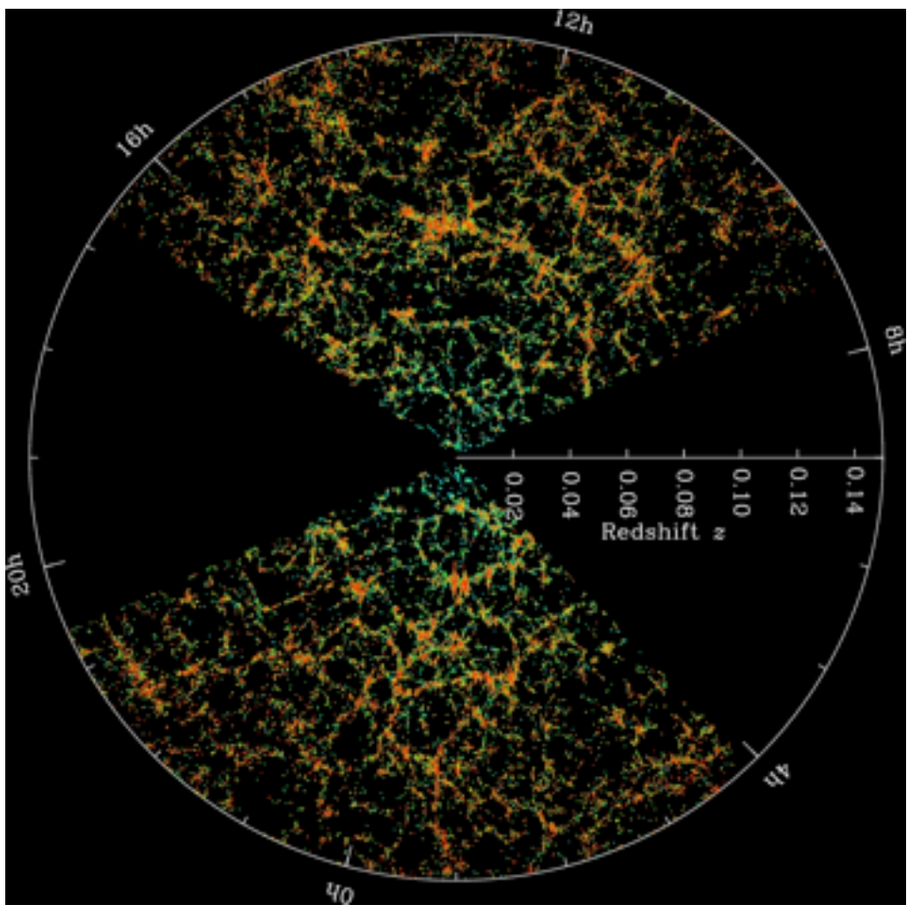

Images and spectra of 1/4 of the sky

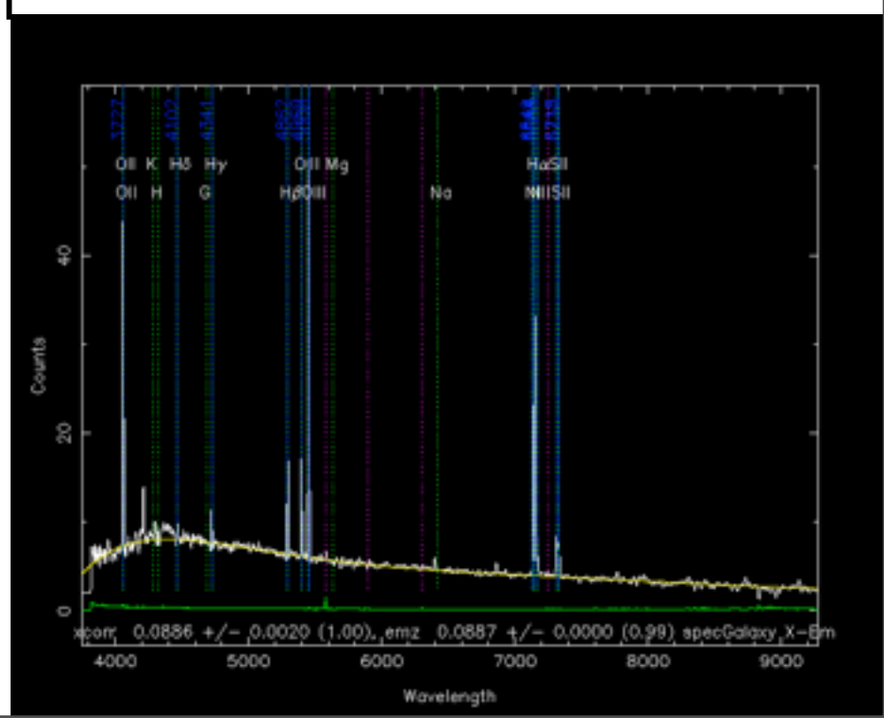

Galaxies are smudges

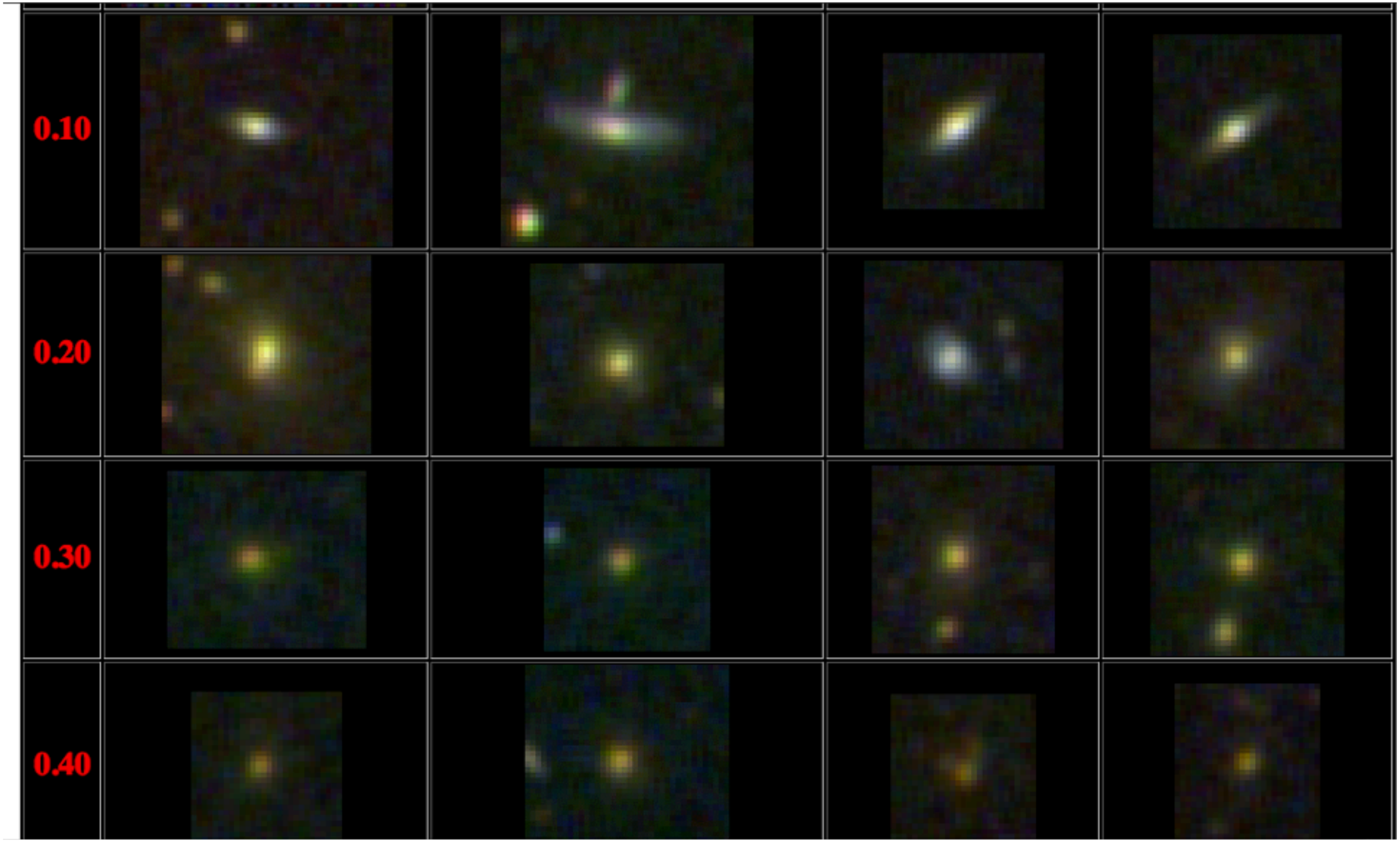

Color-Structure-Spectral Types

THE ASTRONOMICAL JOURNAL, 122:1861–1874, 2001 October

COLOR SEPARATION OF GALAXY TYPES IN THE SLOAN DIGITAL SKY SURVEY IMAGING DATA

ISKRA STRATEVA,[1] ŽELJKO IVEZIĆ,[1] GILLIAN R. KNAPP,[1] VIJAY K. NARAYANAN,[1] MICHAEL A. STRAUSS,[1] JAMES E. GUNN,[1] ROBERT H. LUPTON,[1] DAVID SCHLEGEL,[1] NETA A. BAHCALL,[1] JON BRINKMANN,[2] ROBERT J. BRUNNER,[3] TAMÁS BUDAVÁRI,[4,5] ISTVÁN CSABAI,[4,5] FRANCISCO JAVIER CASTANDER,[6] MAMORU DOI,[7] MASATAKA FUKUGITA,[8,9] ZSUZSANNA GYŐRY,[4,5] MASARU HAMABE,[7] GREG HENNESSY,[10] TAKASHI ICHIKAWA,[11] PETER Z. KUNSZT,[4] DON Q. LAMB,[6] TIMOTHY A. MCKAY,[12] SADANORI OKAMURA,[7] JUDITH RACUSIN,[12] MAKI SEKIGUCHI,[8] DONALD P. SCHNEIDER,[13] KAZUHIRO SHIMASAKU,[7] AND DONALD YORK[6]

Received 2001 February 2; accepted 2001 July 10

ABSTRACT

We study the optical colors of 147,920 galaxies brighter than $g^* = 21$, observed in five bands by the Sloan Digital Sky Survey (SDSS) over ~ 100 deg^2 of high Galactic latitude sky along the celestial equator. The distribution of galaxies in the g^*-r^* versus u^*-g^* color-color diagram is strongly bimodal, with an optimal color separator of $u^*-r^* = 2.22$. We use visual morphology and spectral classification of subsamples of 287 and 500 galaxies, respectively, to show that the two peaks correspond roughly to early- (E, S0, and Sa) and late-type (Sb, Sc, and Irr) galaxies, as expected from their different stellar populations. We also find that the colors of galaxies are correlated with their radial profiles, as measured by the concentration index and by the likelihoods of exponential and de Vaucouleurs' profile fits. While it is well known that late-type galaxies are bluer than early-type galaxies, this is the first detection of a local minimum in their color distribution. In all SDSS bands, the counts versus apparent magnitude relations for the two color types are significantly different and demonstrate that the fraction of blue galaxies increases toward the faint end.

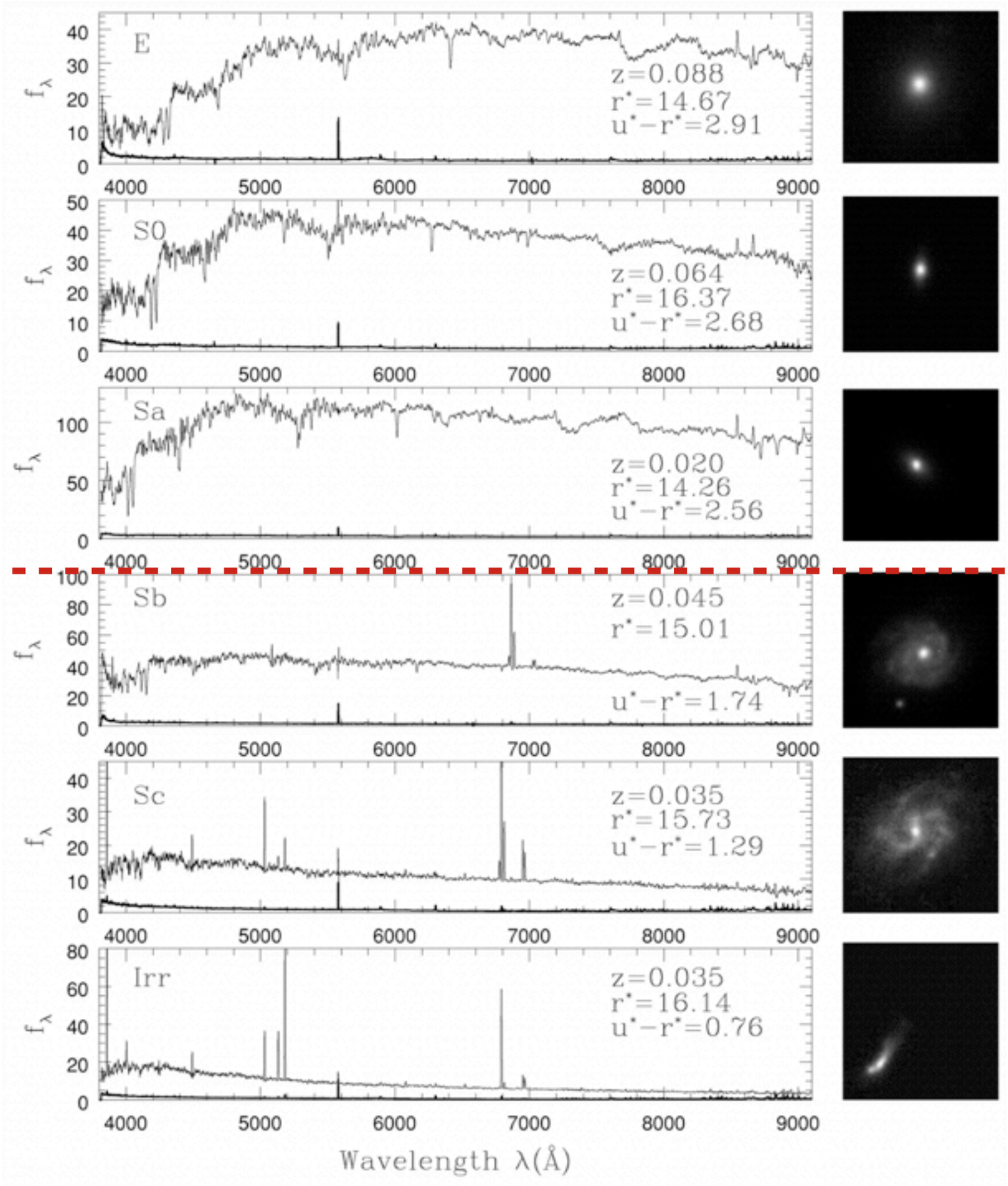

Elliptical

Spiral

bimodality

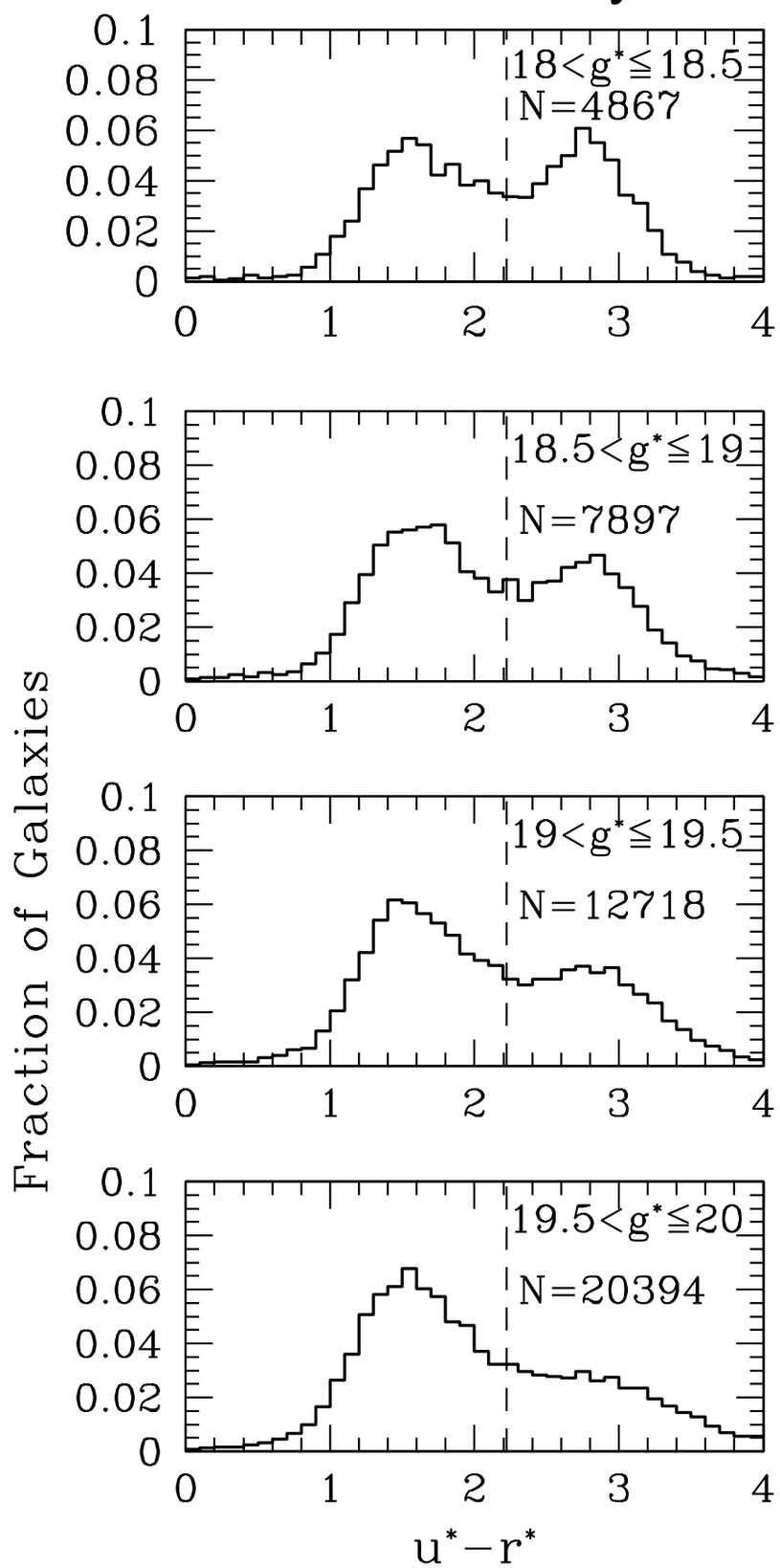

faint galaxies are blue

C=concentration -- stand-in for bulge-to-total ratio. Just the ratio of the light in two apertures.

red galaxies are more compact

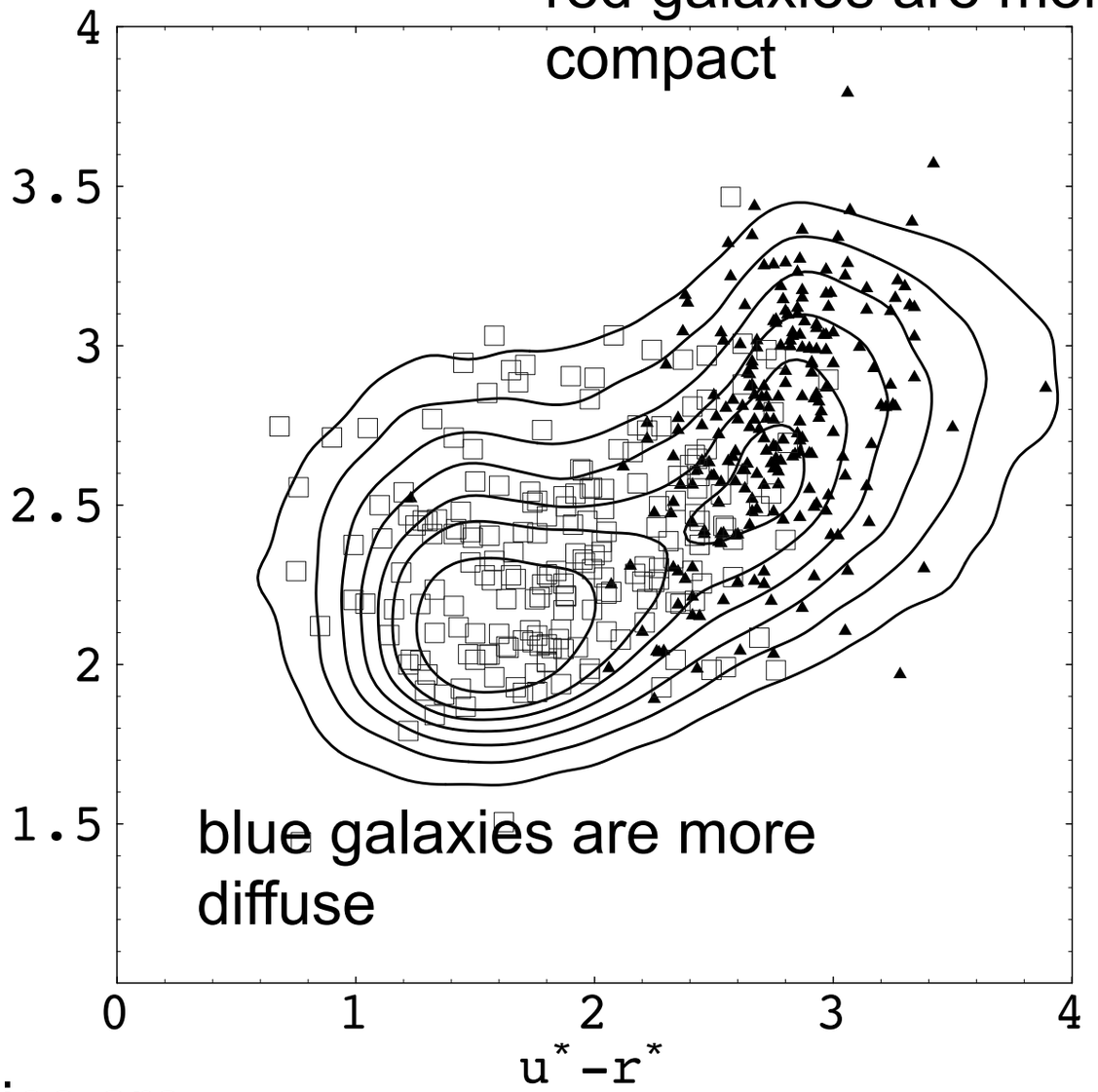

blue galaxies are more diffuse

Mon. Not. R. Astron. Soc. **341,** 54–69 (2003)

The dependence of star formation history and internal structure on stellar mass for 10^5 low-redshift galaxies

Guinevere Kauffmann,[1⋆] Timothy M. Heckman,[2] Simon D. M. White,[1] Stéphane Charlot,[1,3] Christy Tremonti,[2] Eric W. Peng,[2] Mark Seibert,[2] Jon Brinkmann,[4] Robert C. Nichol,[5] Mark SubbaRao[6] and Don York[6]

[1]*Max-Planck Institut für Astrophysik, D-85748 Garching, Germany*
[2]*Department of Physics and Astronomy, Johns Hopkins University, Baltimore, MD 21218, USA*
[3]*Institut d'Astrophysique du CNRS, 98 bis Boulevard Arago, F-75014 Paris, France*
[4]*Apache Point Observatory, PO Box 59, Sunspot, NM 88349, USA*
[5]*Department of Physics, Carnegie Mellon University, 5000 Forbes Ave, Pittsburgh, PA 15232, USA*
[6]*Department of Astronomy, University of Chicago, 5640 South Ellis Ave, Chicago, IL 60637, USA*

Accepted 2002 November 22. Received 2002 October 30; in original form 2002 May 08

ABSTRACT

We study the relations between stellar mass, star formation history, size and internal structure for a complete sample of 122 808 galaxies drawn from the Sloan Digital Sky Survey. We show that low-redshift galaxies divide into two distinct families at a stellar mass of 3×10^{10} $M_\odot$. Lower-mass galaxies have young stellar populations, low surface mass densities and the low concentrations typical of discs. Their star formation histories are more strongly correlated with surface mass density than with stellar mass. A significant fraction of the lowest-mass galaxies in our sample have experienced recent starbursts. At given stellar mass, the sizes of low-mass galaxies are lognormally distributed with dispersion $\sigma(\ln R_{50}) \sim 0.5$, in excellent agreement with the idea that they form with little angular momentum loss through cooling and condensation in a gravitationally dominant dark matter halo. Their median stellar surface mass density scales with stellar mass as $\mu_* \propto M_*^{0.54}$, suggesting that the stellar mass of a disc galaxy is proportional to the three halves power of its halo mass. All of this suggests that the efficiency of the conversion of baryons into stars in low-mass galaxies increases in proportion to halo mass, perhaps as a result of supernova feedback processes. At stellar masses above 3×10^{10} $M_\odot$, there is a rapidly increasing fraction of galaxies with old stellar populations, high surface mass densities and the high concentrations typical of bulges. In this regime, the size distribution remains lognormal, but its dispersion decreases rapidly with increasing mass and the median stellar mass surface density is approximately constant. This suggests that the star formation efficiency decreases in the highest-mass haloes, and that little star formation occurs in massive galaxies after they have assembled.

strength of 4000A break -- a spectral feature indicating old populations

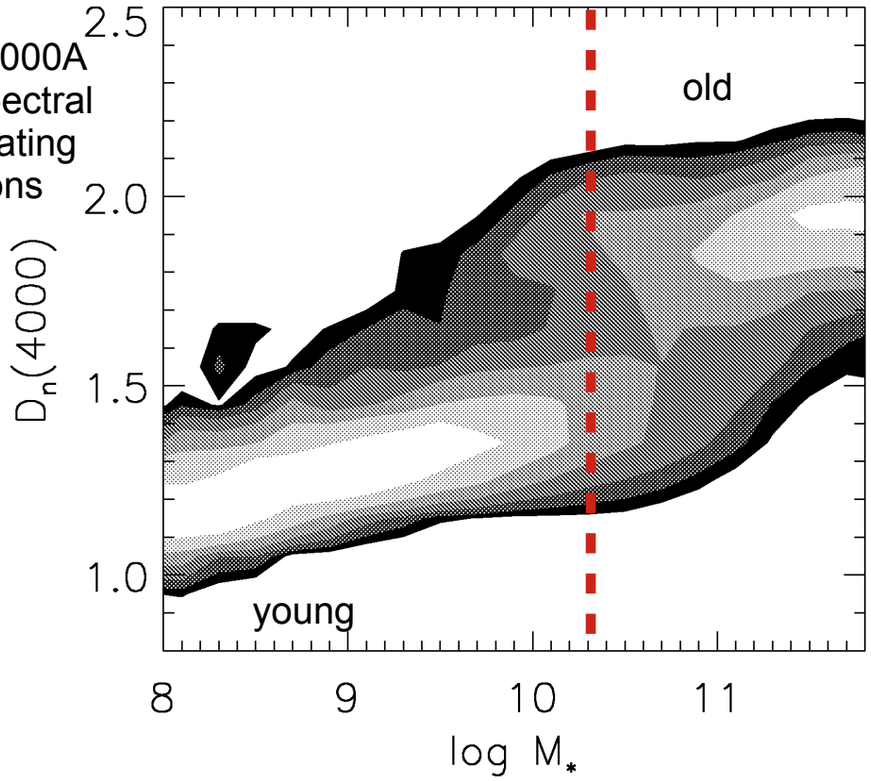

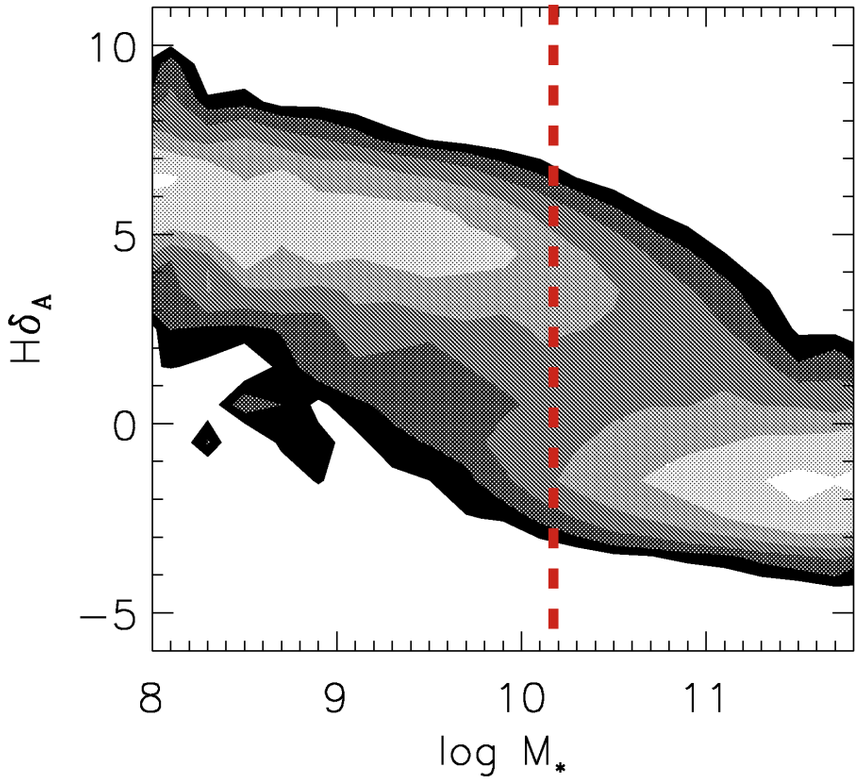

stellar mass

See the same transition as a function of galaxy structure (here concentration).

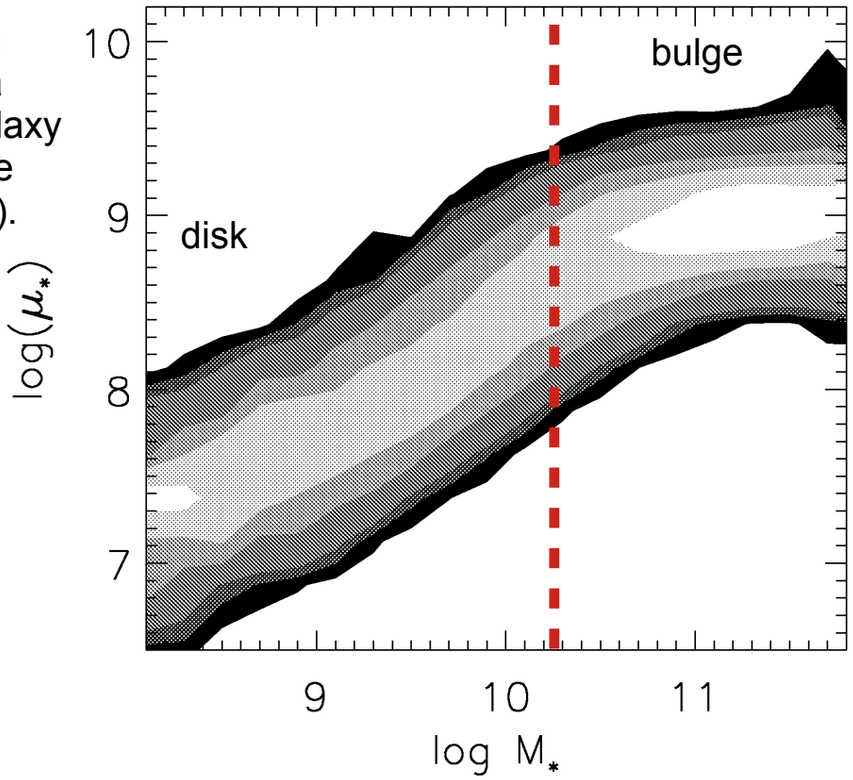

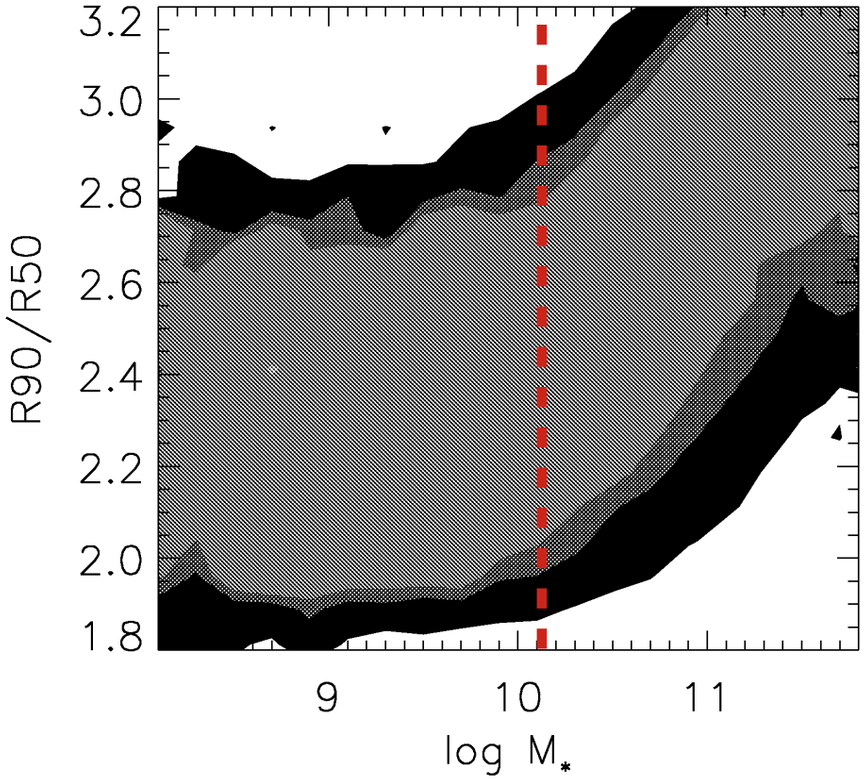

Galaxy bimodality, note the magic scale of $3 \times 10^{10}\ M_\odot$

Annu. Rev. Astron. Astrophys. 2009. 47:159–210

Physical Properties and Environments of Nearby Galaxies

Michael R. Blanton and John Moustakas

Center for Cosmology and Particle Physics, New York University, New York, NY 10003;
email: michael.blanton@nyu.edu

Key Words

galaxy environment, morphological type, star-formation history

Abstract

We review the physical properties of nearby, relatively luminous galaxies, using results from newly available massive data sets together with more detailed observations. First, we present the global distribution of properties, including the optical and ultraviolet (UV) luminosity, stellar mass, and atomic gas mass functions. Second, we describe the shift of the galaxy population from late galaxy types in underdense regions to early galaxy types in overdense regions. We emphasize that the scaling relations followed by each galaxy type change very little with environment, with the exception of some minor but detectable effects. The shift in the population is apparent even at the densities of small groups and therefore cannot be exclusively due to physical processes operating in rich clusters. Third, we divide galaxies into four crude types—spiral, lenticular, elliptical, and merging systems—and describe some of their more detailed properties. We attempt to put these detailed properties into the global context provided by large surveys.

Color

Absolute Magnitude

Sersic index low n - disk

surface brightness

color -- stellar age

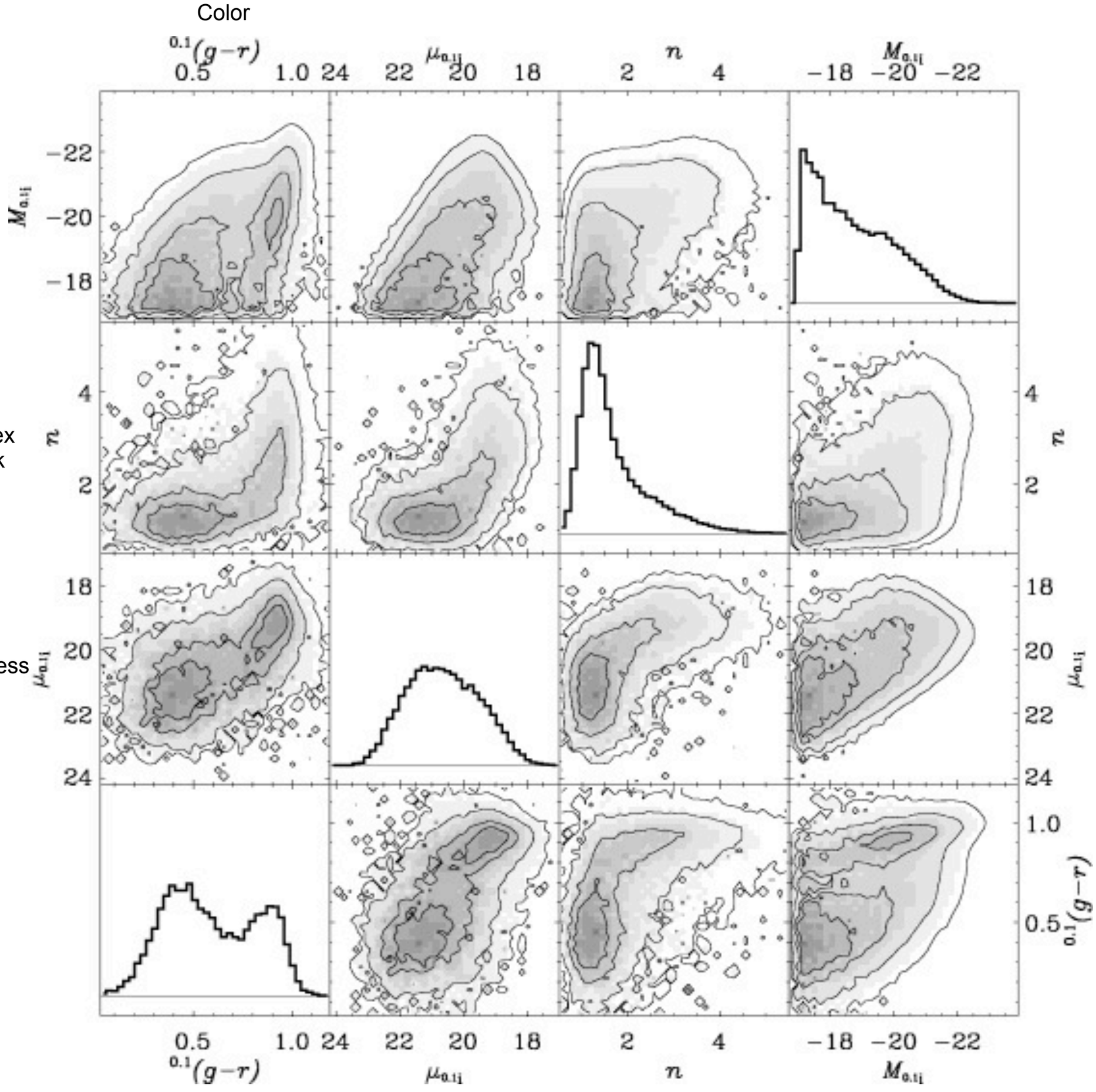

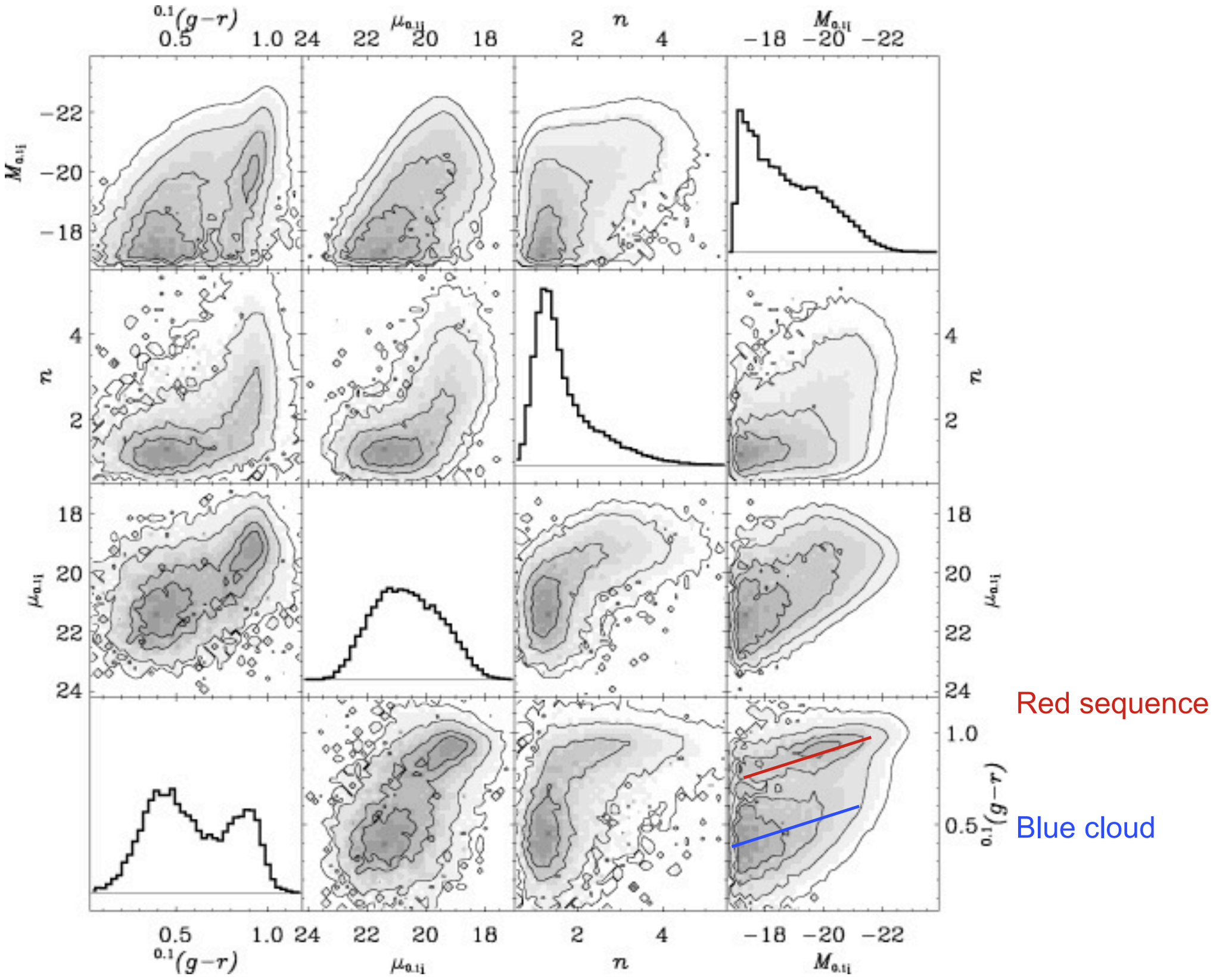
$^{0.1}(g-r)$
$\mu_{0.1i}$
n
$M_{0.1i}$
Red sequence
Blue cloud

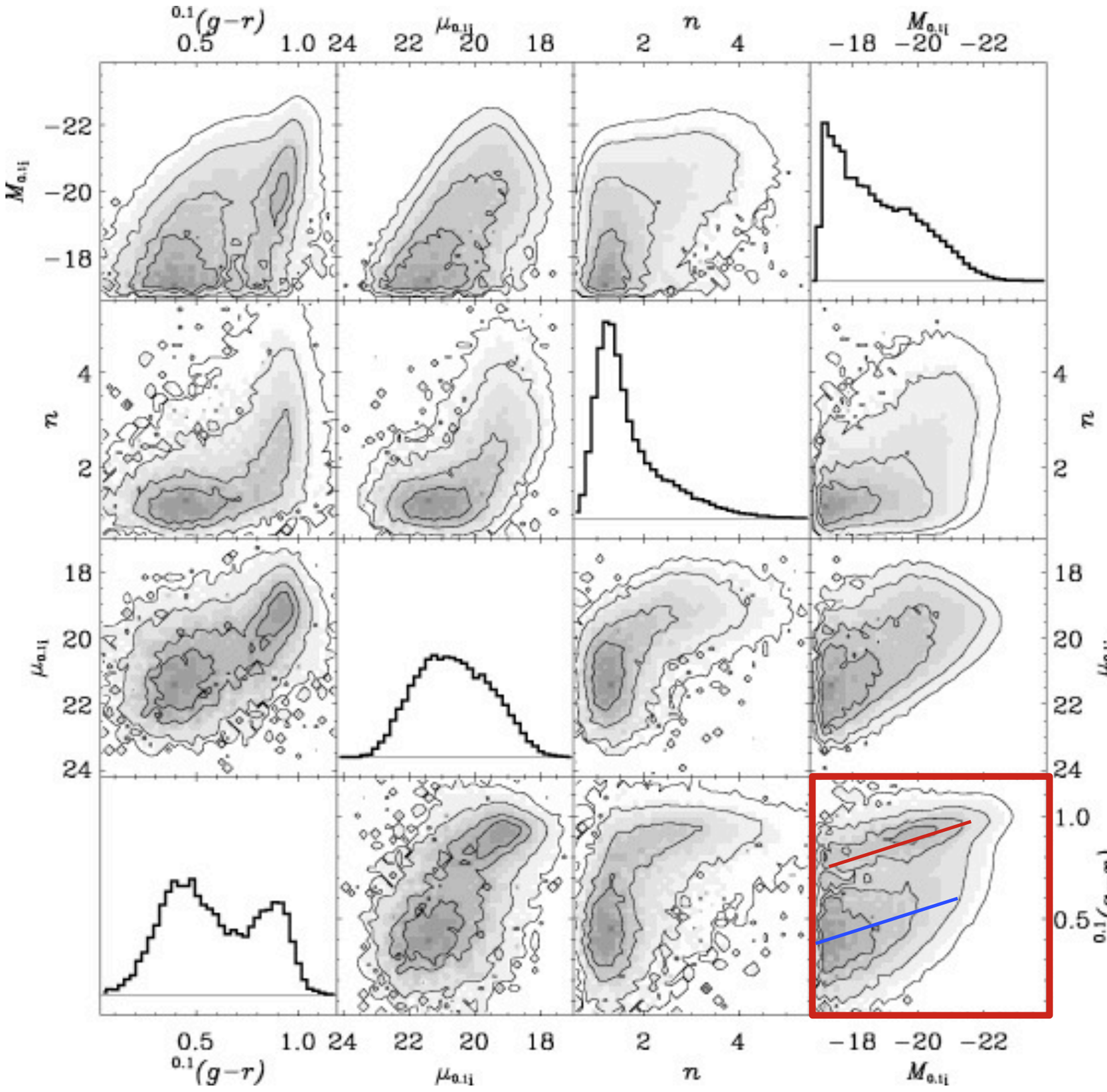

Color-magnitude relation

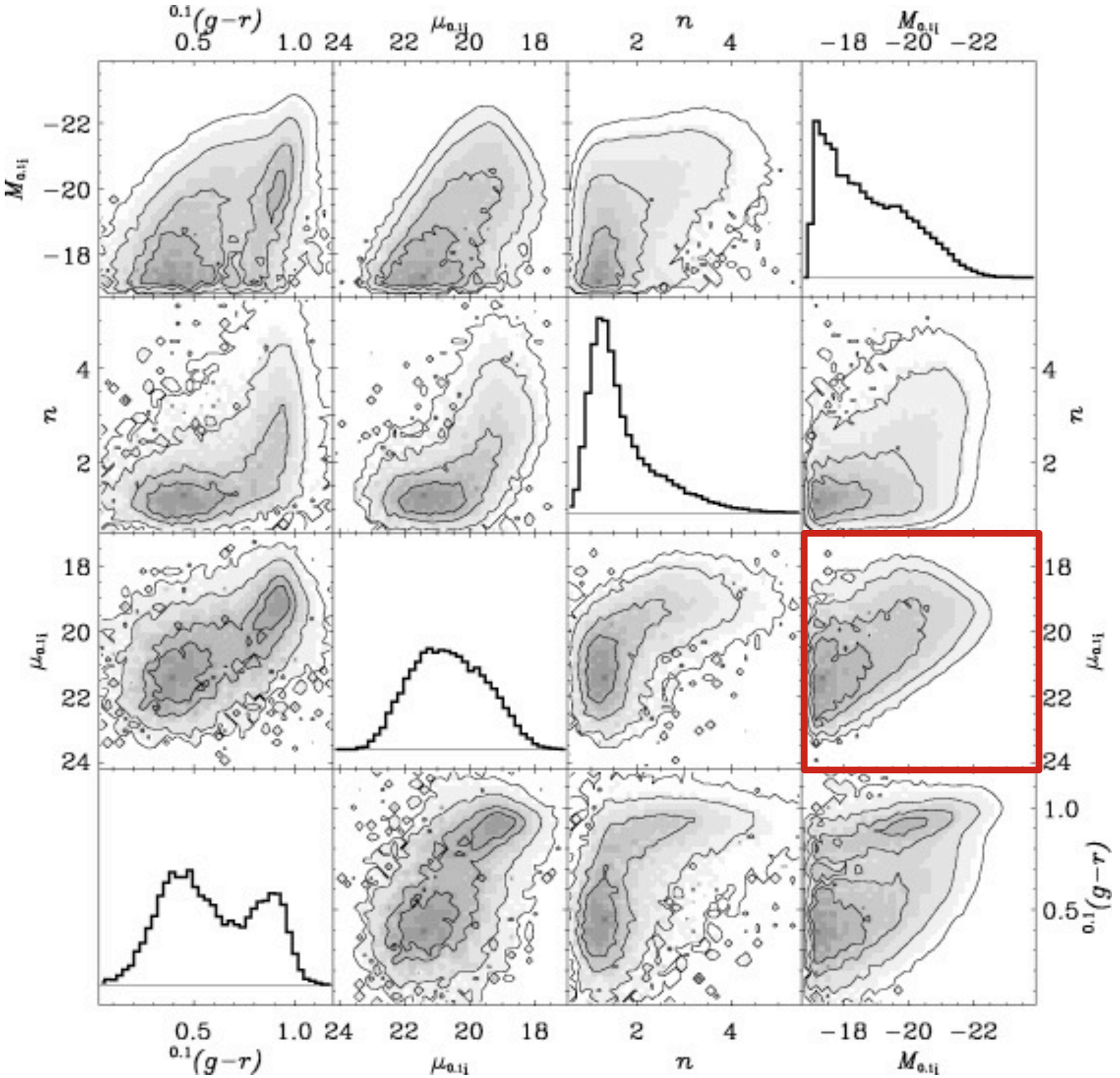

Kormendy relation
(Fundamental Plane)

Structure correlates with mass

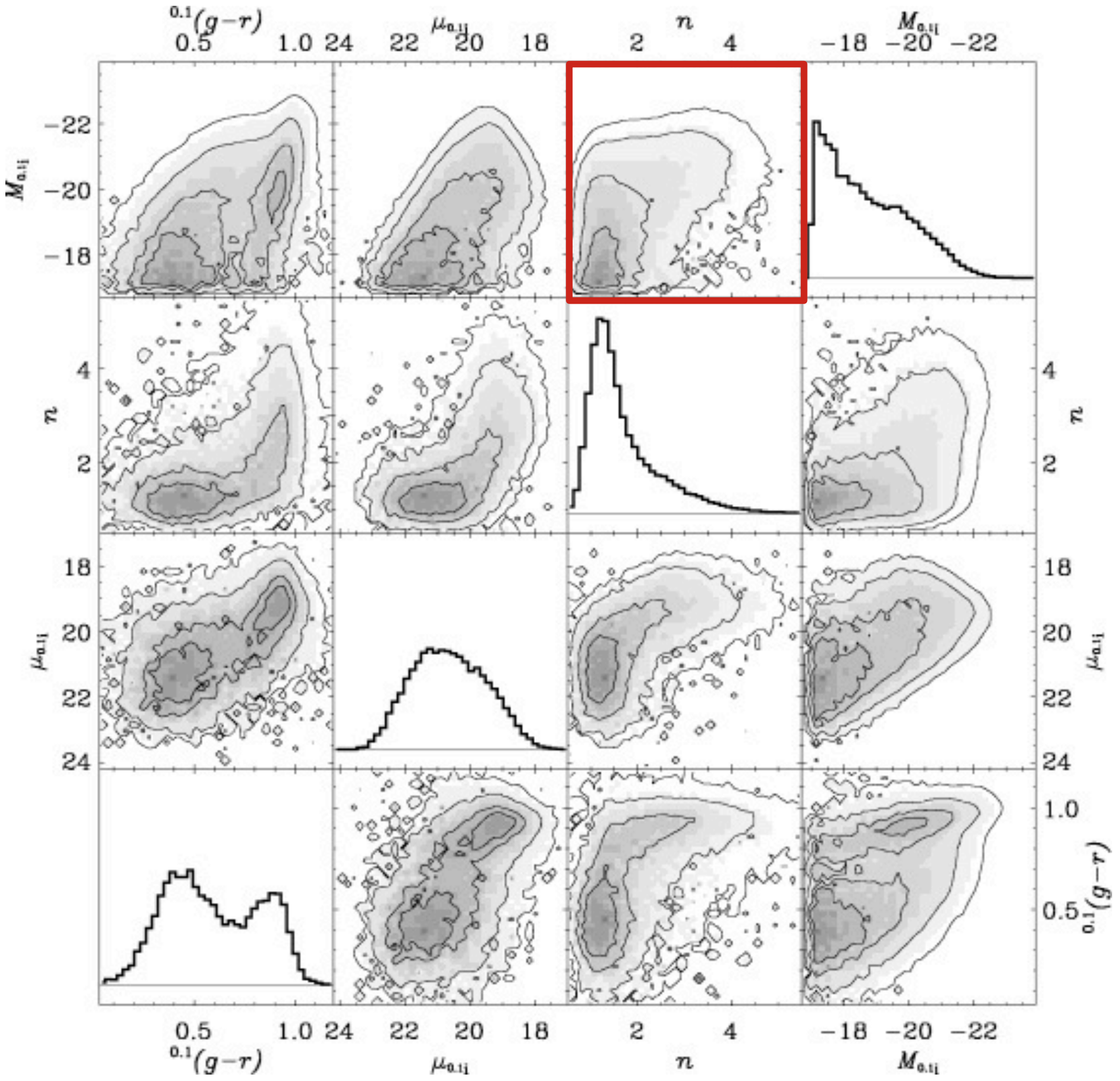

THE ASTROPHYSICAL JOURNAL, 613:898–913, 2004 October 1

THE ORIGIN OF THE MASS-METALLICITY RELATION: INSIGHTS FROM 53,000 STAR-FORMING GALAXIES IN THE SLOAN DIGITAL SKY SURVEY

CHRISTY A. TREMONTI,[1,2] TIMOTHY M. HECKMAN,[1] GUINEVERE KAUFFMANN,[3] JARLE BRINCHMANN,[3,4] STÉPHANE CHARLOT,[3,5] SIMON D. M. WHITE,[3] MARK SEIBERT,[1,6] ERIC W. PENG,[1,7] DAVID J. SCHLEGEL,[8] ALAN UOMOTO,[1,9] MASATAKA FUKUGITA,[10] AND JON BRINKMANN[11]

Received 2003 December 21; accepted 2004 May 28

ABSTRACT

We utilize Sloan Digital Sky Survey imaging and spectroscopy of ~53,000 star-forming galaxies at $z \sim 0.1$ to study the relation between stellar mass and gas-phase metallicity. We derive gas-phase oxygen abundances and stellar masses using new techniques that make use of the latest stellar evolutionary synthesis and photoionization models. We find a tight (±0.1 dex) correlation between stellar mass and metallicity spanning over 3 orders of magnitude in stellar mass and a factor of 10 in metallicity. The relation is relatively steep from $10^{8.5}$ to $10^{10.5}\ M_{\odot}\ h_{70}^{-2}$, in good accord with known trends between luminosity and metallicity, but flattens above $10^{10.5}\ M_{\odot}$. We use indirect estimates of the gas mass based on the Hα luminosity to compare our data to predictions from simple closed box chemical evolution models. We show that metal loss is strongly anticorrelated with baryonic mass, with low-mass dwarf galaxies being 5 times more metal depleted than L^* galaxies at $z \sim 0.1$. Evidence for metal depletion is not confined to dwarf galaxies but is found in galaxies with masses as high as $10^{10}\ M_{\odot}$. We interpret this as strong evidence of both the ubiquity of galactic winds and their effectiveness in removing metals from galaxy potential wells.

Metallicity in gas

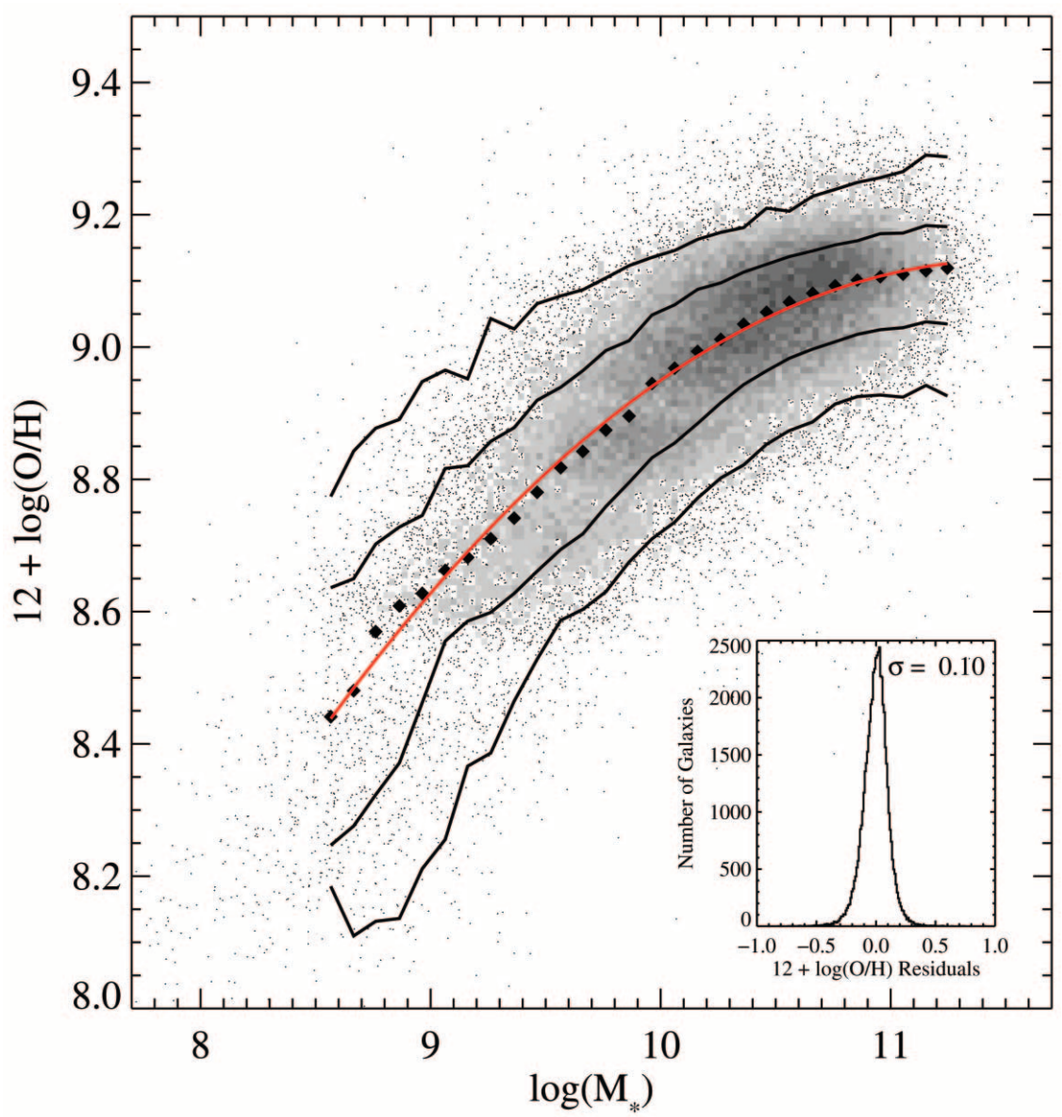

stellar mass

FIG. 6.—Relation between stellar mass, in units of solar masses, and gas-phase oxygen abundance for ~53,400 star-forming galaxies in the SDSS. The large black filled diamonds represent the median in bins of 0.1 dex in mass that include at least 100 data points. The solid lines are the contours that enclose 68% and 95% of the data. The red line shows a polynomial fit to the data. The inset plot shows the residuals of the fit. Data for the contours are given in Table 3.

High-mass galaxies retain metals due to deep potential wells

Low-mass galaxies lose metals in star-formation driven winds (“feedback”)

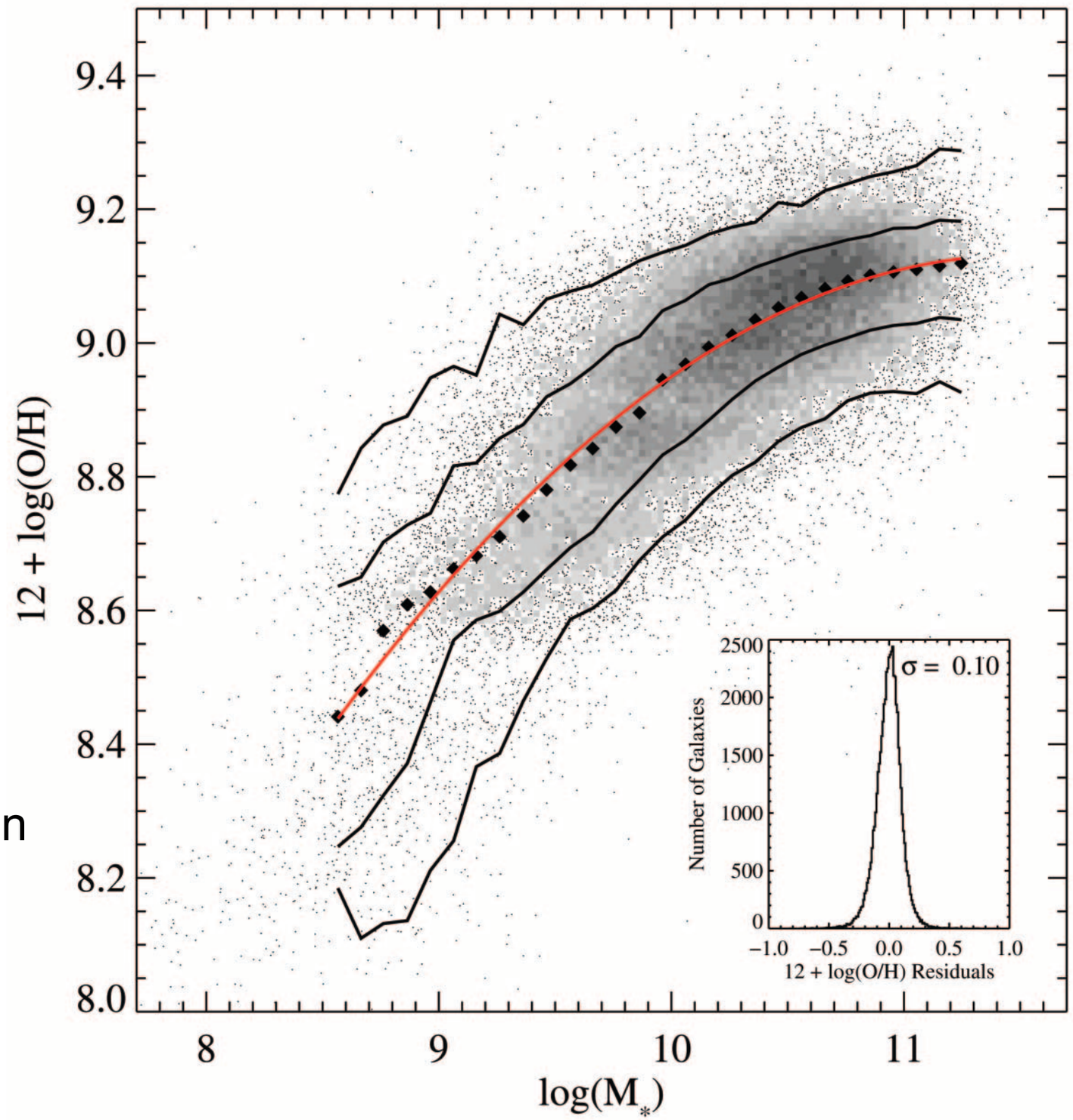

FIG. 6.—Relation between stellar mass, in units of solar masses, and gas-phase oxygen abundance for ∼53,400 star-forming galaxies in the SDSS. The large black filled diamonds represent the median in bins of 0.1 dex in mass that include at least 100 data points. The solid lines are the contours that enclose 68% and 95%

Outflow

There are many lines of evidence for outflows driven by star formation.

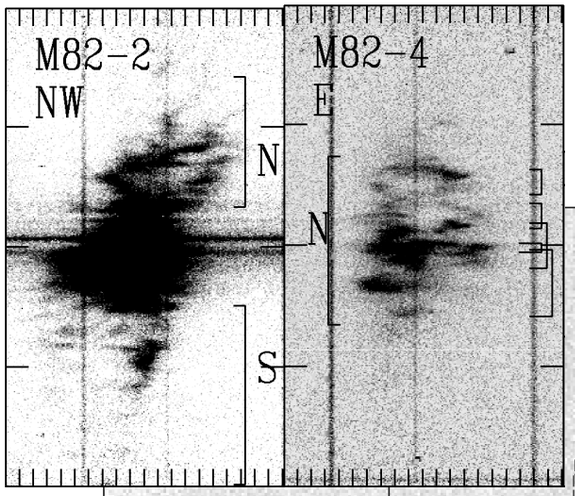

Hα long-slit observations

Hα image

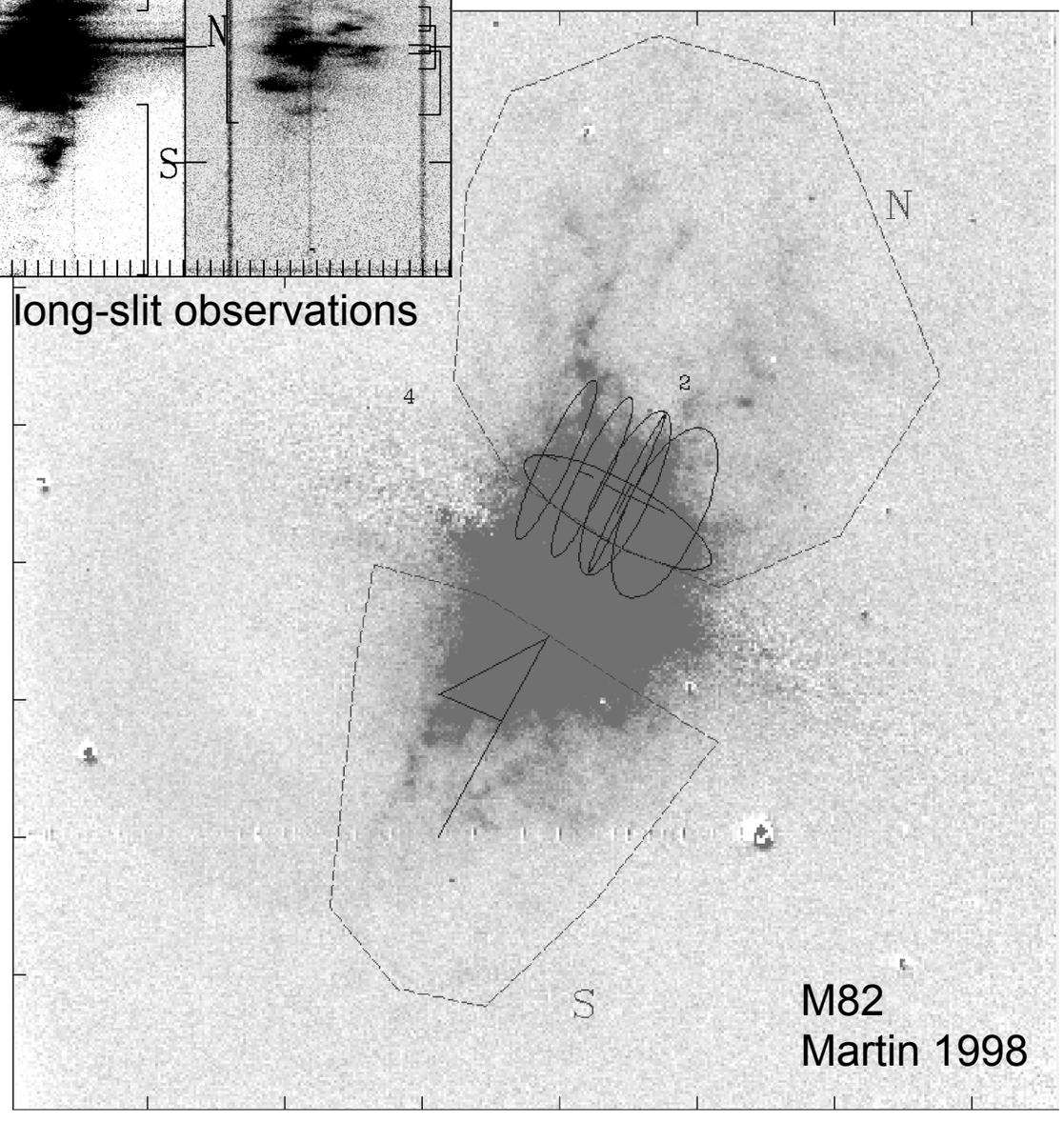

FIG. 2*d*

Strickland & Heckman 2009

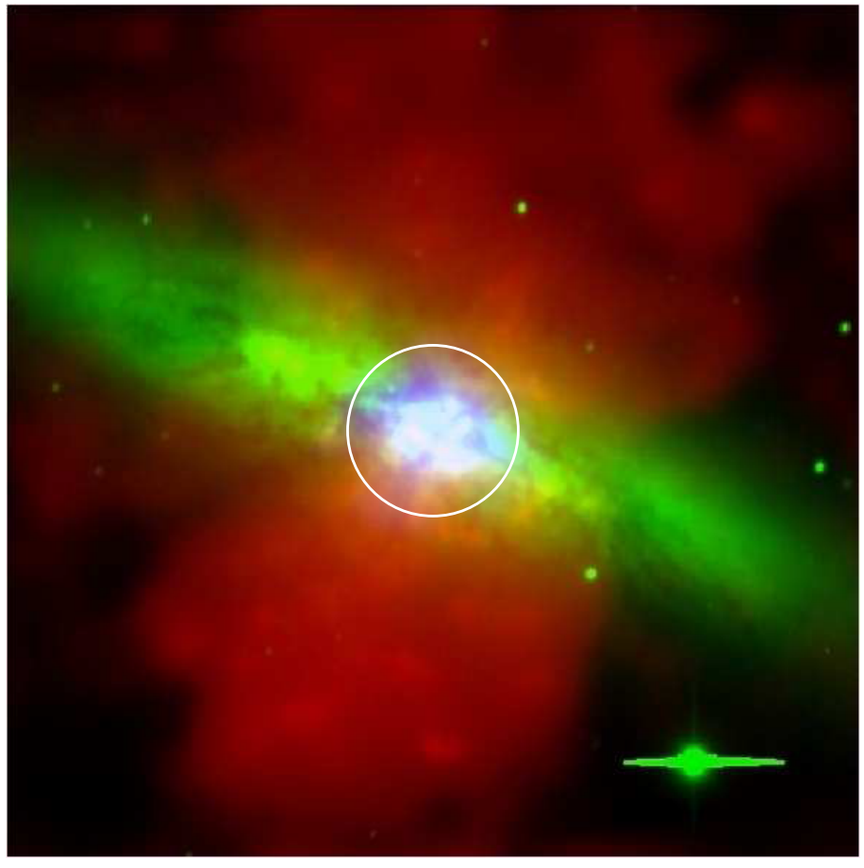

Figure 1. Three-color composite image of M82 showing the region within a 500 pc radius of the nucleus (white circle) in comparison to the galaxy and superwind. Soft X-ray emission in the 0.3–2.8 keV energy band is shown in red, optical *R*-band emission (starlight) in green, and diffuse hard X-ray emission in the 3–7 keV energy band in blue. The X-ray images are adaptively smoothed *Chandra* ACIS-S images with point-source emission removed and interpolated over. The image is 4.′8 (∼5 kpc) on a side.

AN ANALYTIC EXPRESSION FOR THE LUMINOSITY FUNCTION FOR GALAXIES*

PAUL SCHECHTER
California Institute of Technology and the Institute for Advanced Study
Received 1975 April 29; revised 1975 June 30

ABSTRACT

A new analytic approximation for the luminosity function for galaxies is proposed, which shows good agreement with both a luminosity distribution for bright nearby galaxies and a composite luminosity distribution for cluster galaxies. The analytic expression is proportional to $L^{-5/4}e^{-L/L*}$, where L^* is a characteristic luminosity corresponding to a characteristic absolute magnitude $M^*_{B(0)} = -20.6$. For an individual cluster, the characteristic magnitude may be determined with an accuracy of ~ 0.25 mag, suggesting its use as a standard candle. The analytic expression is used to compute an expected richness–absolute magnitude correlation for first ranked cluster galaxies and an expected dispersion, which are compared with the data of Sandage and Hardy.

Subject headings: galaxies: clusters of — galaxies: photometry

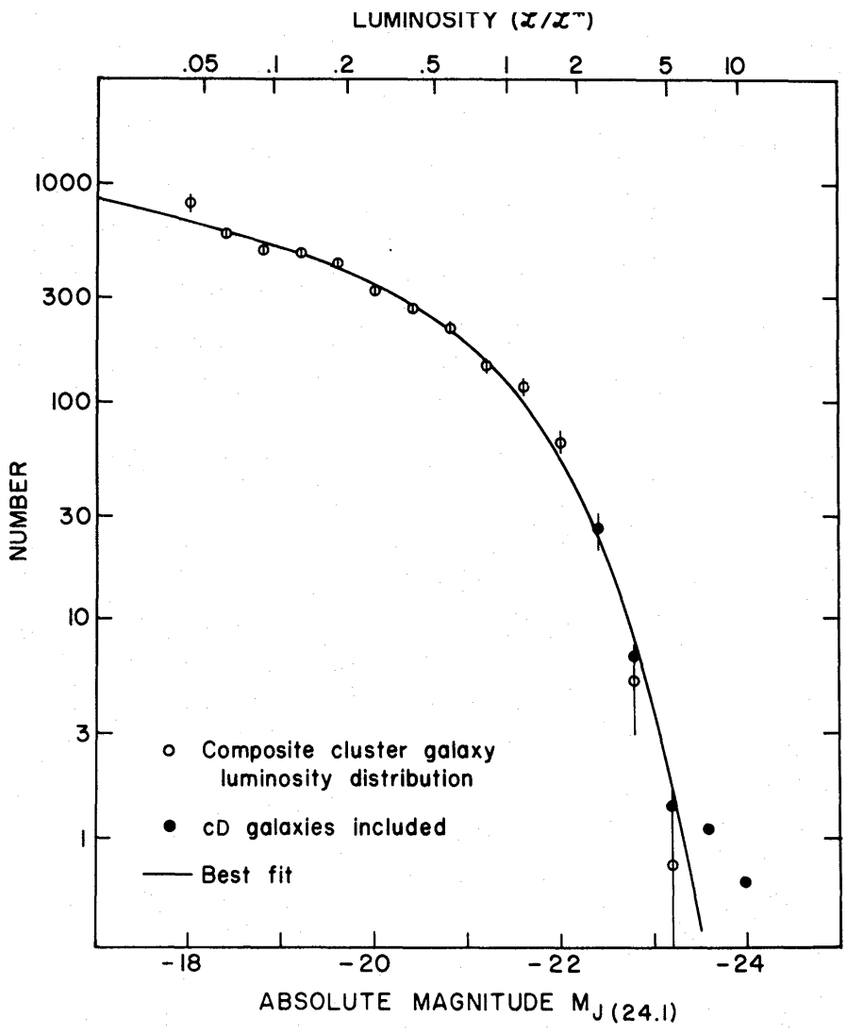

FIG. 2.—Best fit of analytic expression to observed composite cluster galaxy luminosity distribution. Filled circles show the effect of including cD galaxies in composite.

$$\varphi(L)dL = \varphi^*(L/L^*)^\alpha \exp(-L/L^*)d(L/L^*)$$

AN ANALYTIC EXPRESSION FOR THE LUMINOSITY FUNCTION FOR GALAXIES*

PAUL SCHECHTER
California Institute of Technology and the Institute for Advanced Study
Received 1975 April 29; revised 1975 June 30

ABSTRACT

A new analytic approximation for the luminosity function for galaxies is proposed, which shows good agreement with both a luminosity distribution for bright nearby galaxies and a composite luminosity distribution for cluster galaxies. The analytic expression is proportional to $L^{-5/4}e^{-L/L*}$, where L^* is a characteristic luminosity corresponding to a characteristic absolute magnitude $M^*_{B(0)} = -20.6$. For an individual cluster, the characteristic magnitude may be determined with an accuracy of ~ 0.25 mag, suggesting its use as a standard candle. The analytic expression is used to compute an expected richness–absolute magnitude correlation for first ranked cluster galaxies and an expected dispersion, which are compared with the data of Sandage and Hardy.

Subject headings: galaxies: clusters of — galaxies: photometry

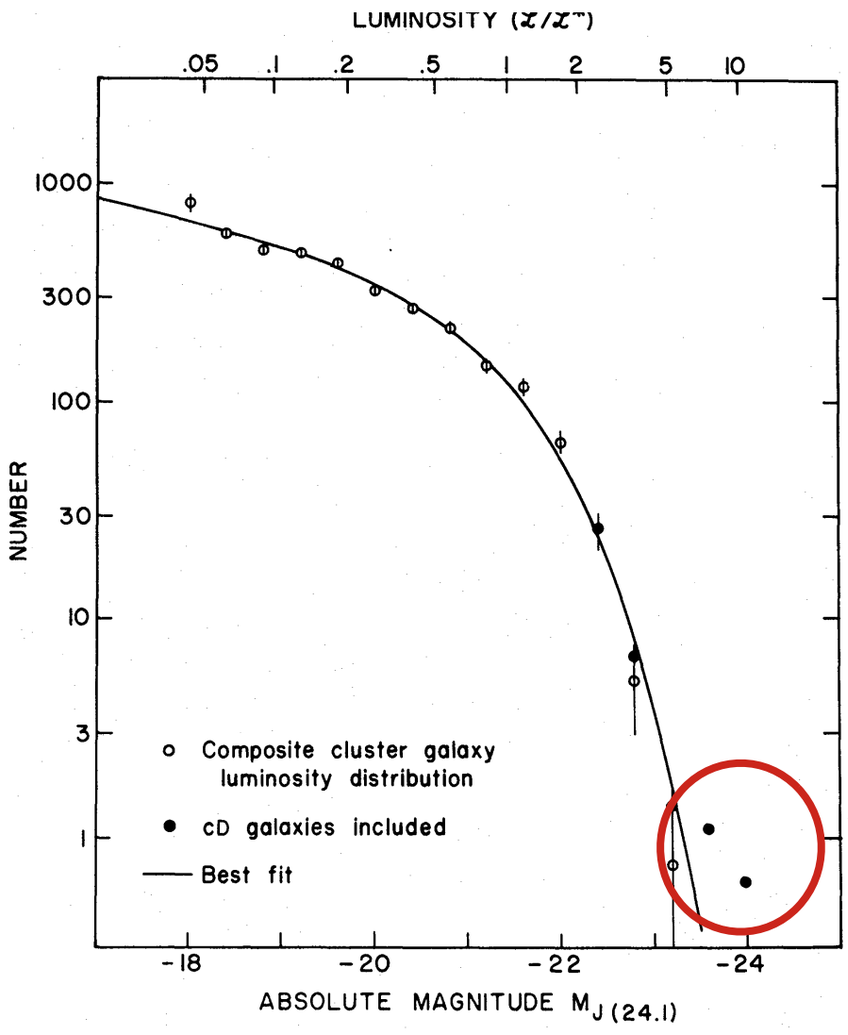

FIG. 2.—Best fit of analytic expression to observed composite cluster galaxy luminosity distribution. Filled circles show the effect of including cD galaxies in composite.

$$\varphi(L)dL = \varphi^*(L/L^*)^{\alpha} \exp(-L/L^*)d(L/L^*)$$

These are brightest cluster galaxies. They sit at the center of the cluster and get stars dumped on them. Different LF then regular galaxies.

Schechter Function

Power-law slope at faint end

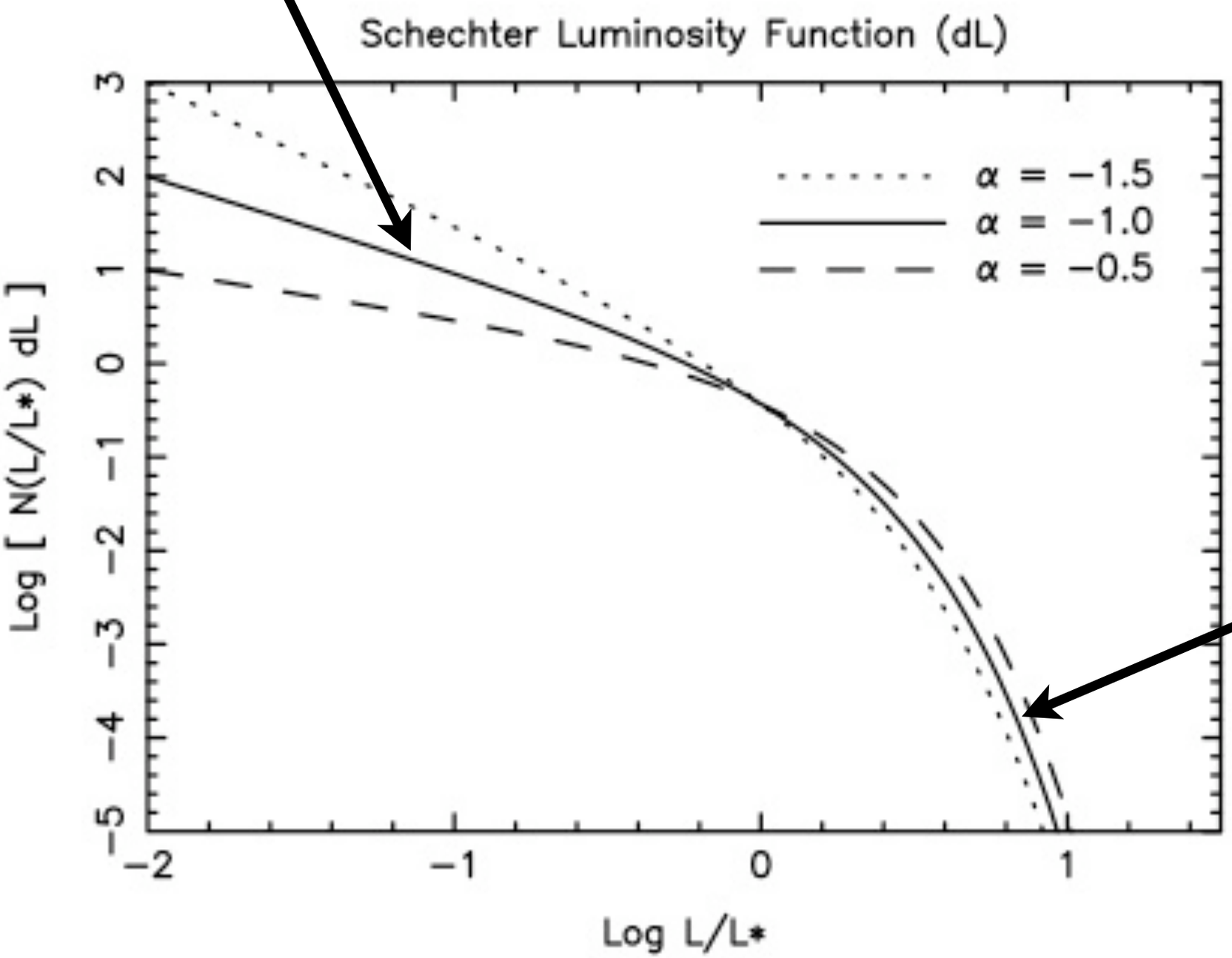

Exponential decline at luminous end

Schechter Function

Power-law slope at faint end

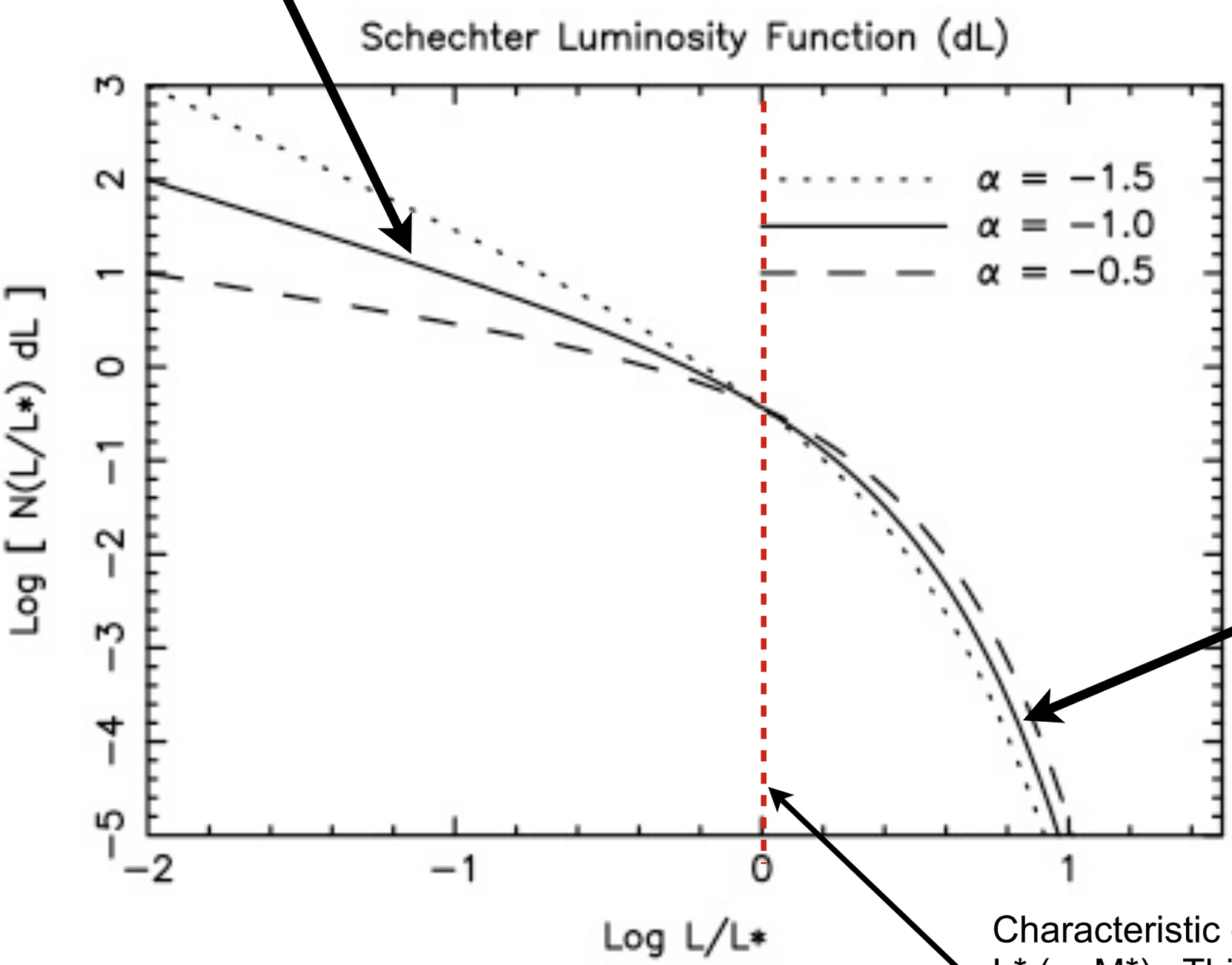

Exponential decline at luminous end

Characteristic or break luminosity is L* (or M*). This is the most common galaxy ($L_B = 10^{10}$ or $M_B = -19.7$). The MW is ~L*.

Schechter Function

Power-law slope at faint end. α varies with environment and is more controversial. α = -1.5 “steep”, α=-0.5 “shallow”.

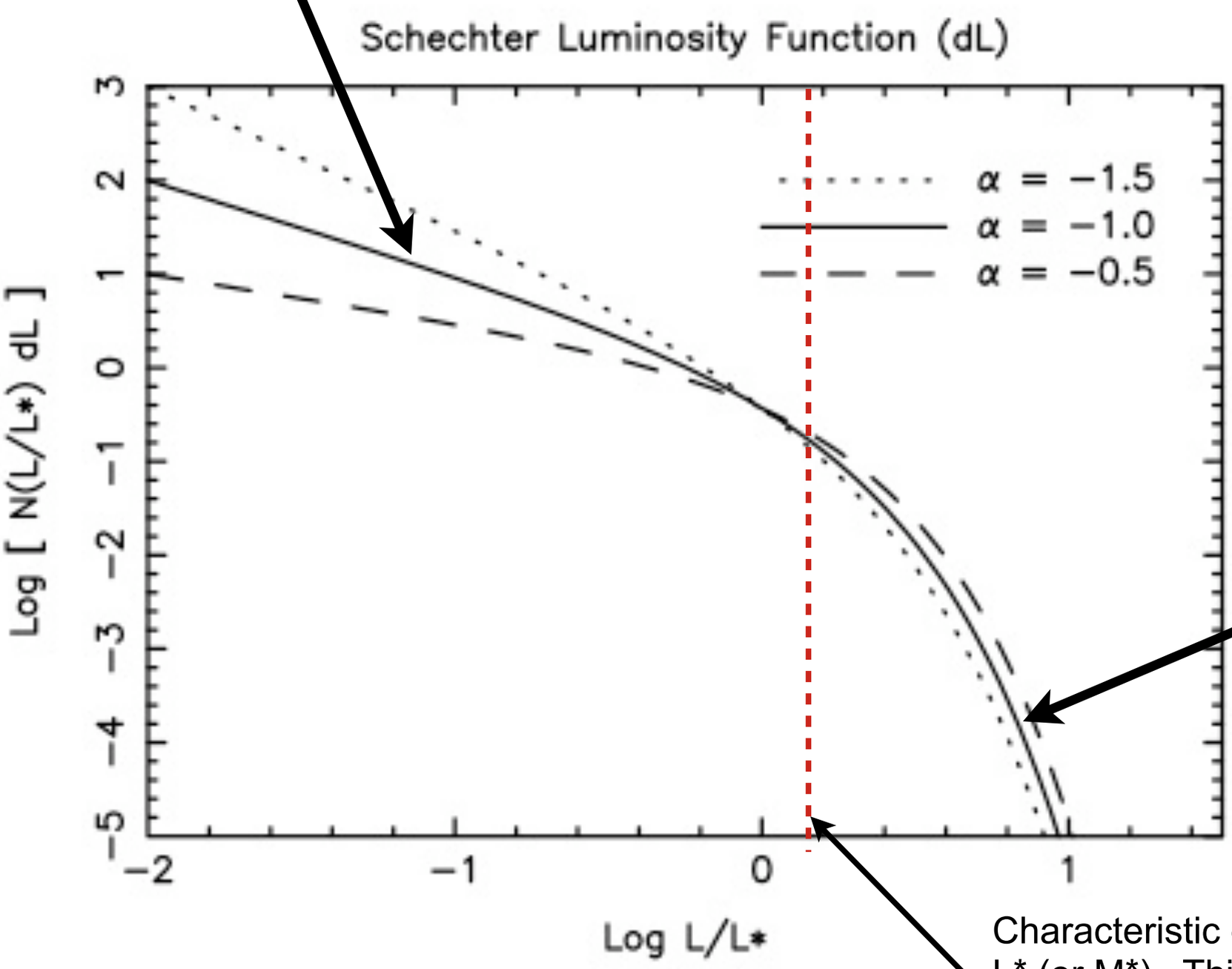

Exponential decline at luminous end

Characteristic or break luminosity is L* (or M*). This is the most common galaxy ($L_B = 10^{10}$ or $M_B = -19.7$). The MW is ~L*.

Blanton et al. 2003

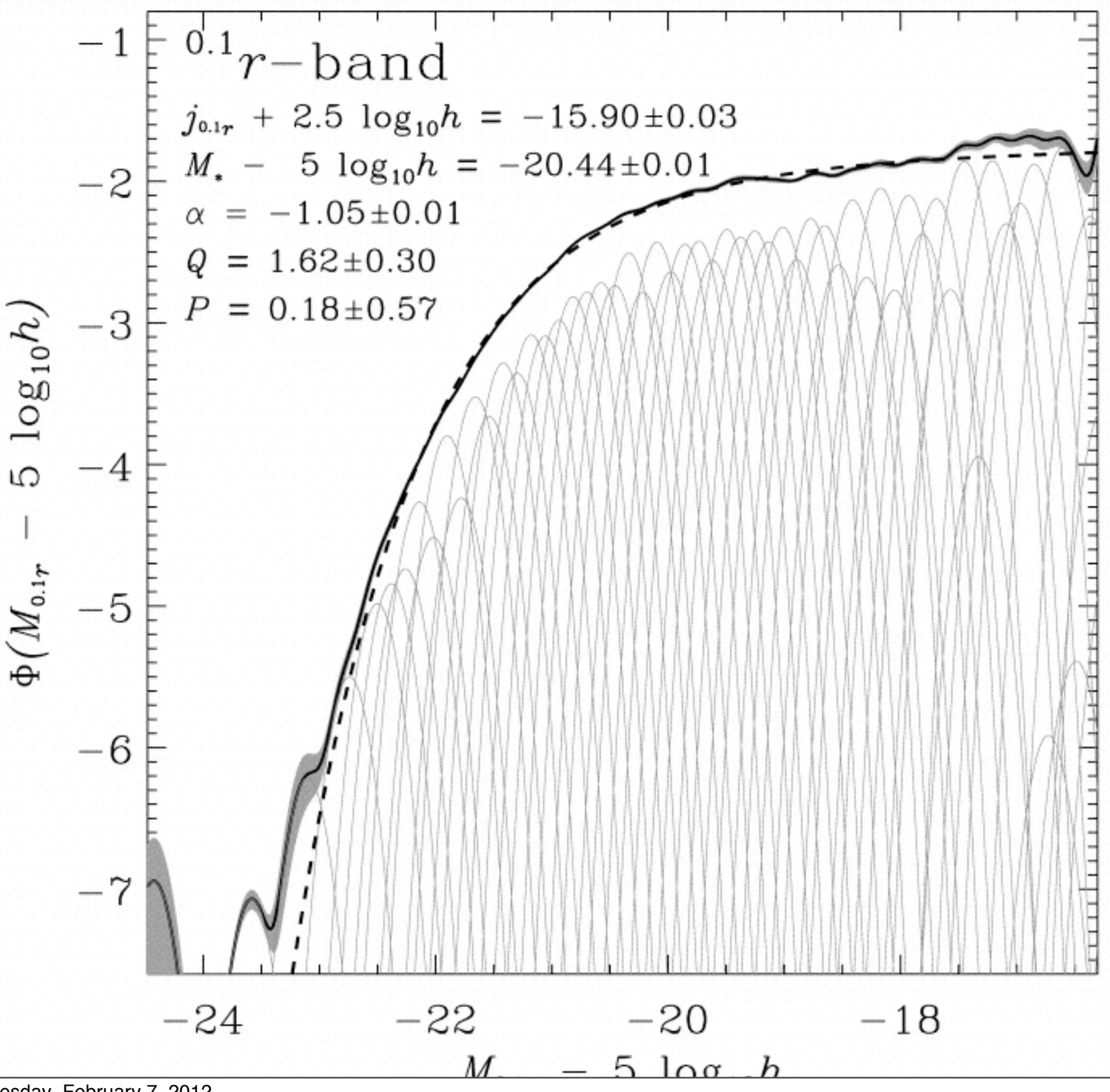

Blanton et al. 2003

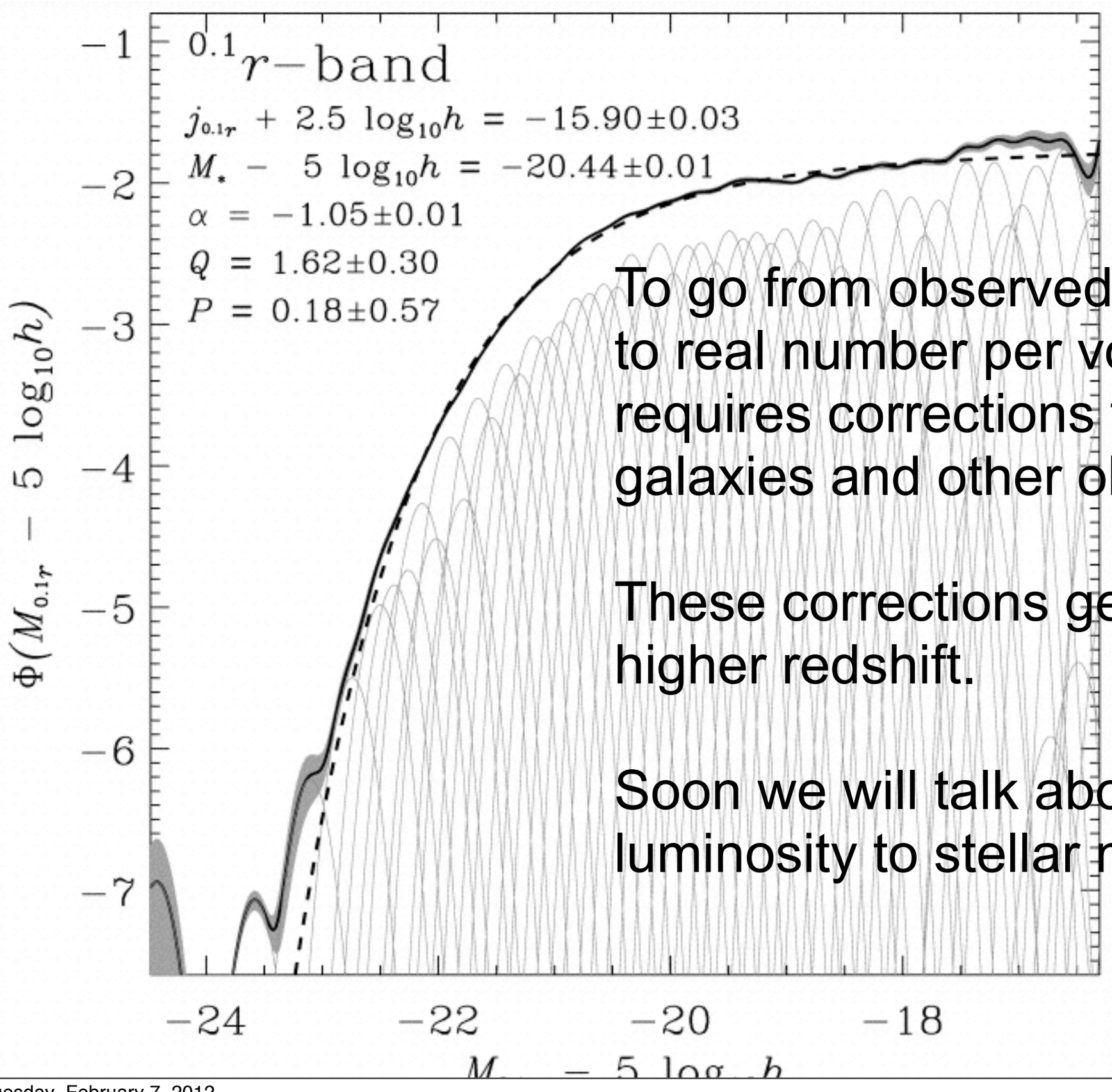

To go from observed galaxies to real number per volume requires corrections for missing galaxies and other observational errors.

These corrections get harder at higher redshift.

Soon we will talk about going from luminosity to stellar mass.

Physical Origins of the LF

The predicted mass function of dark matter halos (in any CDM cosmology) is a featureless power-law which turns over at the largest scales.

The galaxy luminosity function and the halo mass function are related by the mass-to-light ration. From plot below, the mass-to-light ratio *must* be a function of luminosity. Galaxy formation efficiency is mass dependent.

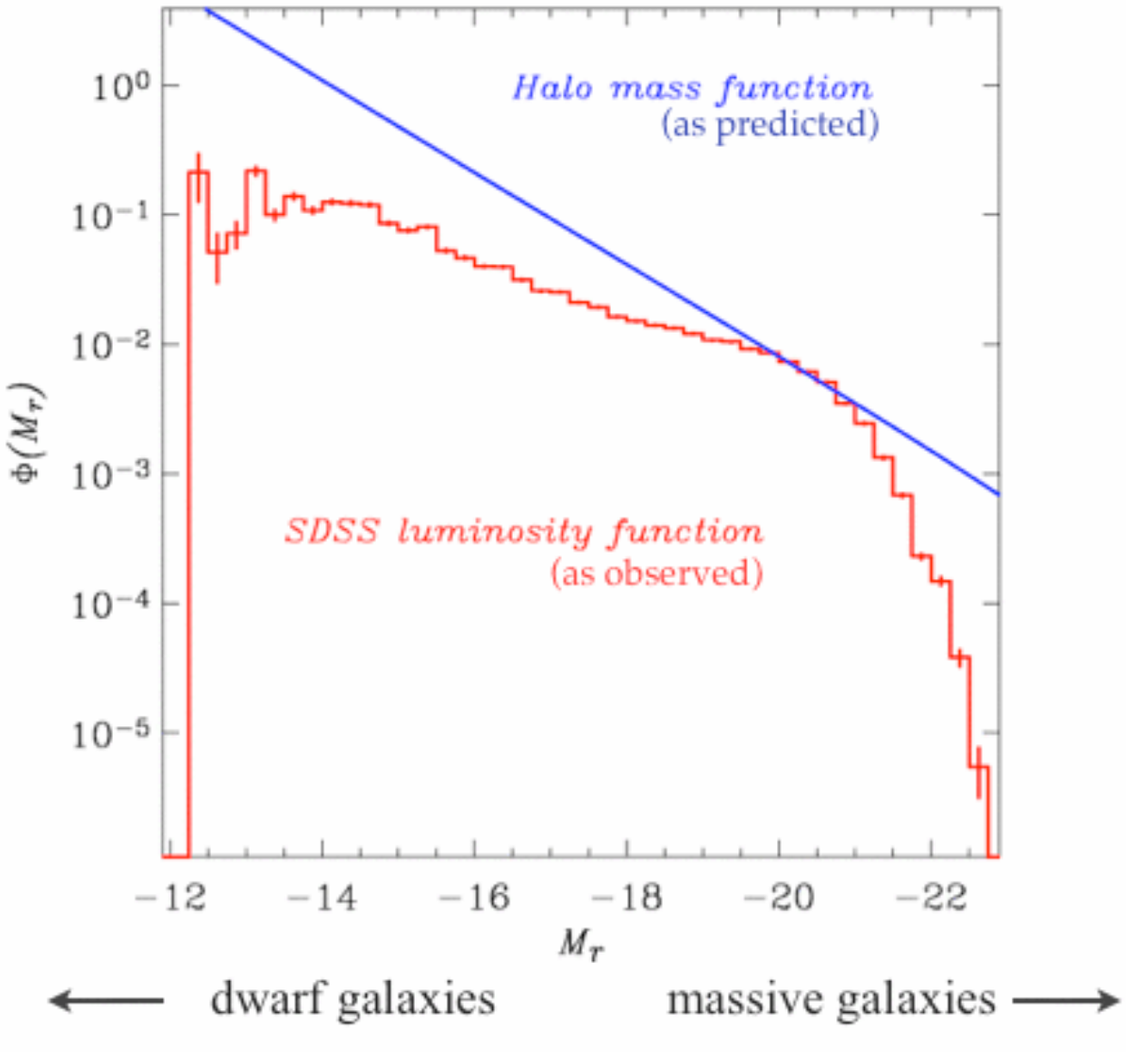

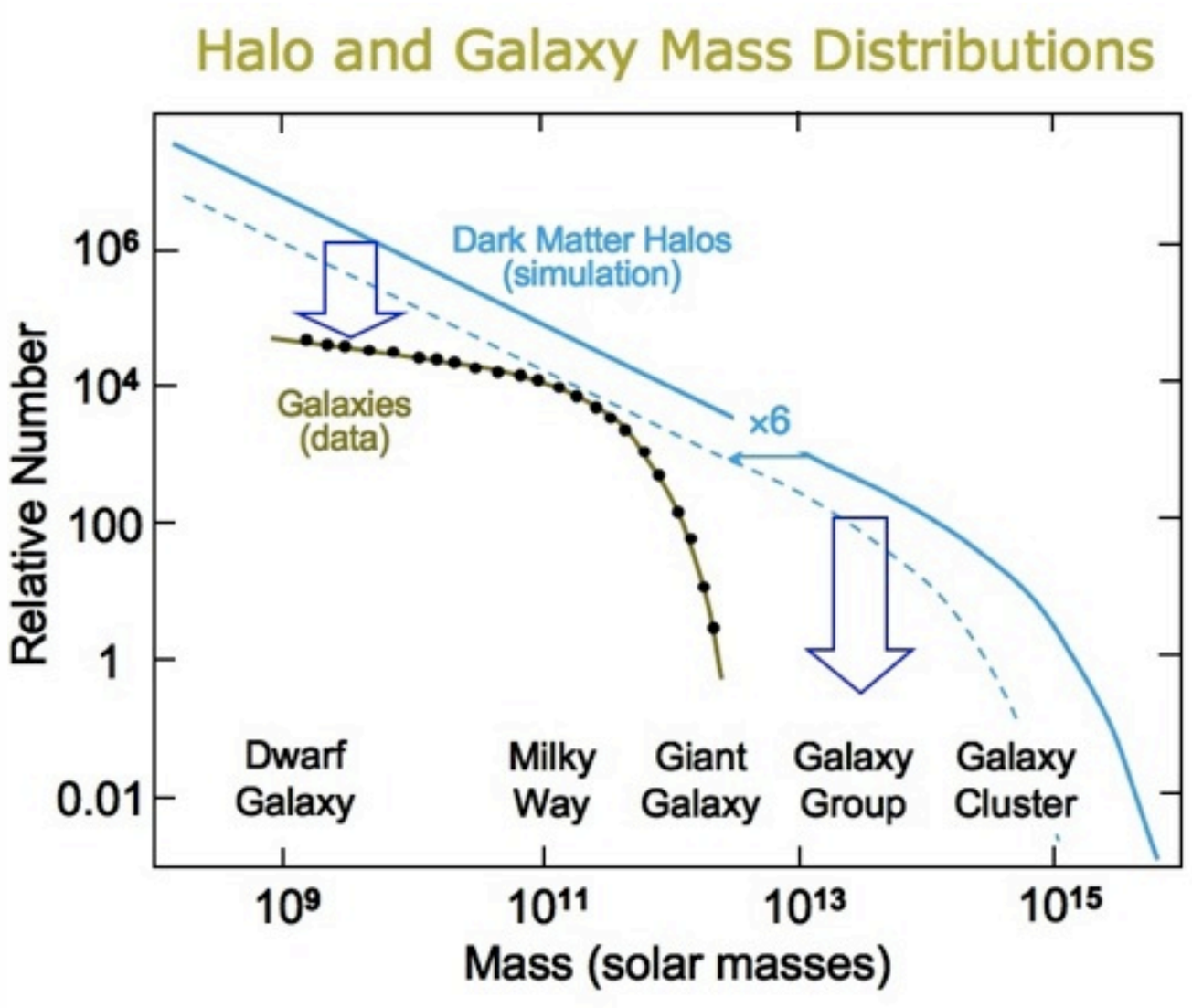

Ann. Rev. Astron. Astrophys. 1988. 26: 509–60

THE LUMINOSITY FUNCTION OF GALAXIES

Bruno Binggeli

Astronomisches Institut der Universität Basel, Venusstrasse 7,
CH-4102 Binningen, Switzerland and Osservatorio Astrofisico di Arcetri,
Largo Enrico Fermi 5, I-50125 Firenze, Italy

Allan Sandage

Mount Wilson and Las Campanas Observatories, Carnegie Institution
of Washington, 813 Santa Barbara Street, Pasadena, California 91101

G. A. Tammann

Astronomisches Institut der Universität Basel, Venusstrasse 7,
CH-4102 Binningen, Switzerland and European Southern Observatory,
Karl-Schwarzschild-Strasse 2, D-8046 Garching, West Germany

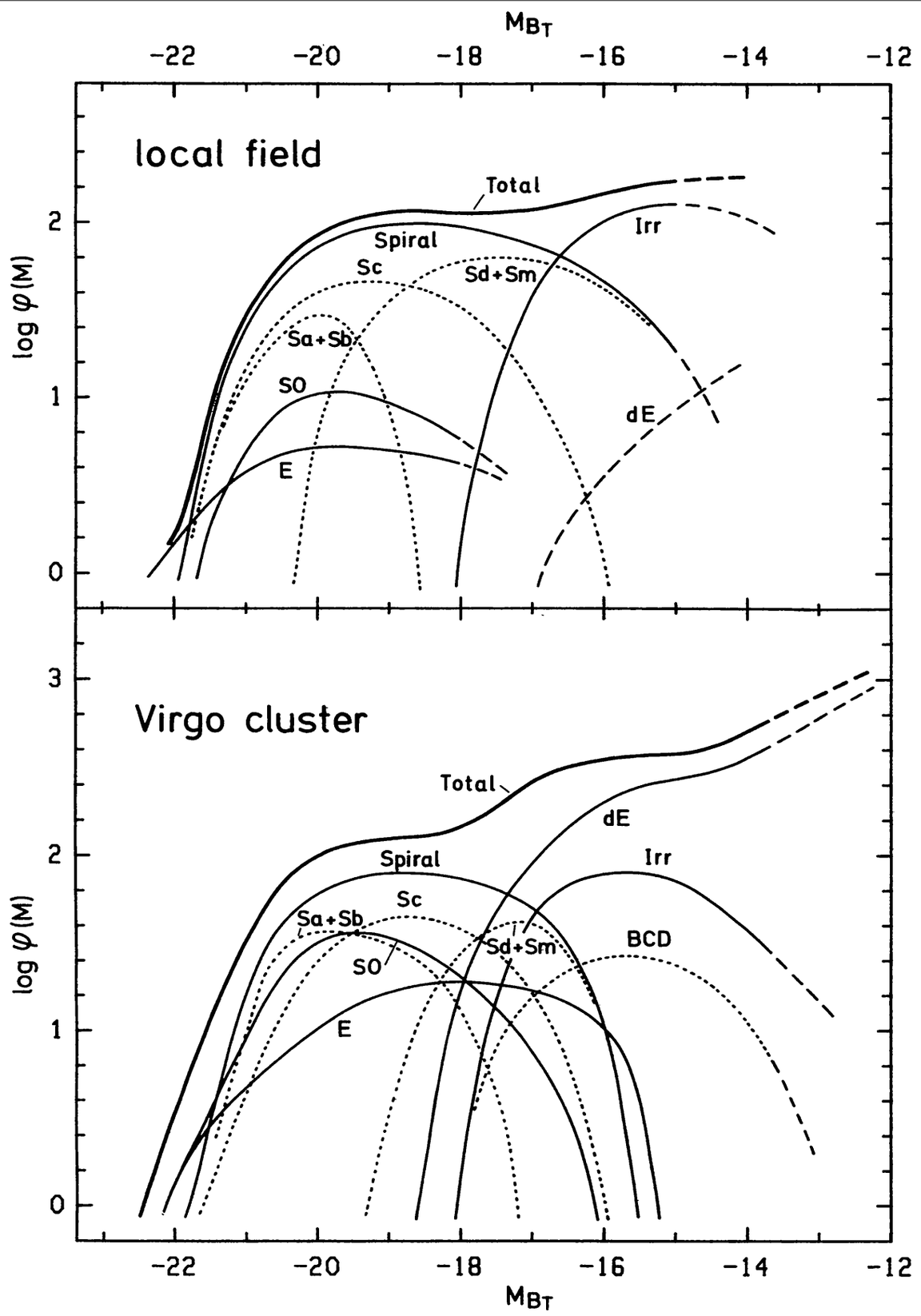

Figure 1 The LF of field galaxies (top) and Virgo cluster members (bottom). The zero point of $\log \varphi(M)$ is arbitrary. The LFs for individual galaxy types are shown. Extrapolations are marked by dashed lines. In addition to the LF of all spirals, the LFs of the subtypes Sa + Sb, Sc, and Sd + Sm are also shown as dotted curves. The LF of Irr galaxies comprises the Im and BCD galaxies; in the case of the Virgo cluster, the BCDs are also shown separately. The classes dS0 and "dE or Im" are not illustrated. They are, however, included in the total LF over all types (heavy line).

The HT-dependent shape of the LF is Gaussian for luminous galaxies.

The shape of the LF for a given Hubble Type is constant with environment

However, the MIX of different Hubble Types changes as a function of environment. More ellipticals in high-density regions.

THE ASTROPHYSICAL JOURNAL, 236:351–365, 1980 March 1

GALAXY MORPHOLOGY IN RICH CLUSTERS: IMPLICATIONS FOR THE FORMATION AND EVOLUTION OF GALAXIES

ALAN DRESSLER
Hale Observatory,[1] Carnegie Institution of Washington
Received 1979 June 8; accepted 1979 September 14

ABSTRACT

A study of the galaxy populations in 55 rich clusters is presented together with a discussion of the implications for the formation and/or evolution of different morphological types. A well-defined relationship is found between local galaxy density and galaxy type, which, in agreement with previous studies, indicates an increasing elliptical and S0 population and a corresponding decrease in spirals with increasing density.

Three lines of evidence are presented which contradict the interpretation that these gradients in population result from the production of S0 galaxies when spirals are swept of their disk gas by an IGM. (1) The relation between density and morphological type is a very slow function of density, so that a significant percentage of S0 galaxies exists in regions where gas density and temperature are too low to effect removal of the gas from spirals by evaporation or ram pressure stripping. (2) The relation between density and morphological type is virtually identical in irregular clusters of low concentration which are presumably not yet relaxed, and regular, high concentration clusters which are thought to be relaxed, despite the expectation that S0 production by gas ablation from spirals should only be important in the latter. (3) The bulges and bulge/disk ratios of S0 galaxies are systematically larger than those of spiral galaxies in all density regimes. Since the tightly bound inner bulges should be unaffected by ablation, the dissimilarity in the bulge and bulge/disk distributions in all density regimes is inconsistent with the idea that most S0 galaxies result from the removal of disk gas from a spiral by ram pressure stripping or evaporation.

As an alternative to the hypothesis of spiral sweeping, it is suggested that the local density/morphological-type relation reflects the long time scale associated with the formation of the disk component of galaxies. If this time scale is comparable to or greater than several billion years, an increase in local galaxy density may slow or even halt the growth of the disk components. This could generally account for the large number of elliptical galaxies in very high density regions and the prevalence of spiral galaxies at very low densities.

The data also indicate a trend of increasing luminosity of the spheroidal component with increasing local density. This may be interpreted as evidence for: (1) relatively late formation of galaxies, (2) mergers, (3) a formation mechanism that is highly sensitive to density, or (4) phase coupling between the high-frequency (galaxy) and low frequency (cluster) perturbations in the early universe.

55 rich clusters with z<0.06

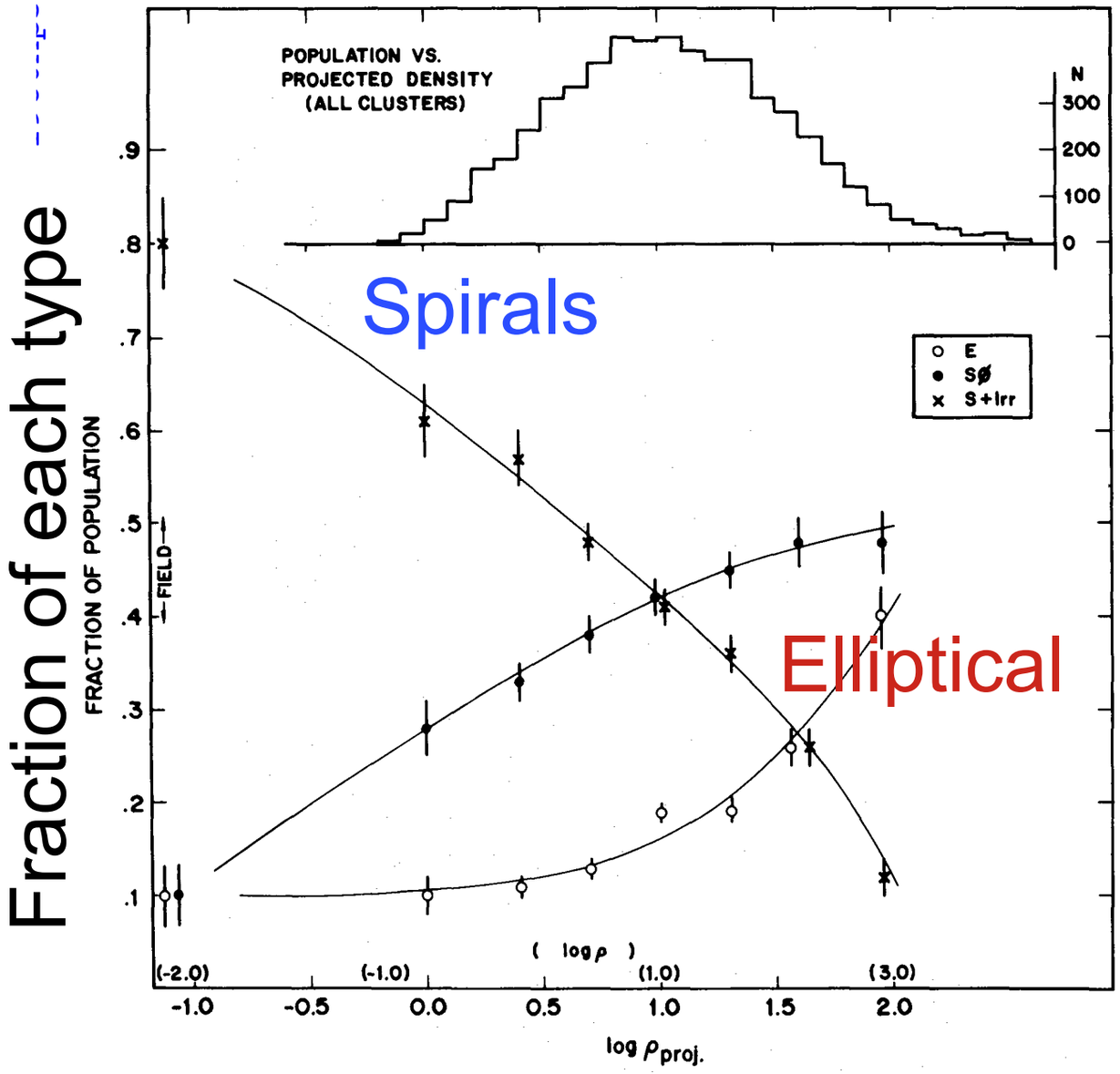

FIG. 4.—The fraction of E, S0, and S+I galaxies as a function of the log of the projected density, in galaxies Mpc^{-2}. The data shown are for all cluster galaxies in the sample and for the field. Also shown is an estimated scale of true space density in galaxies Mpc^{-3}. The upper histogram shows the number distribution of the galaxies over the bins of projected density.

Number of nearby galaxies

Morphology-density relation: Elliptical fraction is strong function of local galaxy density (e.g., projected number of neighbors).

What physical mechanisms drive these trends?

- ram-pressure stripping within the cluster
- tidal stripping
- galaxy-galaxy harrassment in the rich environment.
- Or pre-processing in group environments?

There is a well-defined relationship between the local density of galaxies in a region of space and the representation of different morphological types. This relationship extends from the low-density field to the dense cores of clusters, some five orders of magnitude in space density. This, combined with the existence of S0 galaxies in substantial numbers in regions where the gas density and temperature are presumably too low to effect the ram pressure stripping or evaporation of gas from spirals, argues that most S0 galaxies are not created by such processes. The similarly of the

Stellar Population Synthesis Modeling

Remember the stellar mass functions from Richard's talk? How do we measure them?

Here is the basic idea. For a given **single-age** stellar population (SSP) we can model the luminous output of the entire stellar population as a function of time using models of stellar evolution.

If we assume we know the **initial mass function (IMF):** the number of stars of a given mass formed in a single burst of stars, then we can model the light from a population as a function of time by modeling the motion of stars through Luminosity-Temperature space (the HR diagram).

Then, to model a generic stellar population, we just need to add up the light from each SSP. The modeling tells us how much stellar **mass** there is, rather than just light. Provided we know the IMF, the dust reddening, and trust our models of stellar evolution...

The Hertzprung-Russel Diagram

Recall that observation HR diagram (or color-magnitude diagram) is measured in color and magnitude, while underlying physics is driven by luminosity and temperature.

Stars evolve through the HR diagram as they complete core H burning, expand, recontract, ignite He burning, etc.

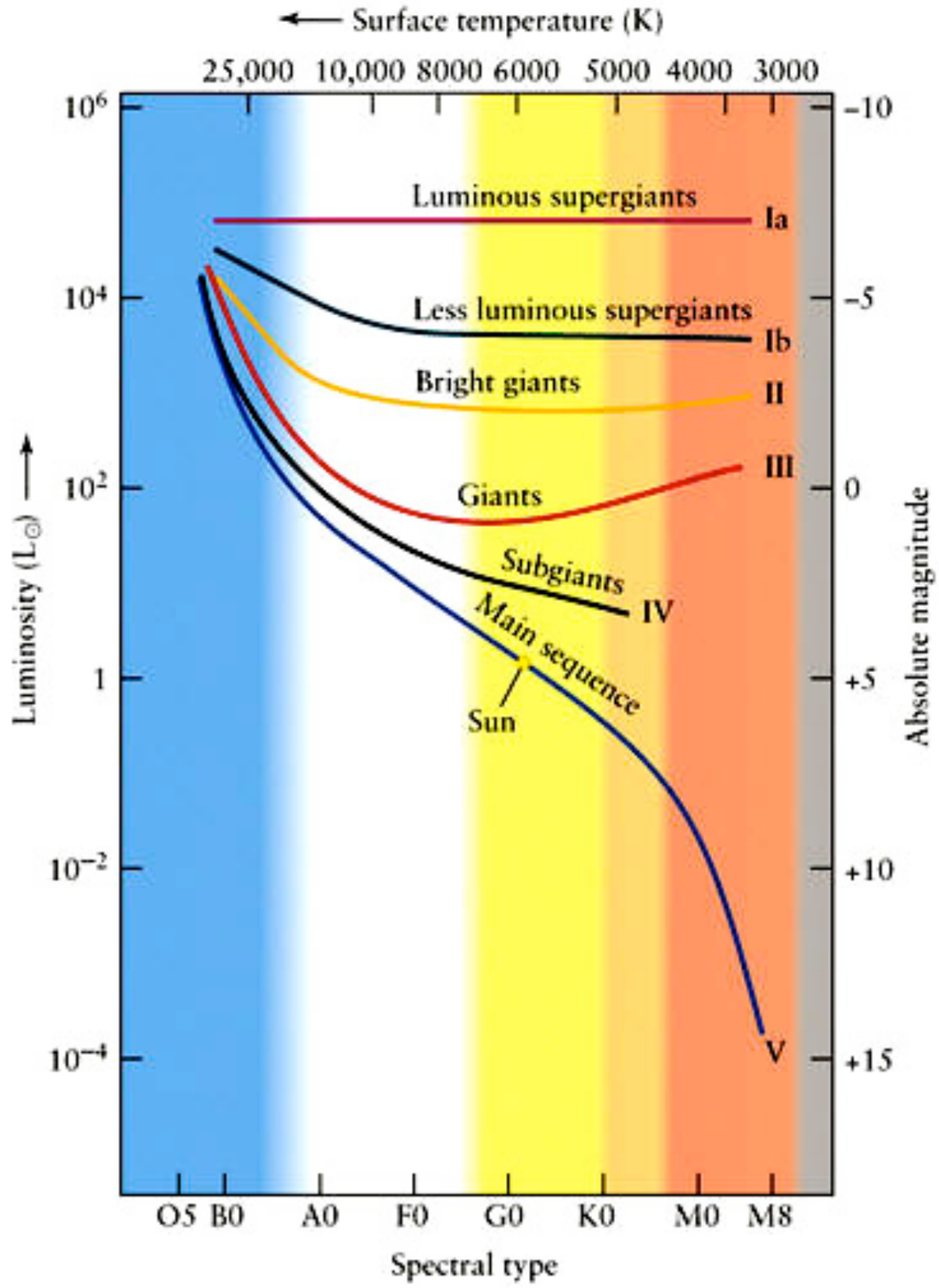

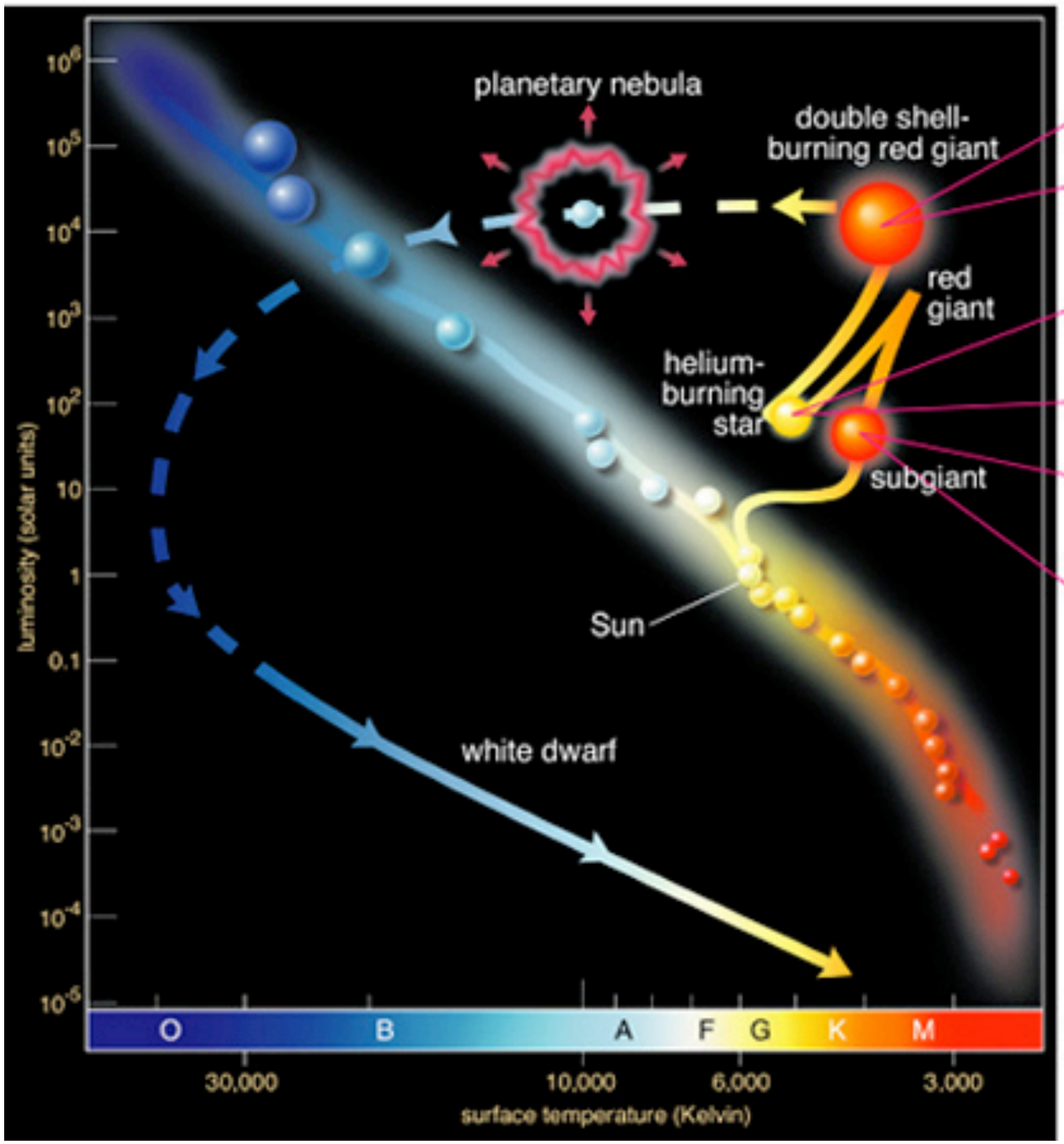
planetary nebula
double shell-
burning red giant
red
giant
helium-
burning
star
subgiant
Sun
white dwarf
luminosity (solar units)
10^6
10^5
10^4
10^3
10^2
10
1
0.1
10^{-2}
10^{-3}
10^{-4}
10^{-5}
O
B
A
F
G
K
M
30,000
10,000
6,000
3,000
surface temperature (Kelvin)

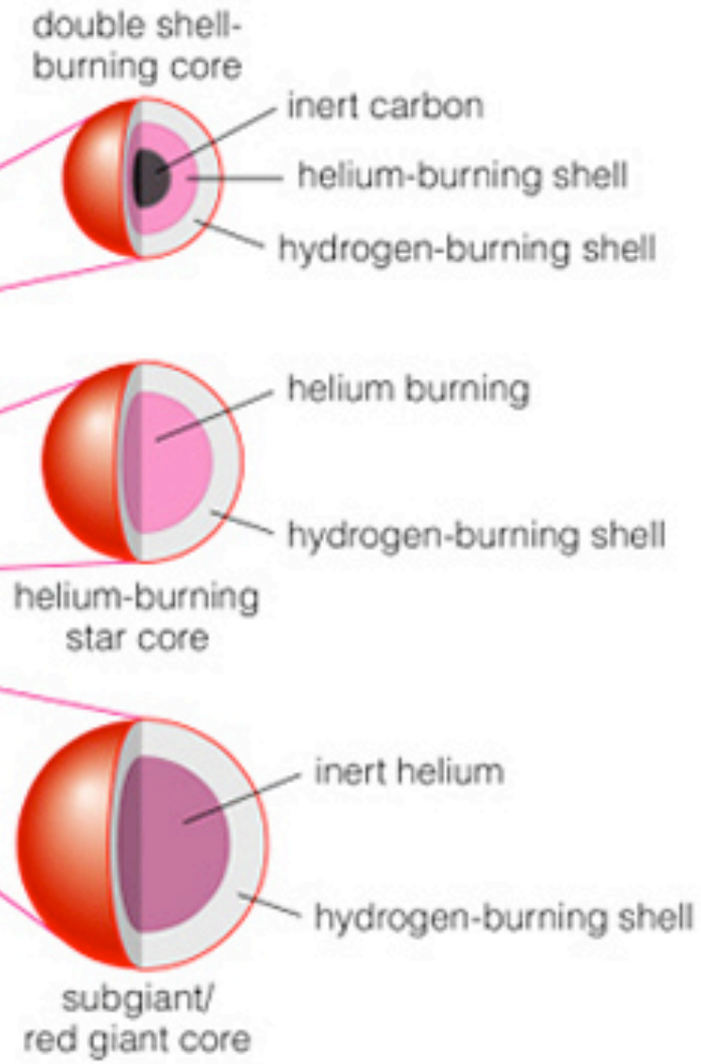
double shell-
burning core
inert carbon
helium-burning shell
hydrogen-burning shell
helium burning
hydrogen-burning shell
helium-burning
star core
inert helium
hydrogen-burning shell
subgiant/
red giant core

$M > 8\ M_\odot$ Stellar Evolution: Massive Stars

Proceeds similarly except that:

1. MS lifetimes are MUCH shorter.

The luminosity doesn't really change much in later stages of evolution.

2. Instead of stopping with He ignition, the star is able to burn elements all the way up until Fe. At which point there is a supernova.

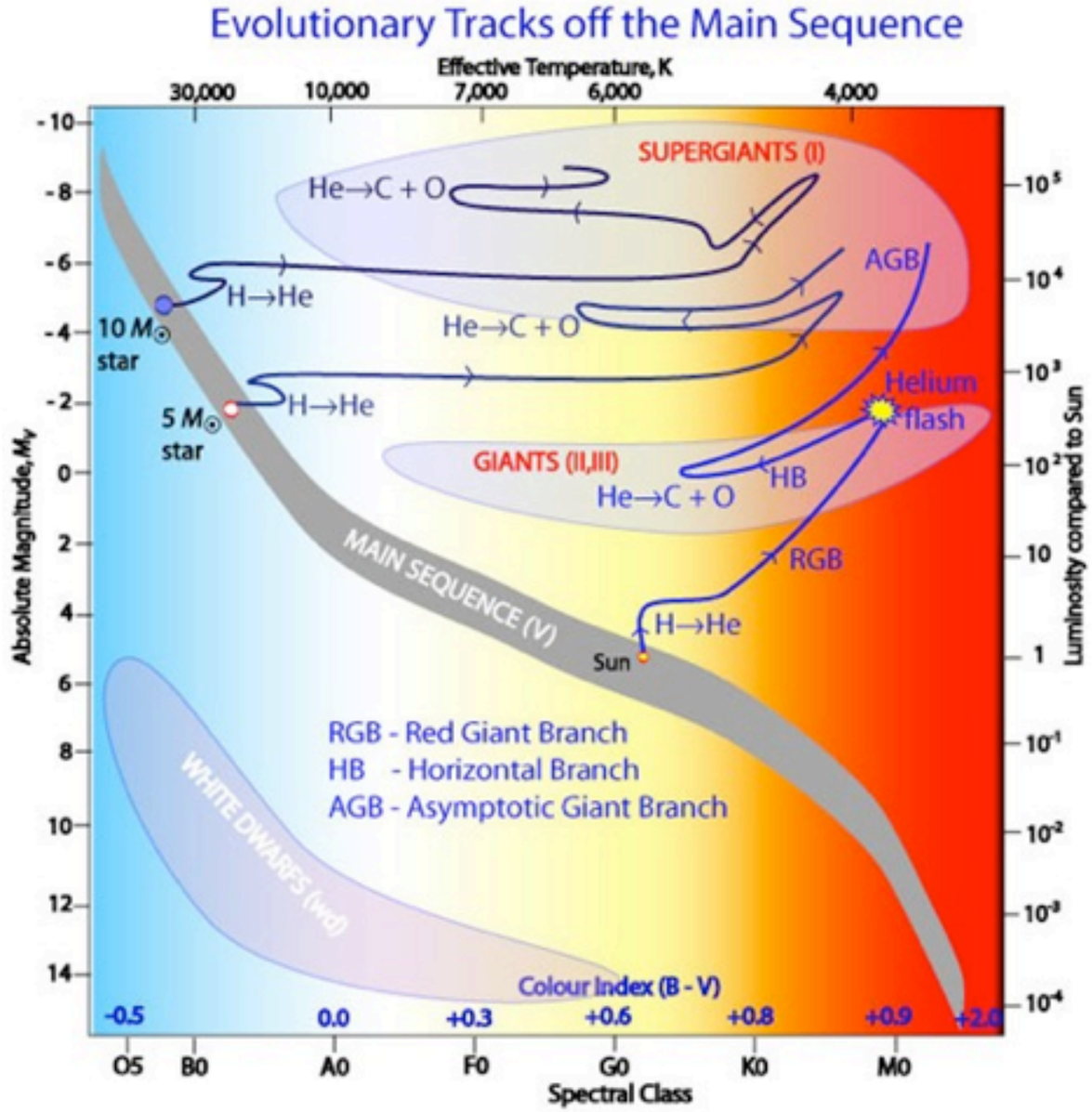

Also note that more massive stars evolve off the MS much faster than low-mass stars.

time(MS) ~ $10\ M/M_\odot\ (L/L_\odot)^{-1}$
Table 5.2 in BM shows time spent in different phases.

Isochrones

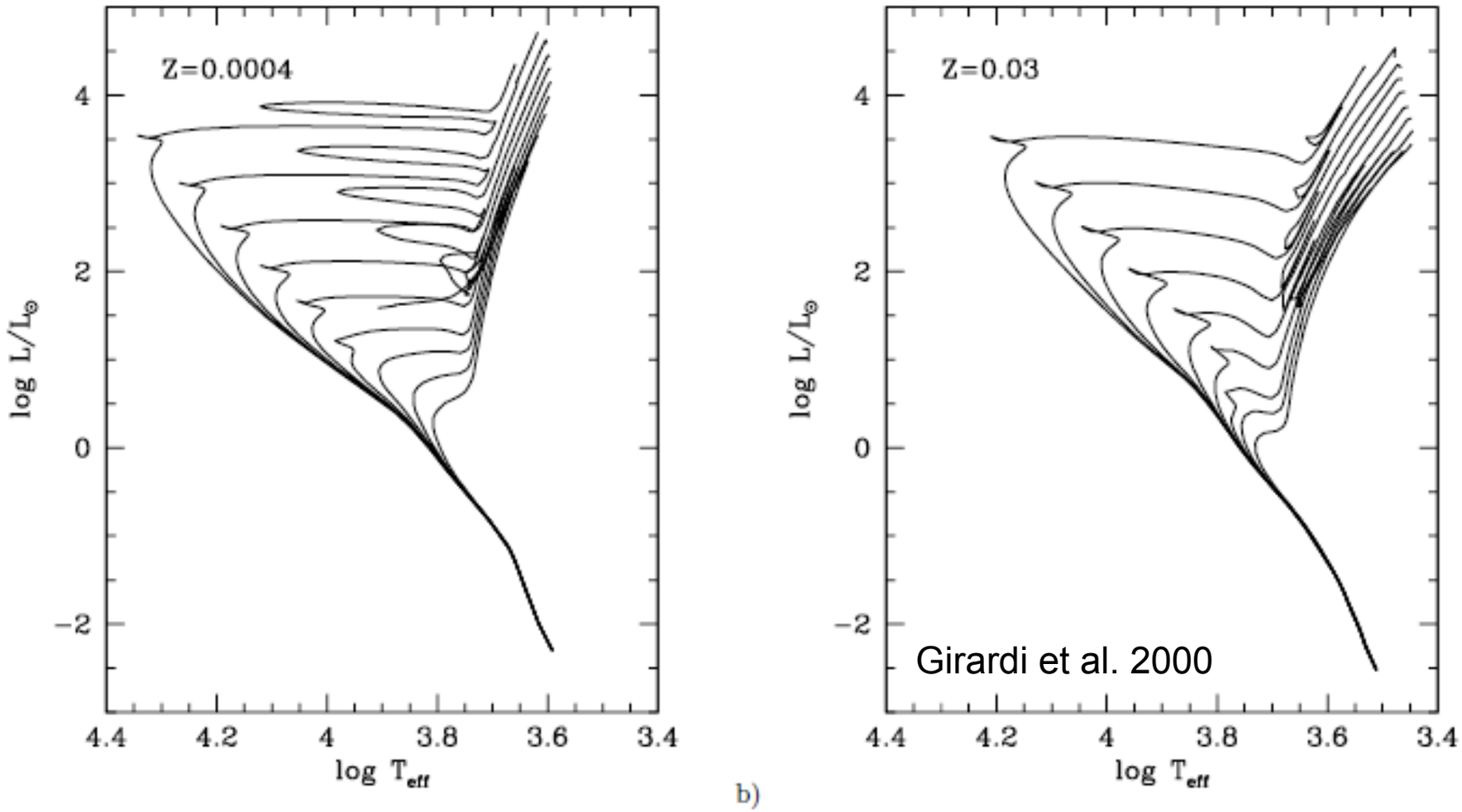

Fig. 5. Theoretical isochrones in the HR diagram, for the compositions $[Z = 0.0004, Y = 0.230]$ (panel a), and $[Z = 0.030, Y = 0.300]$ (panel b). The age range goes from $\log(t/\mathrm{yr}) = 7.8$ to 10.2, at equally spaced intervals of $\Delta \log t = 0.3$. In both cases, the main sequence is complete down to 0.15 $M_\odot$

Here are example theoretical isochrones (same time) as a function of metallicity that allow us to synthesize the evolution of stellar populations.

CMD / stellar evolution depends on metallicity

At lower metallicity, individual stars are brighter and hotter at fixed mass.

Location of MS also is affected (shifted to the left).

1955ApJ...121..161S

THE LUMINOSITY FUNCTION AND STELLAR EVOLUTION

EDWIN E. SALPETER*
Australian National University, Canberra, and Cornell University
Received July 29, 1954

ABSTRACT

The evolutionary significance of the observed luminosity function for main-sequence stars in the solar neighborhood is discussed. The hypothesis is made that stars move off the main sequence after burning about 10 per cent of their hydrogen mass and that stars have been created at a uniform rate in the solar neighborhood for the last five billion years.

Using this hypothesis and the observed luminosity function, the rate of star creation as a function of stellar mass is calculated. The total number and mass of stars which have moved off the main sequence is found to be comparable with the total number of white dwarfs and with the total mass of all fainter main-sequence stars, respectively.

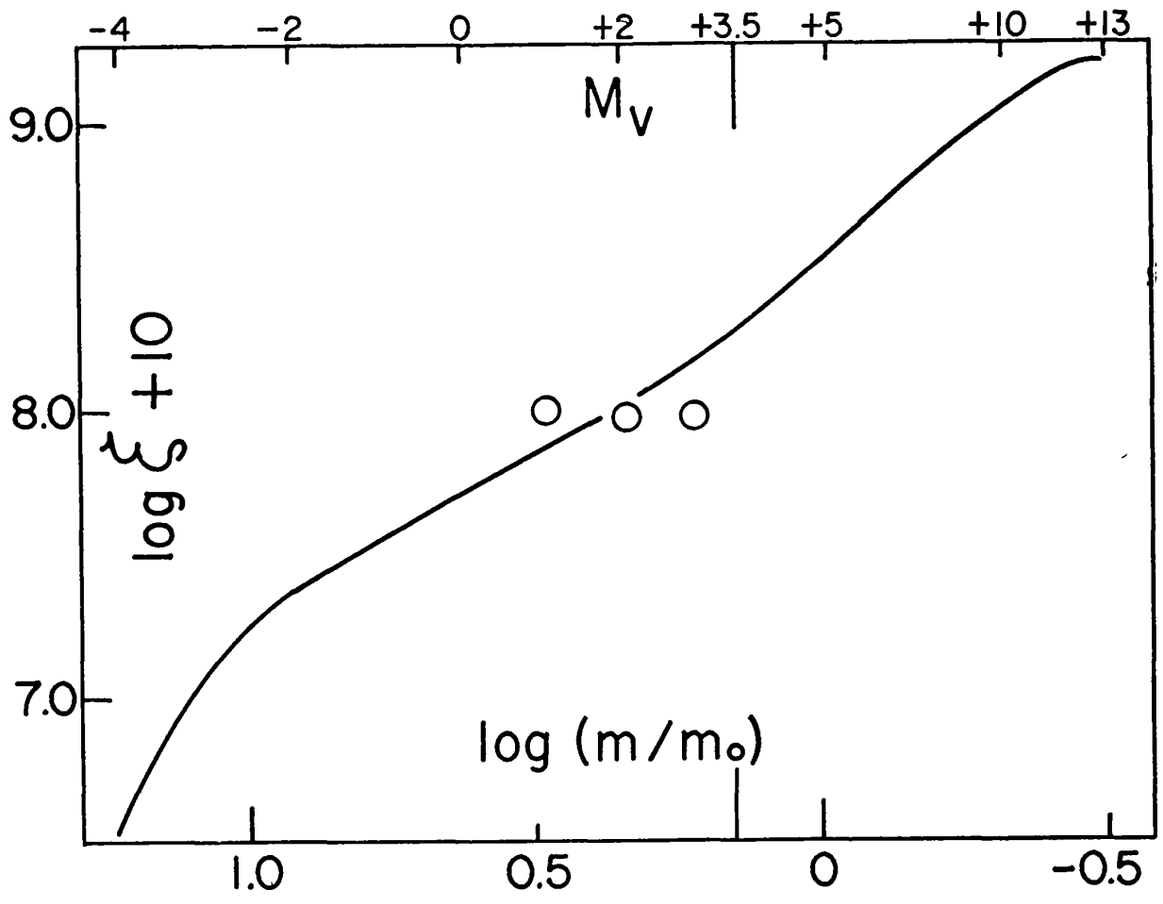

FIG. 2.—The logarithm of the "original mass function," ξ, plotted against the mass, $\mathfrak{M}$, in solar units.

Stellar Population Synthesis

Start with a single burst of star formation: Single Stellar Population (SSP)

Then, to evolve this group of stars forward in time, you need to know:

(a) The Luminosity and Temp of each star as a function of mass and time (isochrones)

(b) The spectrum of each star as a function of L, T -- usually from an observed spectral library

(c) The relative number of stars of each mass (IMF).

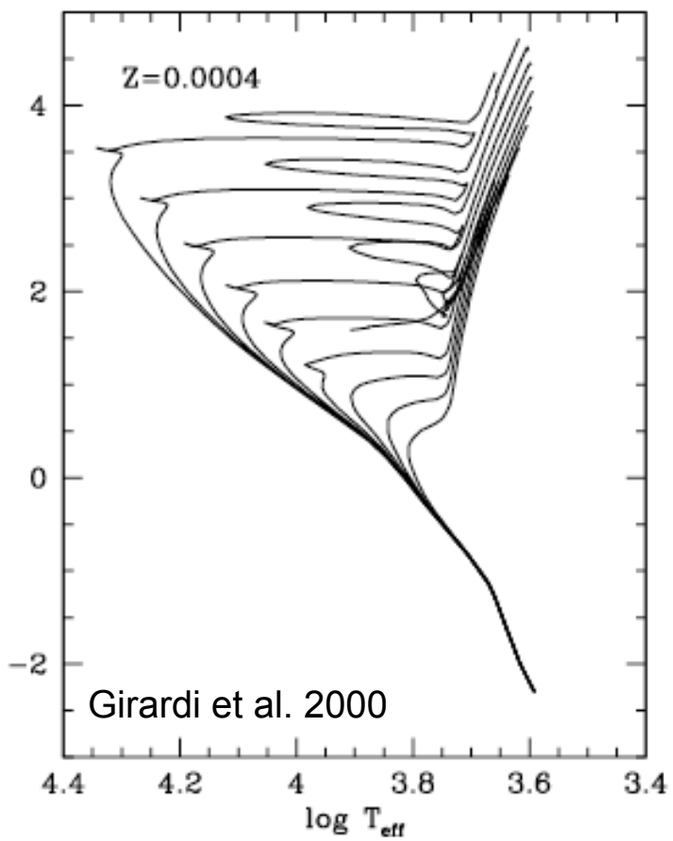

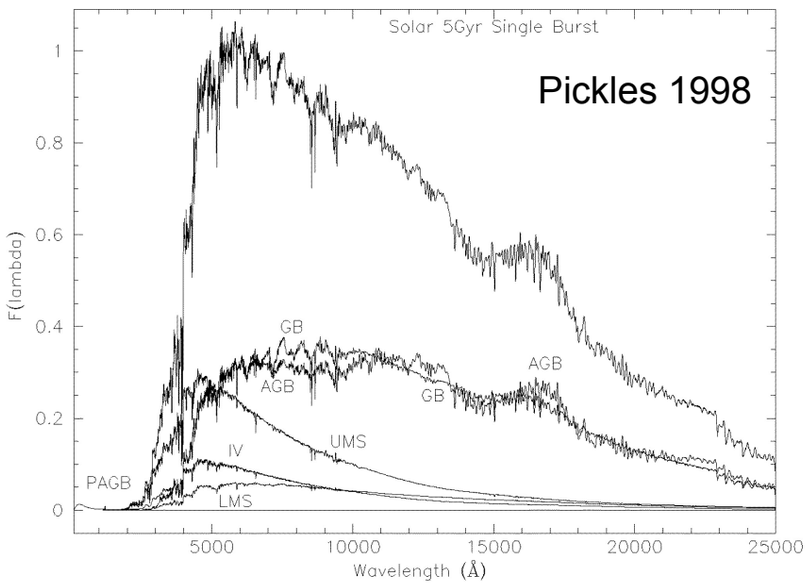

Fig. 8: Library spectra co-added in the ratios determined from the previous figure. Spectra are grouped into lower main sequence (LMS: KM dwarfs), upper main sequence (UMS: FG dwarfs), subgiant (IV), first giant branch (GB: K–M7 giants), second and third giant branches (AGB: K–M9 III), and post–asymptotic giant branch (PAGB), which is primarily contributed by an EP at log*Te = 4.29* and represented here by a combination of blackbody spectra. The top trace is the sum of the six components and represents the emergent spectrum of a single-burst stellar population of solar age and solar metallicity.

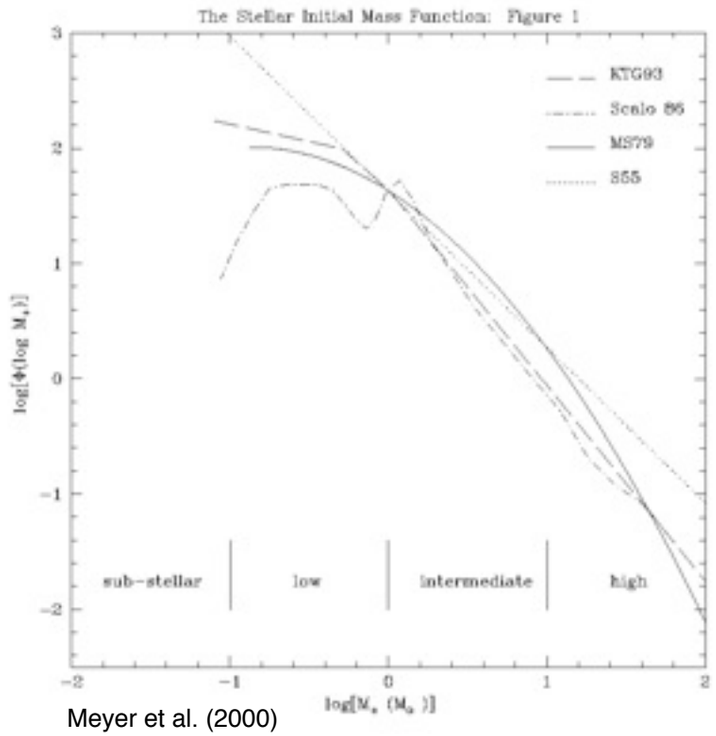

Meyer et al. (2000)

Simple Stellar Populations (SSPs)

Compute "isochrone" of age t, based on tracks in H-R diagram. Populate the regions of the H-R diagram according to the IMF. Use the stellar spectral library to assign spectra to stars in various evolutionary stages.

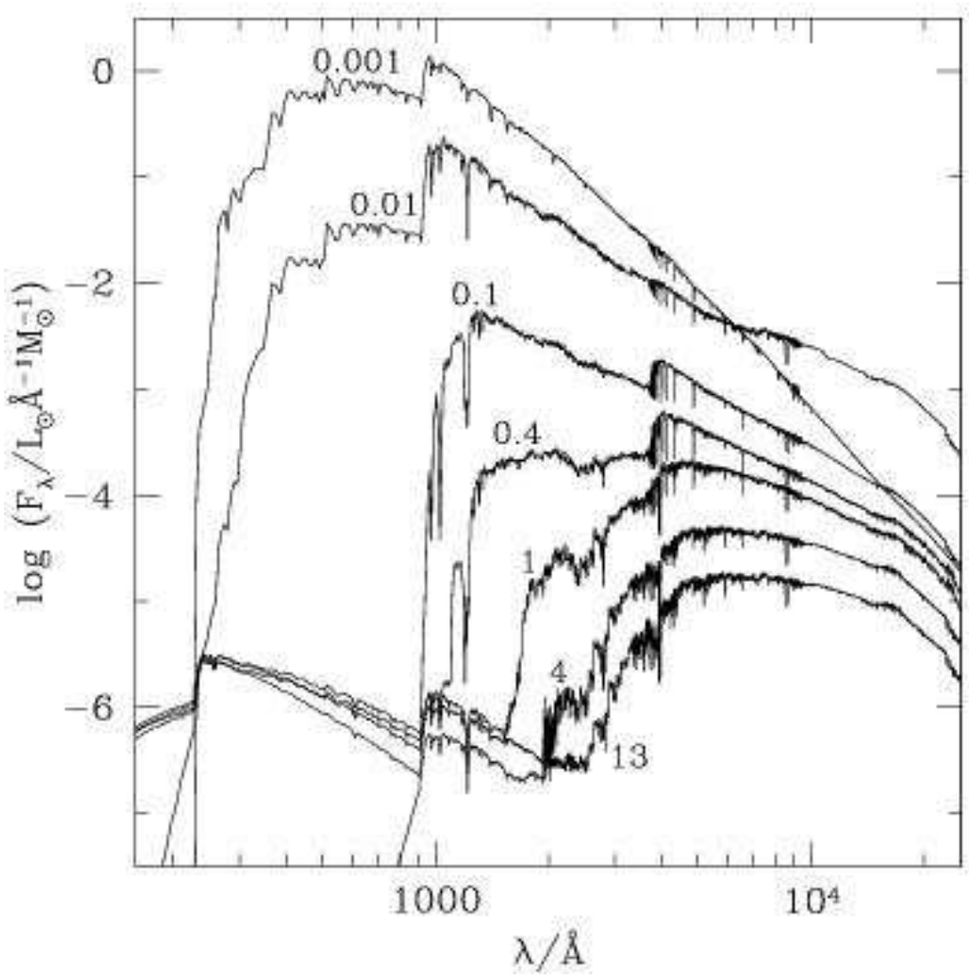

Figure 9. Spectral evolution of the standard SSP model of Section 3 for the solar metallicity. The STELIB/BaSeL 3.1 spectra have been extended blueward of 3200 Å and redward of 9500 Å using the Pickles medium-resolution library. Ages are indicated next to the spectra (in Gyr).

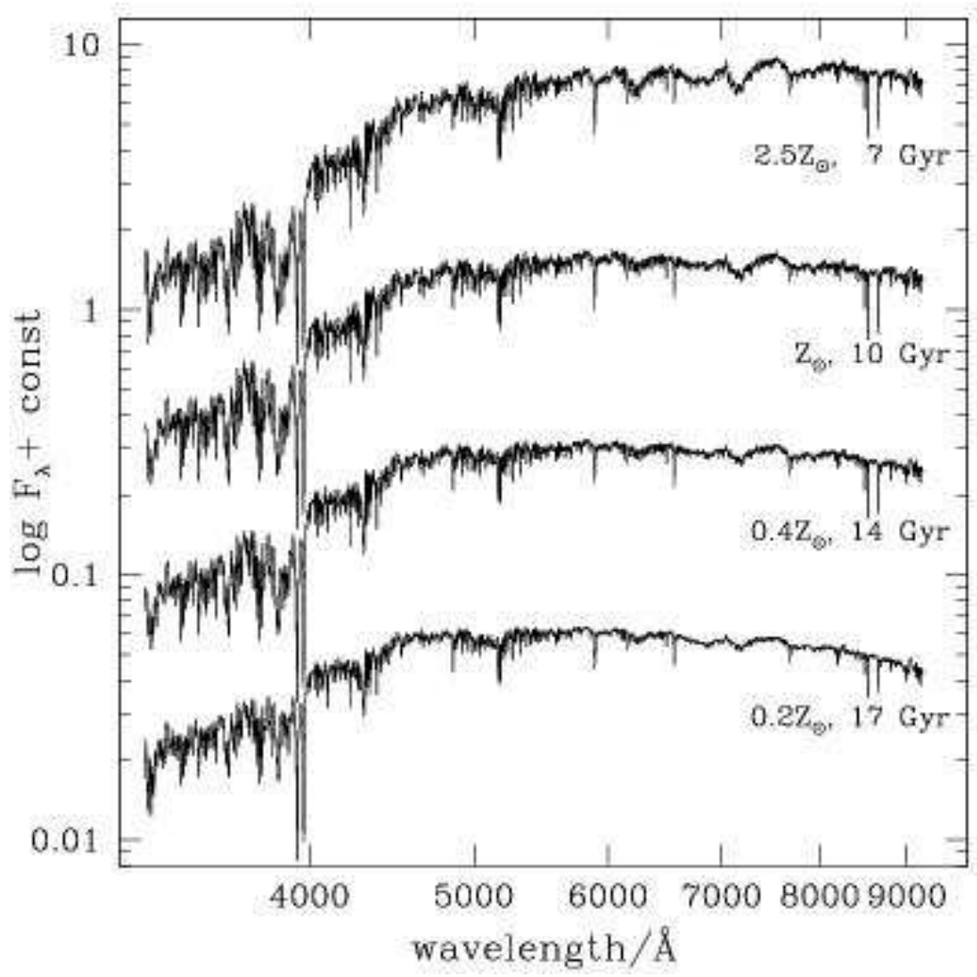

Figure 10. Spectra of the standard SSP model of Section 3 at different ages for different metallicities, as indicated. The prominent metallic features show a clear strengthening from the most metal-poor to the most metal-rich models, even though the shape of the spectral continuum is roughly similar in all models.

Bruzual & Charlot 2003

Stellar Population Synthesis

Once there are SSPs, a general stellar population follows with some parametrization of the star formation rate (and perhaps chemical enrichment) as a function of time.

$$F_\lambda(t) = \int_0^t \Psi(t-\tau) f_\lambda(\tau) d\tau \ ,$$

$\Psi(t)$: Star formation rate per unit time

$f_\lambda(t)$: light from an SSP of age t

Typically, a few forms are assumed for SFR $\Psi(t)$:

- Delta function (SSP)
- Constant
- Exponentially declining, with e-folding time τ. You often hear about “tau” models.

In practice, one must also assume dust extinction. It is common to assume that stars are completely extinguished at very young ages ($< 10^7$ yrs; Charlot & Fall 2000).

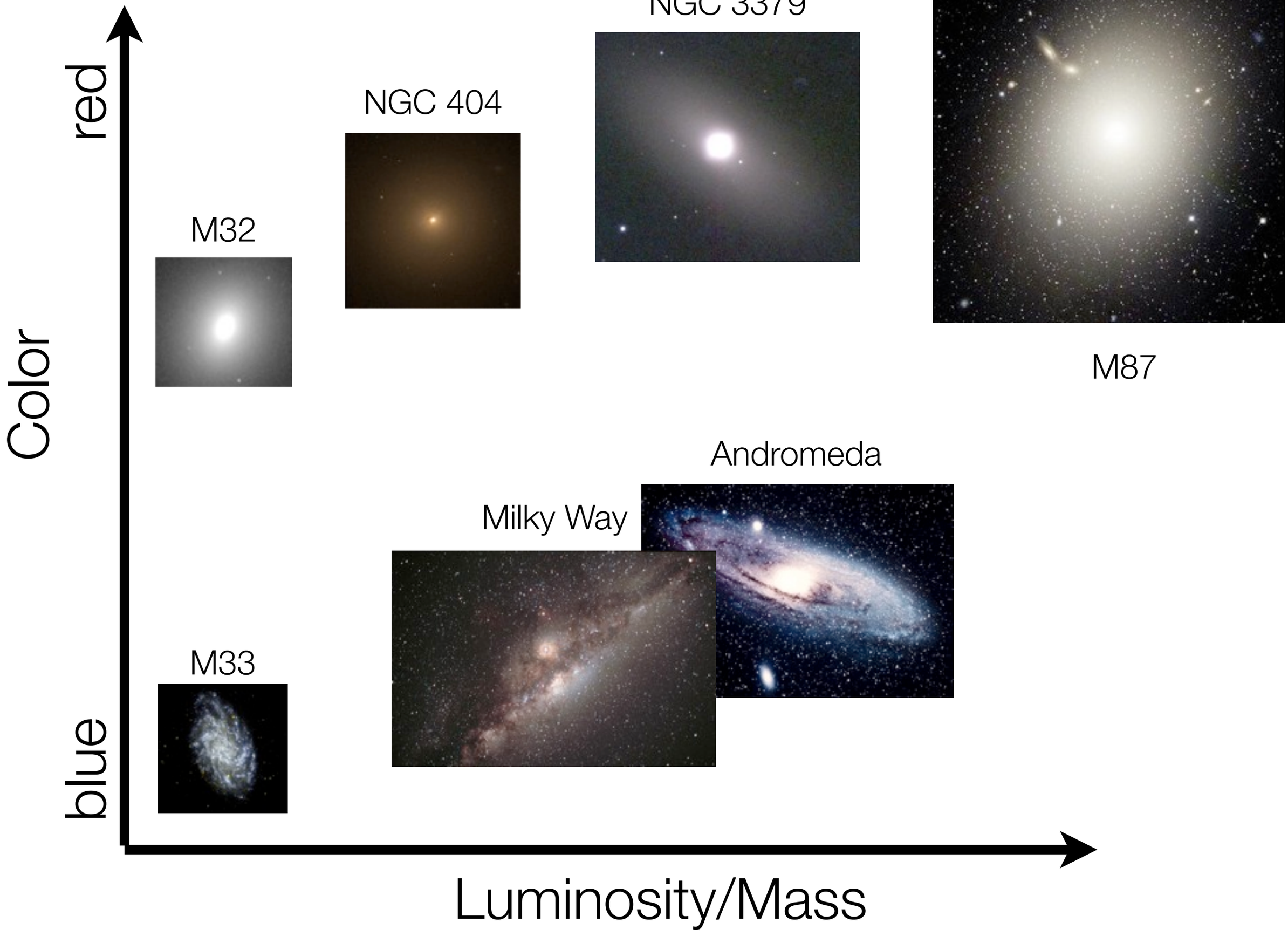
NGC 3379
NGC 404
M32
M87
red
Color
Andromeda
Milky Way
M33
blue
Luminosity/Mass

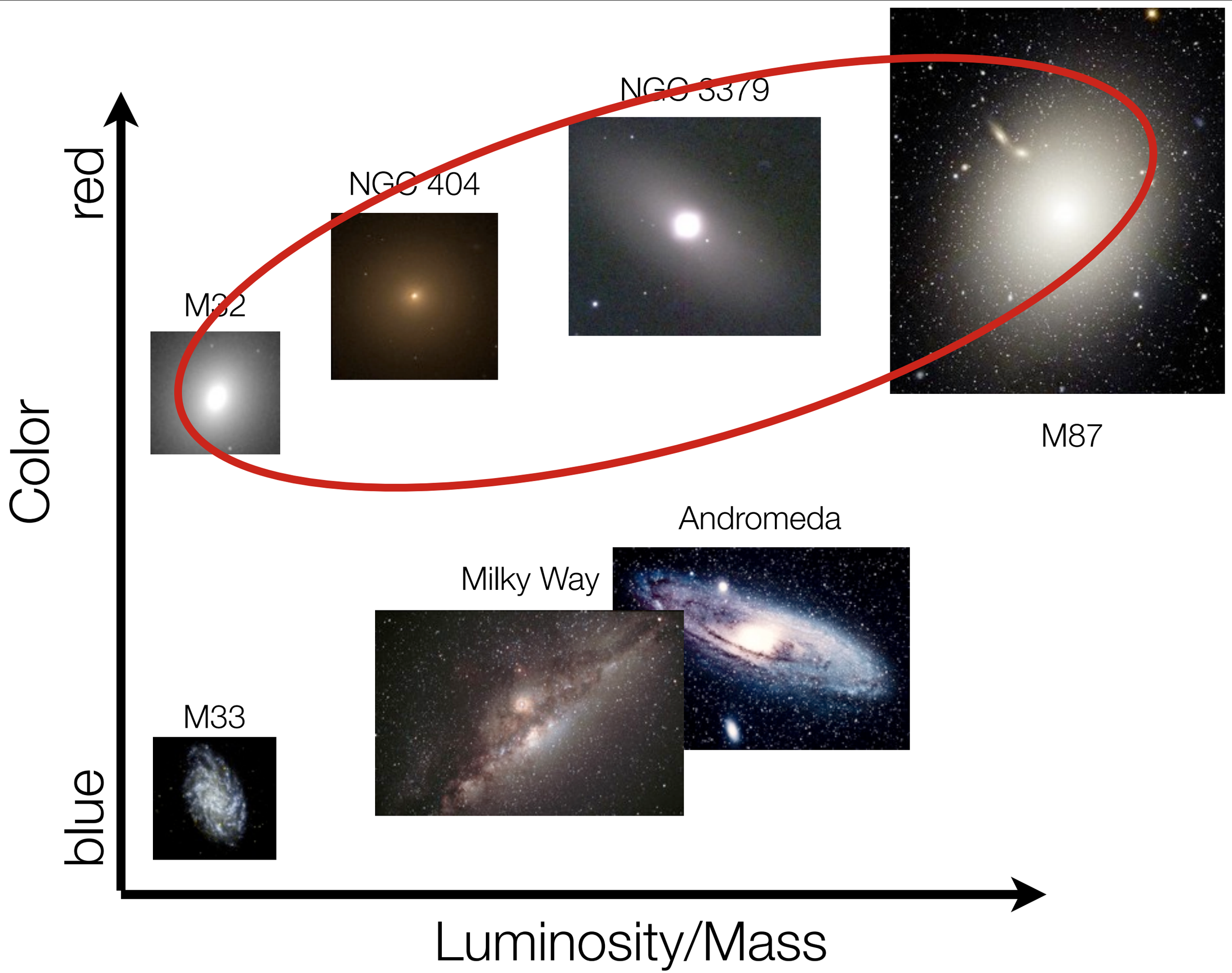
red
Color
blue
M32
NGC 404
NGC 3379
M87
Andromeda
Milky Way
M33
Luminosity/Mass

Brightness Profiles of Elliptical Galaxies

de Vaucouleurs and Capaccioli (1979) claimed that NGC 3379, like other ellipticals, is well described by a de Vaucouleurs law.

Brightness per unit area. Will see I and μ for this quantity

de Vaucouleurs 1948, Ann. d'Ap., 11, 247:

$$\log (I/I_e) = -3.3307127 \left[(r/r_e)^{1/4} - 1 \right]$$

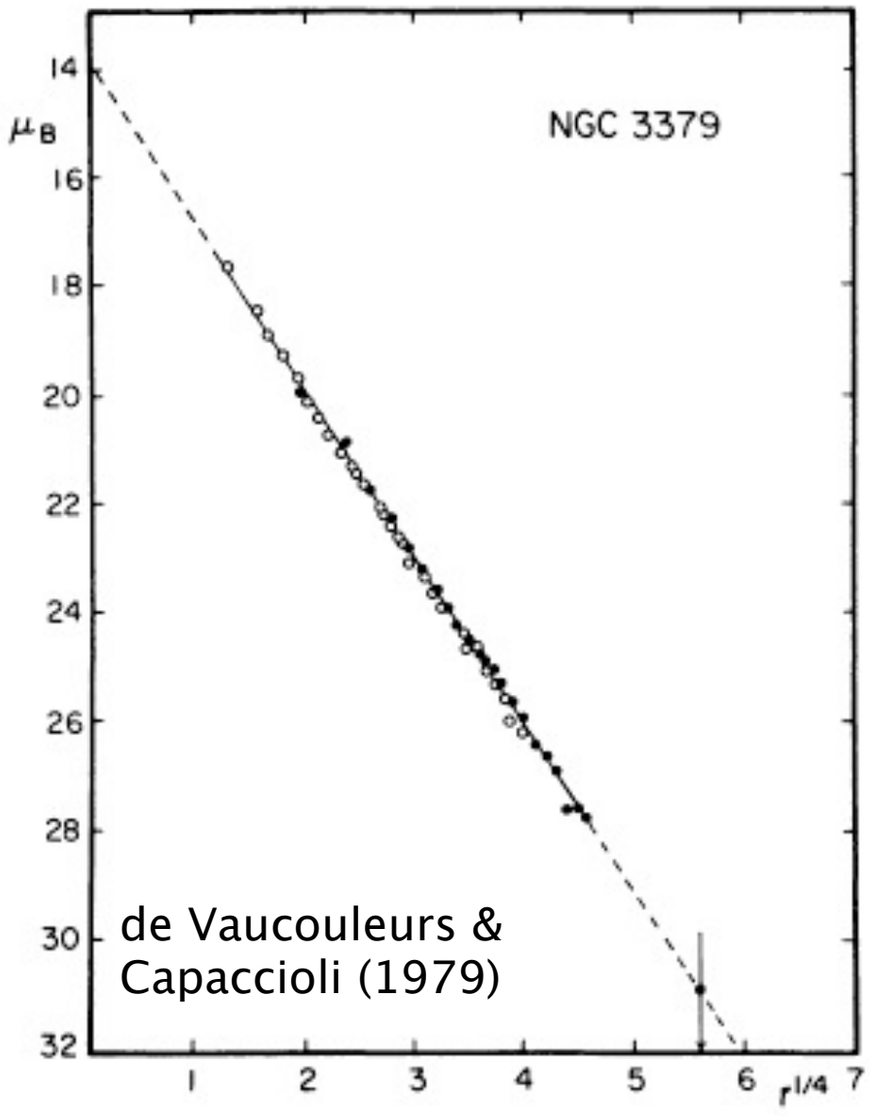

FIG. 2.—Mean E-W luminosity profile of NGC 3379 derived from McDonald photoelectric data. ●, Pe 4 data with 90 cm reflector; ○, Pe 1 data (M + P) with 2 m reflector. Note close agreement with $r^{1/4}$ law.

Ellipticals are not de Vaucouleurs (1948) $r^{1/4}$ laws – Profile shape correlates with luminosity.

Schombert (1986) template mean profiles for M_V = -18, …, -22.5:

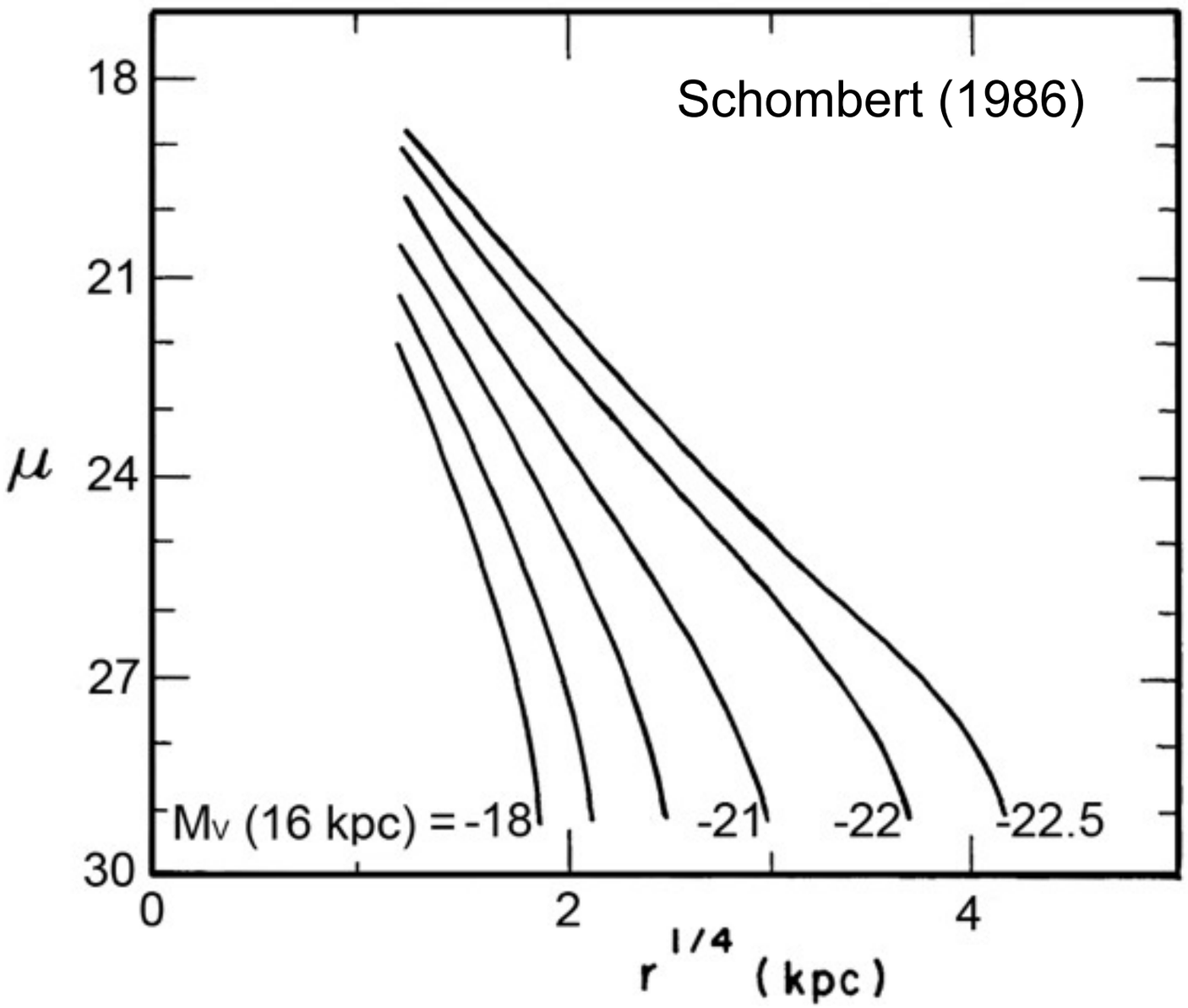

The Sérsic (1968) Function

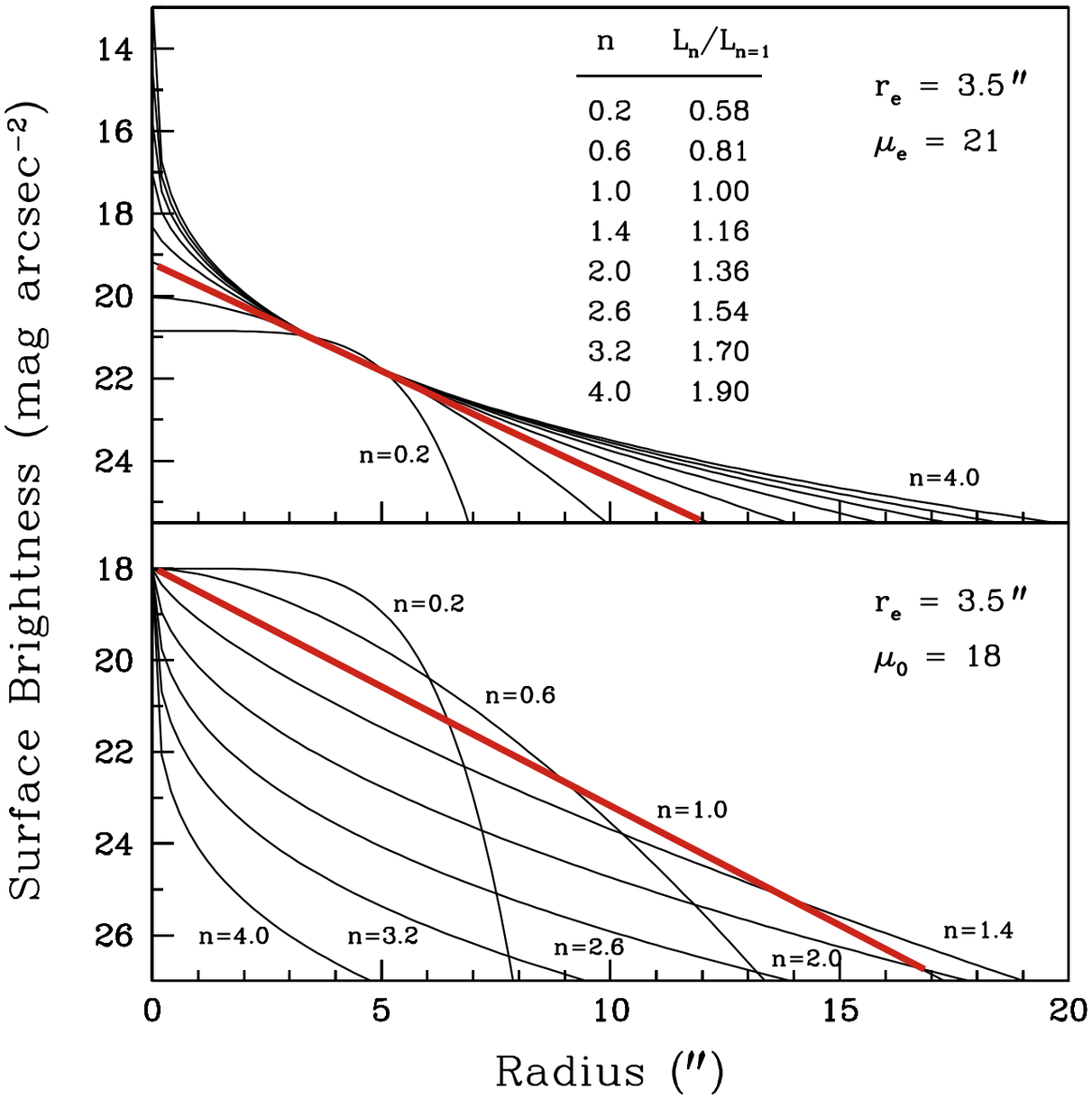

FIG. 2.—Sérsic n profiles for different values of n. The top panel shows profiles with $\mu_e = 21$ mag arcsec^{-2} and $r_e = 3\farcs5$ for values of n in the range $0.2 < n < 4$. The table lists the relative light contributions of the different profiles normalized to the $n = 1$ case. The bottom panel shows the same profiles except for a constant CSB of $\mu_0 = 18$ mag arcsec^{-2}.

$$\mu_{ser} = \mu_0 \exp\left[-\left(\frac{r}{r_0}\right)^{\frac{1}{n}}\right]$$

This figure (MacArthur et al. 2003) shows how the shape of the profile depends on the index n.

n=1 is highlighted in red for reference.

Note the large wings at high n.

Also note -- the x-axis in arcsec here.

The Astrophysical Journal Supplement Series, 182:216–309, 2009 May doi:10.1088/0067-0049/182/1/216

STRUCTURE AND FORMATION OF ELLIPTICAL AND SPHEROIDAL GALAXIES*,†,‡

John Kormendy[1,2,3], David B. Fisher[1,2,3], Mark E. Cornell[1], and Ralf Bender[1,2,3]
[1] Department of Astronomy, University of Texas, Austin, TX 78712, USA; kormendy@astro.as.utexas.edu, dbfisher@astro.as.utexas.edu, cornell@astro.as.utexas.edu
[2] Universitäts-Sternwarte, Scheinerstrasse 1, München D-81679, Germany; bender@usm.uni-muenchen.de
[3] Max-Planck-Institut für Extraterrestrische Physik, Giessenbachstrasse, D-85748 Garching-bei-München, Germany; bender@mpe.mpg.de
Received 2006 September 2; accepted 2008 October 7; published 2009 April 30

ABSTRACT

New surface photometry of all known elliptical galaxies in the Virgo cluster is combined with published data to derive composite profiles of brightness, ellipticity, position angle, isophote shape, and color over large radius ranges. These provide enough leverage to show that Sérsic $\log I \propto r^{1/n}$ functions fit the brightness profiles $I(r)$ of nearly all ellipticals remarkably well over large dynamic ranges. Therefore, we can confidently identify departures from these profiles that are diagnostic of galaxy formation. Two kinds of departures are seen at small radii. All 10 of our ellipticals with total absolute magnitudes $M_{VT} \leqslant -21.66$ have cuspy cores—"missing light"—at small radii. Cores are well known and naturally scoured by binary black holes (BHs) formed in dissipationless ("dry") mergers. All 17 ellipticals with $-21.54 \leqslant M_{VT} \leqslant -15.53$ do not have cores. We find a new distinct component in these galaxies: all coreless ellipticals in our sample have extra light at the center above the inward extrapolation of the outer Sérsic profile. In large ellipticals, the excess light is spatially resolved and resembles the central components predicted in numerical simulations of mergers of galaxies that contain gas. In the simulations, the gas dissipates, falls toward the center, undergoes a starburst, and builds a compact stellar component that, as in our observations, is distinct from the Sérsic-function main body of the elliptical. But ellipticals with extra light also contain supermassive BHs. We suggest that the starburst has swamped core scouring by binary BHs. That is, we interpret extra light components as a signature of formation in dissipative ("wet") mergers.

Besides extra light, we find three new aspects to the ("E–E") dichotomy into two types of elliptical galaxies. Core galaxies are known to be slowly rotating, to have relatively anisotropic velocity distributions, and to have boxy isophotes. We show that they have Sérsic indices $n > 4$ uncorrelated with M_{VT}. They also are α-element enhanced, implying short star-formation timescales. And their stellar populations have a variety of ages but mostly are very old. Extra light ellipticals generally rotate rapidly, are more isotropic than core Es, and have disky isophotes. We show that they have $n \simeq 3 \pm 1$ almost uncorrelated with M_{VT} and younger and less α-enhanced stellar populations. These are new clues to galaxy formation. We suggest that extra light ellipticals got their low Sérsic indices by forming in relatively few binary mergers, whereas giant ellipticals have $n > 4$ because they formed in larger numbers of mergers of more galaxies at once plus later heating during hierarchical clustering.

We confirm that core Es contain X-ray-emitting gas whereas extra light Es generally do not. This leads us to suggest why the E–E dichotomy arose. If energy feedback from active galactic nuclei (AGNs) requires a "working surface" of hot gas, then this is present in core galaxies but absent in extra light galaxies. We suggest that AGN energy feedback is a strong function of galaxy mass: it is weak enough in small Es not to prevent merger starbursts but strong enough in giant Es and their progenitors to make dry mergers dry and to protect old stellar populations from late star formation.

Finally, we verify that there is a strong dichotomy between elliptical and spheroidal galaxies. Their properties are consistent with our understanding of their different formation processes: mergers for ellipticals and conversion of late-type galaxies into spheroidals by environmental effects and by energy feedback from supernovae.

In an appendix, we develop machinery to get realistic error estimates for Sérsic parameters even when they are strongly coupled. And we discuss photometric dynamic ranges necessary to get robust results from Sérsic fits.

n increases with L

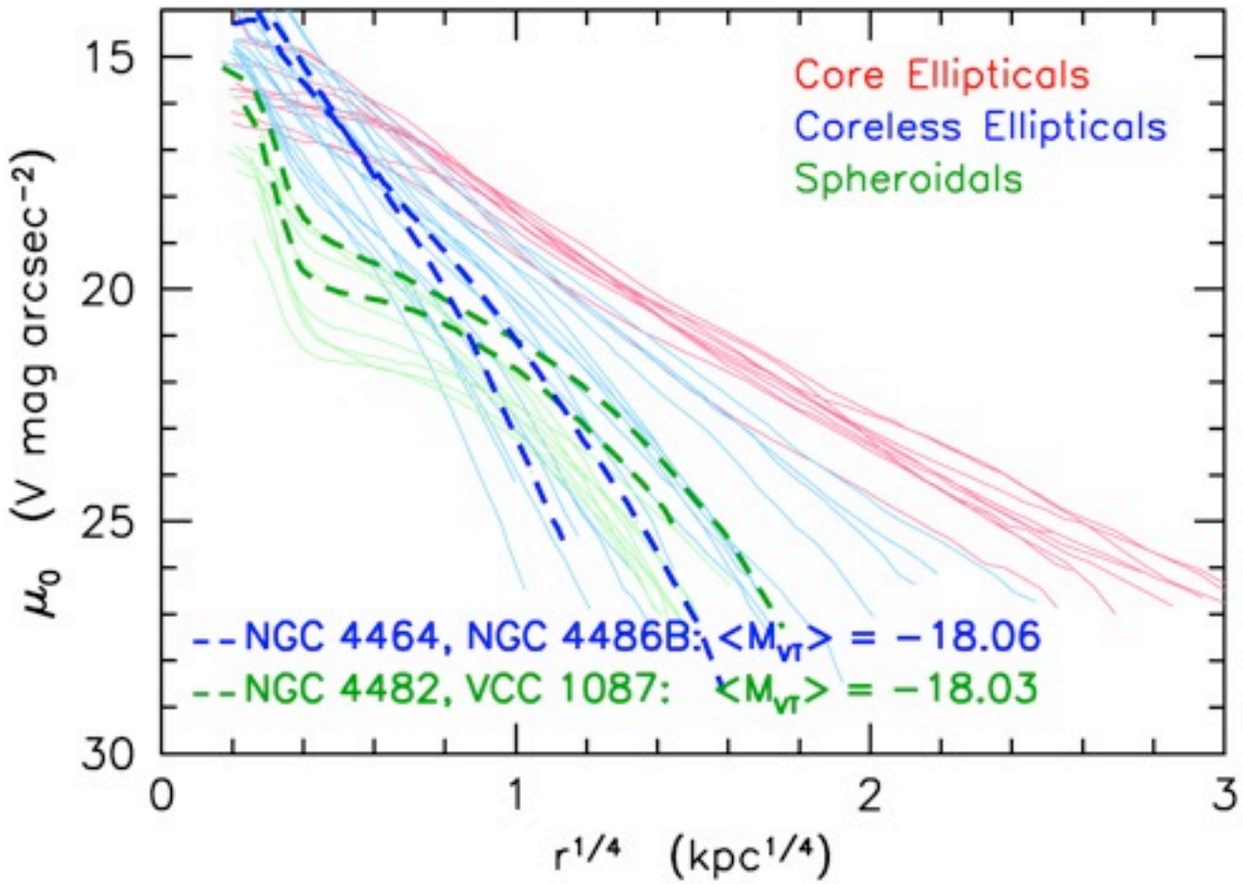

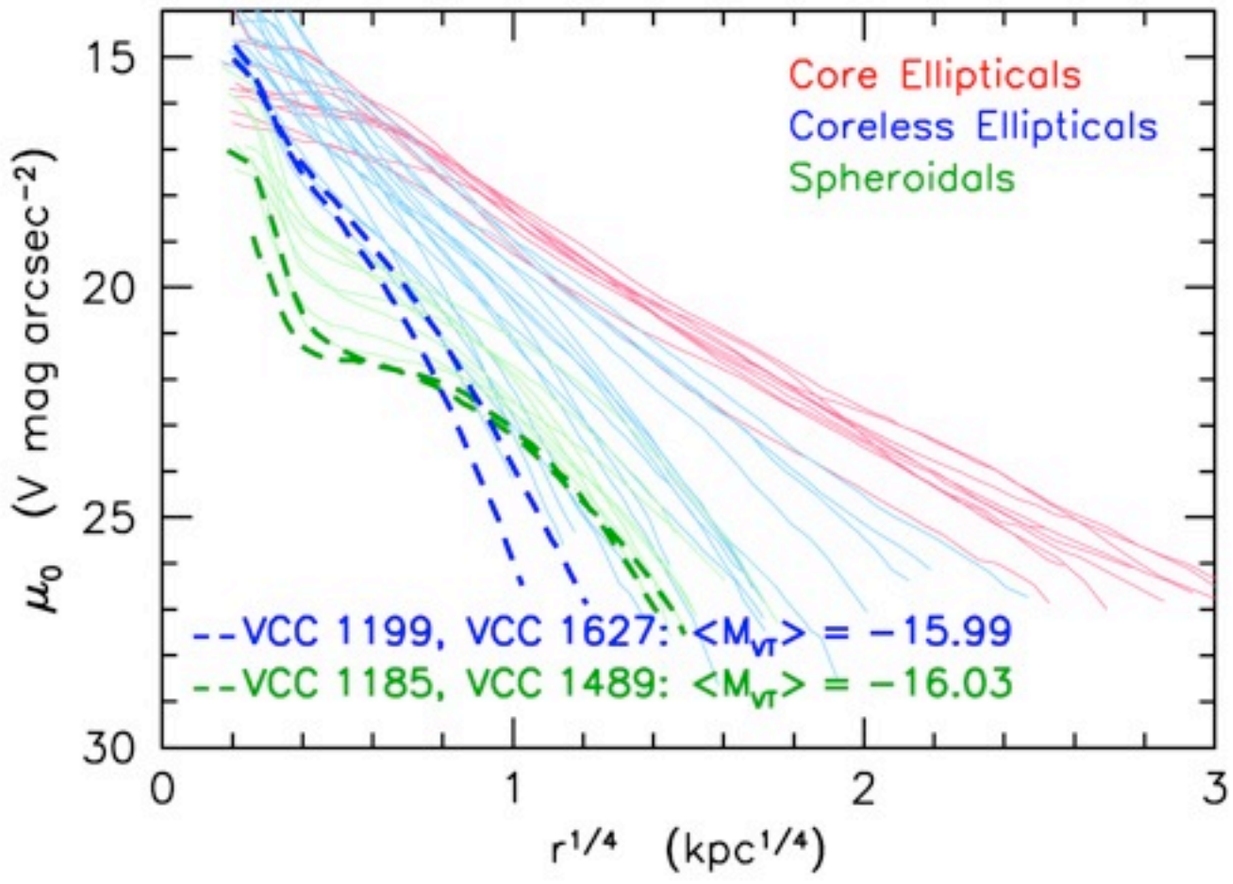

Note: more and more light in the wings for the most luminous galaxies.

In other words, higher value of n.

Sersic index correlates with luminosity

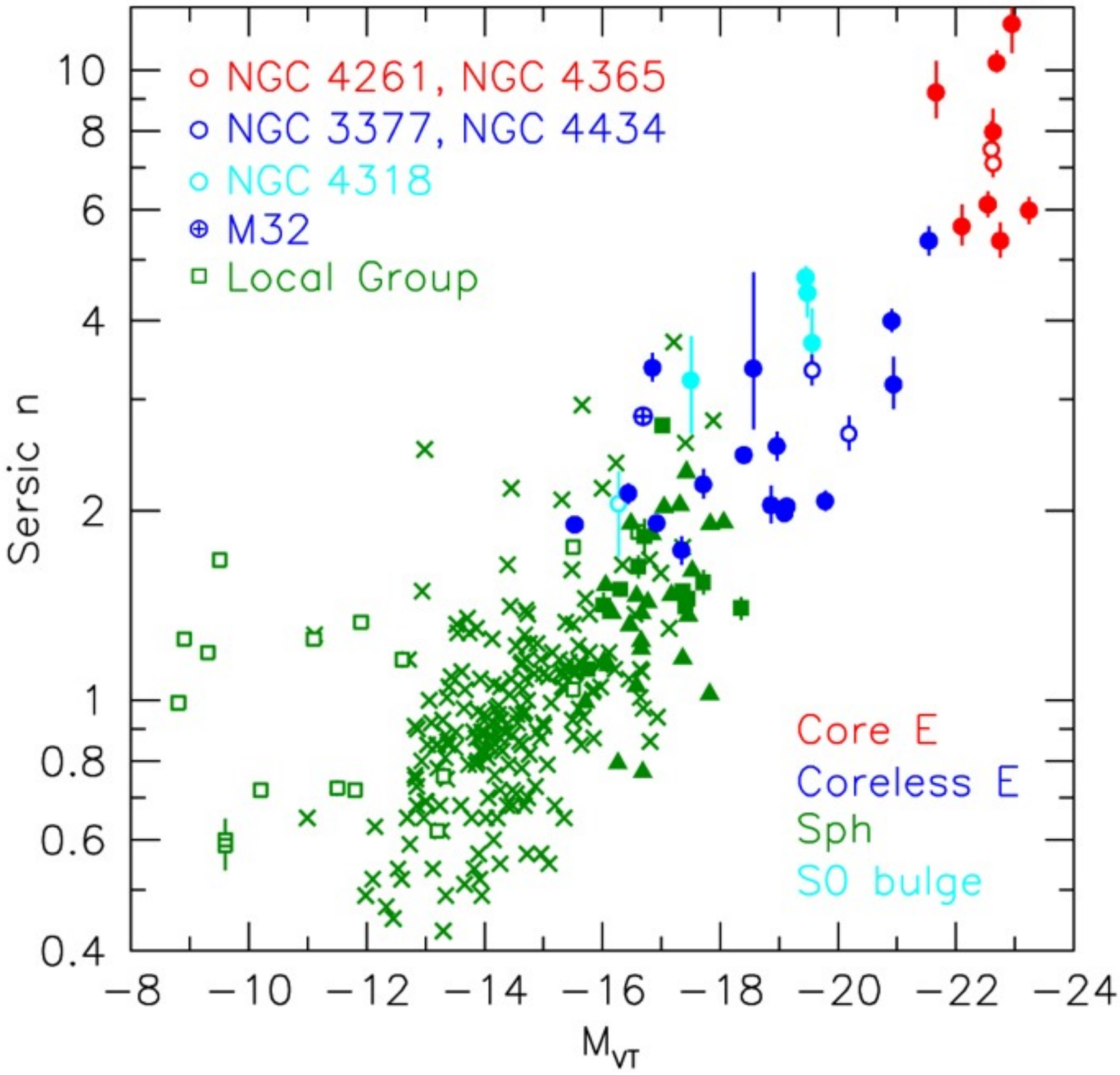

Kormendy Relation

THE ASTROPHYSICAL JOURNAL, **218**:333–346, 1977 December 1

BRIGHTNESS DISTRIBUTIONS IN COMPACT AND NORMAL GALAXIES. II. STRUCTURE PARAMETERS OF THE SPHEROIDAL COMPONENT

JOHN KORMENDY
Hale Observatories, California Institute of Technology, Carnegie Institution of Washington
Received 1977 April 14; accepted 1977 May 23

ABSTRACT

Systematic properties of galaxy spheroids are studied by using simple fitting functions to derive the brightness, size, and shape parameters of their brightness profiles. Fitting the de Vaucouleurs $r^{1/4}$-law to the profiles of 16 red compact and 19 normal galaxies yields the following results.

1. Ellipticals with close, massive neighbors have bright outer halos which are not possessed by more isolated objects. Possible tidal explanations are considered.

2. The brightness and radius parameters are related by $B_{0V} = 3.02 \log r_0 + 19.74$ B mag arcsec^{-2}. The half-light radius r_0 varies from 1.0 to 14.1 kpc, and the brightness B_{0V} at r_0 varies from 19.8 to 23.3 B mag arcsec^{-2}. The parameter along the $B_{0V}(\log r_0)$ relation is absolute magnitude. With much scatter, more luminous galaxies are more diffuse (i.e., have larger r_0 and fainter B_{0V}).

3. Most red compacts are not abnormally compact.

4. The $B_{0V}(\log r_0)$ relation can be used to measure relative distances. We use it to examine the consistency of velocity distances to galaxies in the Virgo cluster versus galaxies 1.6–3.5 times farther away. This suggests that Virgo is closer than its redshift distance by $\delta(m - M) \leq 0.07 \pm 0.23$ mag, a null result supporting the uniform Hubble flow advocated by Sandage and Tammann.

In the Appendix, detailed comparisons are made of how well the fitting functions of de Vaucouleurs, Hubble, and King describe galaxy profiles. The Hubble and King functions fully confirm results obtained above with the de Vaucouleurs law. Relations among the parameters of different models show that they all measure the same physical quantities. To varying degrees, the Hubble and King models fit tidal halos, while the $r^{1/4}$-law does not. However, the de Vaucouleurs law fits unperturbed galaxies best, and is generally the most convenient fitting function.

Kormendy relation

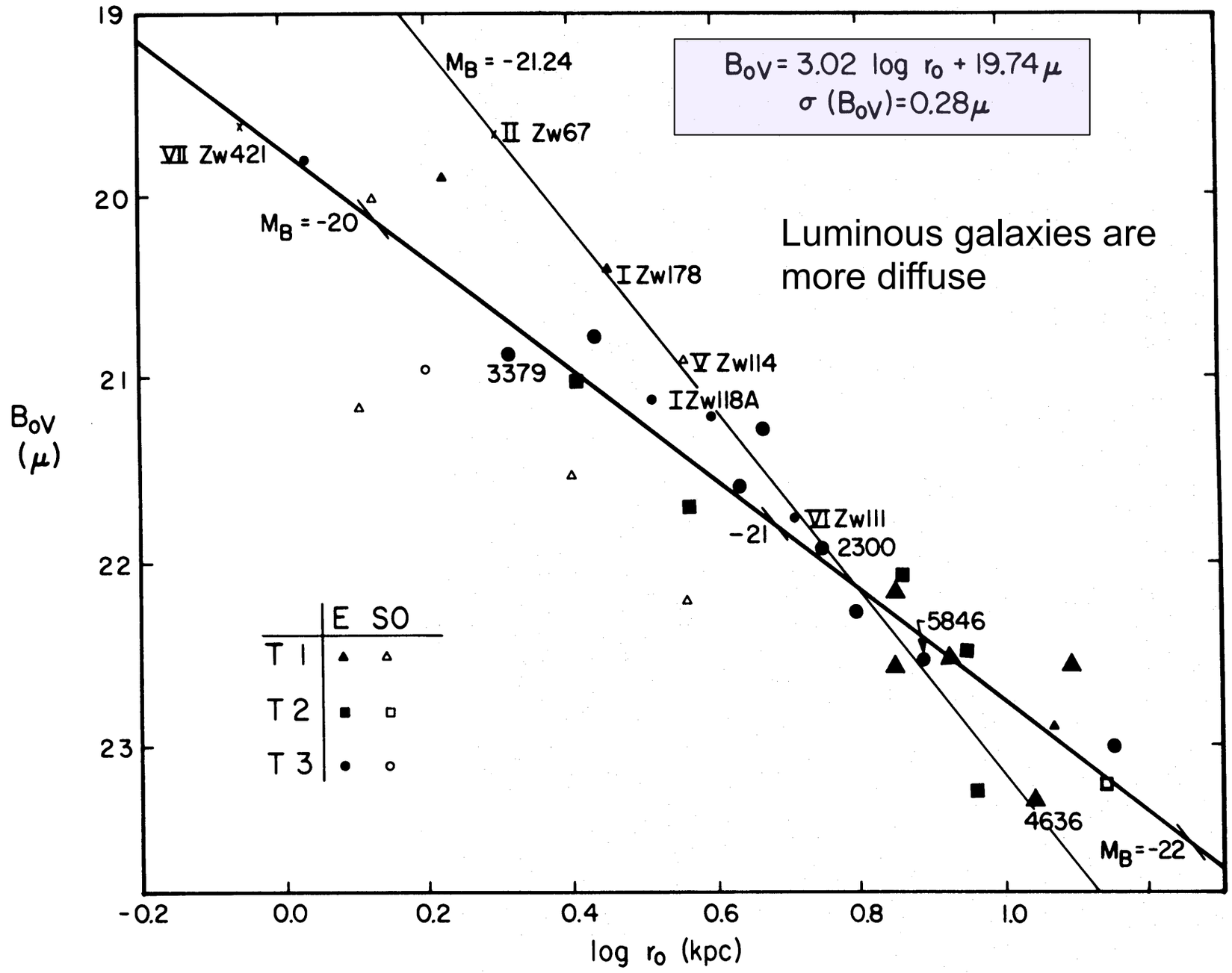

FIG. 2.—B_{0V} versus log r_0 for de Vaucouleurs law fits to compact (*small symbols*) and normal (*large symbols*) galaxies. The heavy line is the least-squares relation for normal galaxies, given at upper right. Average absolute magnitude ticks are defined by eq. (5). Also shown is a typical line of constant M_B, defined by the labeled galaxies.

Stellar Velocity Dispersion

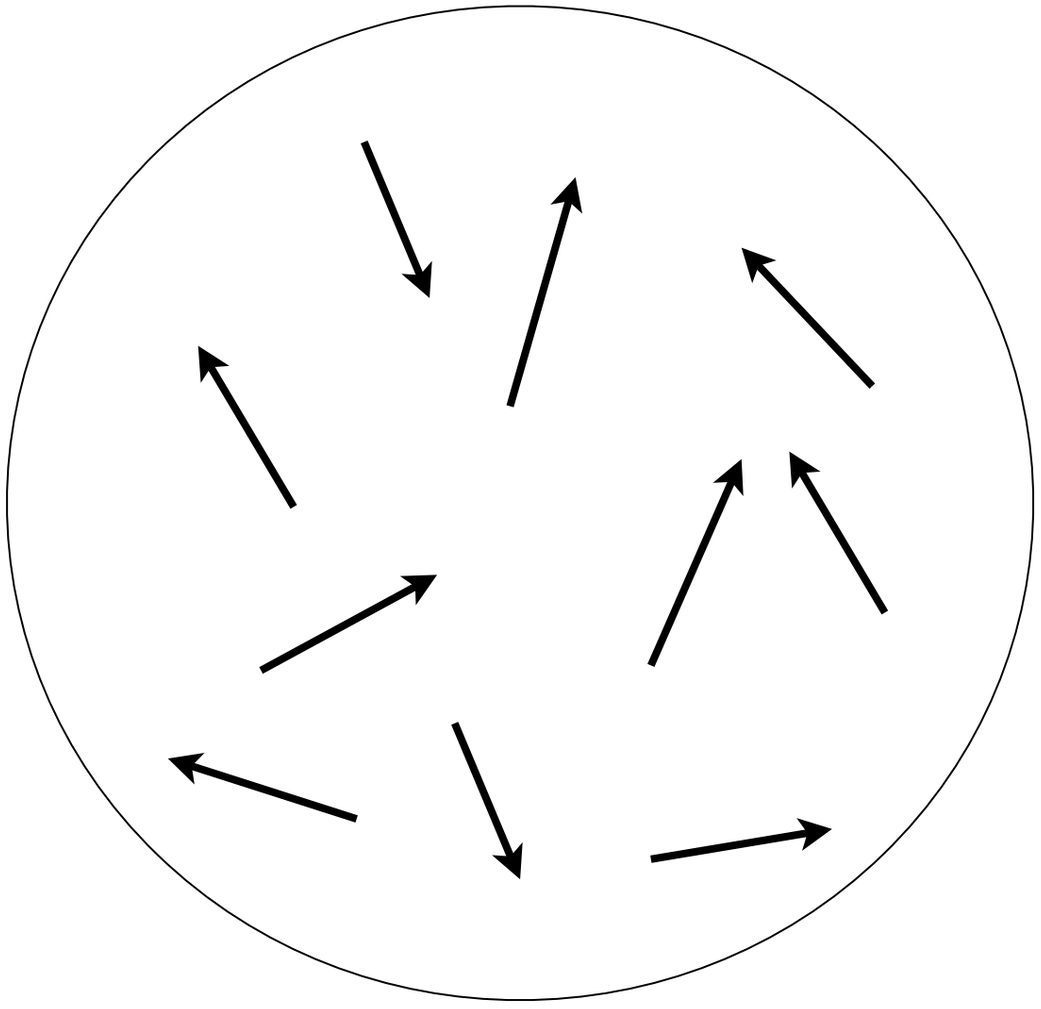

Schematic bulge

Barth et al. 2002

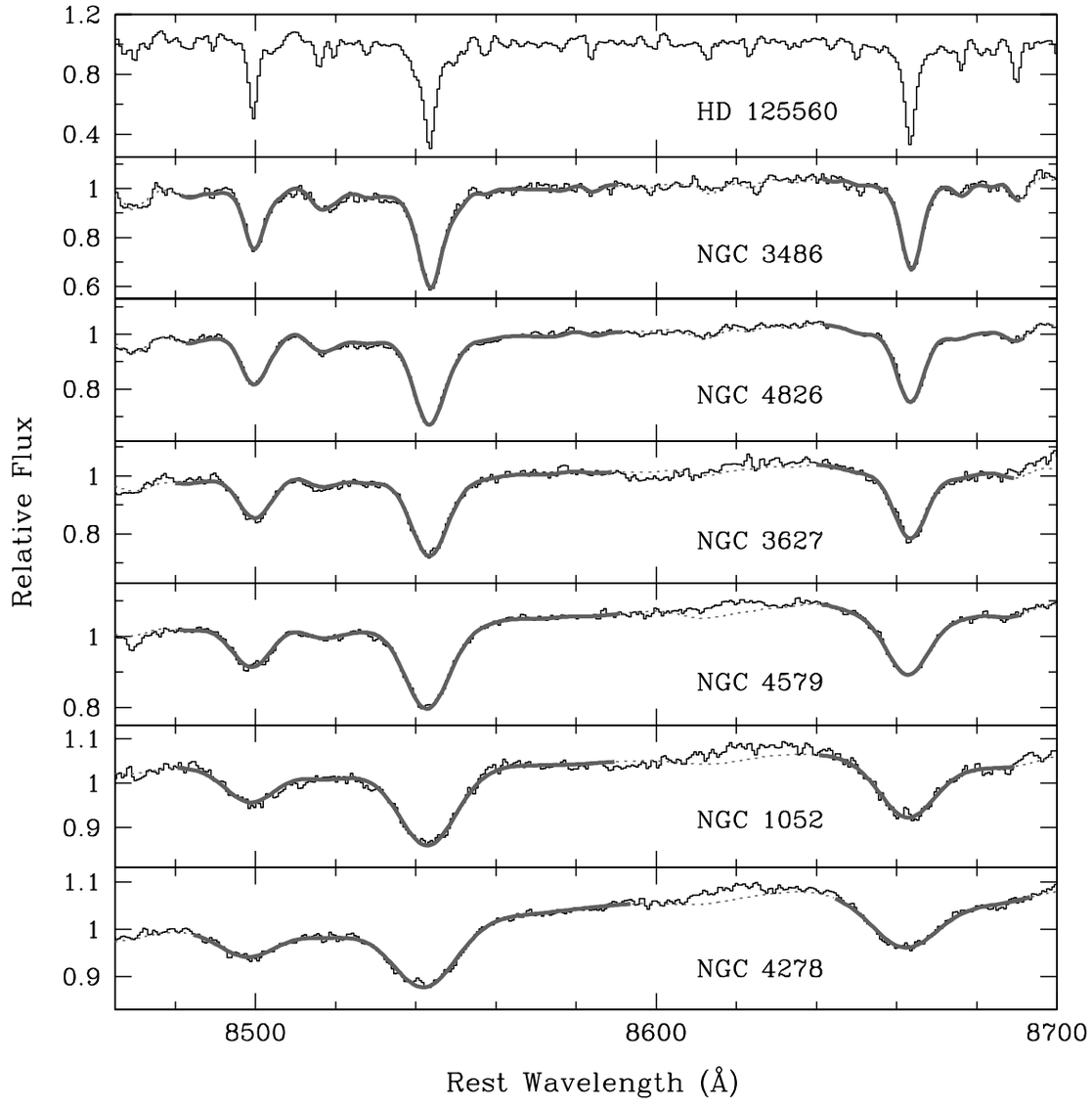

Usually denoted σ* because it denotes RMS velocity.
Related to the kinetic energy of the galaxy.

THE ASTROPHYSICAL JOURNAL, **204**: 668–683, 1976 March 15

VELOCITY DISPERSIONS AND MASS-TO-LIGHT RATIOS FOR ELLIPTICAL GALAXIES*

S. M. FABER AND ROBERT E. JACKSON
Lick Observatory and Board of Studies in Astronomy and Astrophysics, University of California, Santa Cruz
Received 1975 June 30; revised 1975 August 28

ABSTRACT

Velocity dispersions for 25 galaxies have been measured using conventional and Fourier techniques. The resultant velocity system is probably accurate to 10–15 percent. Internal rms errors are on the order of 10 percent. Using unpublished data of King, we have computed core values of M/L_B. For luminous ellipticals with $M_B < -20$, M/L_B averages $7(H/50\ \mathrm{km\ s^{-1}\ Mpc^{-1}})$, considerably smaller than previous estimates. This value agrees well with M/L_B for early-type spirals, indicating that there is no large discontinuity in M/L_B between ellipticals and early-type spirals. This result is consistent with the observed small color differences between ellipticals and Sa's.

Velocity dispersions increase with luminosity for normal elliptical galaxies of moderate ellipticity. The data also suggest that M/L_B generally increases with luminosity. This conclusion is consistent with predictions based on King's data on core radii and central surface brightness (to be discussed fully in a separate paper). This increase in M/L_B might be due at least in part to the known increase in metal abundance with luminosity for normal elliptical galaxies.

The close correlation between luminosity and dynamical properties for normal ellipticals is further evidence that the ellipticals are very nearly a one-parameter family with total mass as the most important independent variable.

It is still debated today
whether mass is the
most important parameter

Faber-Jackson Relation

log σ*

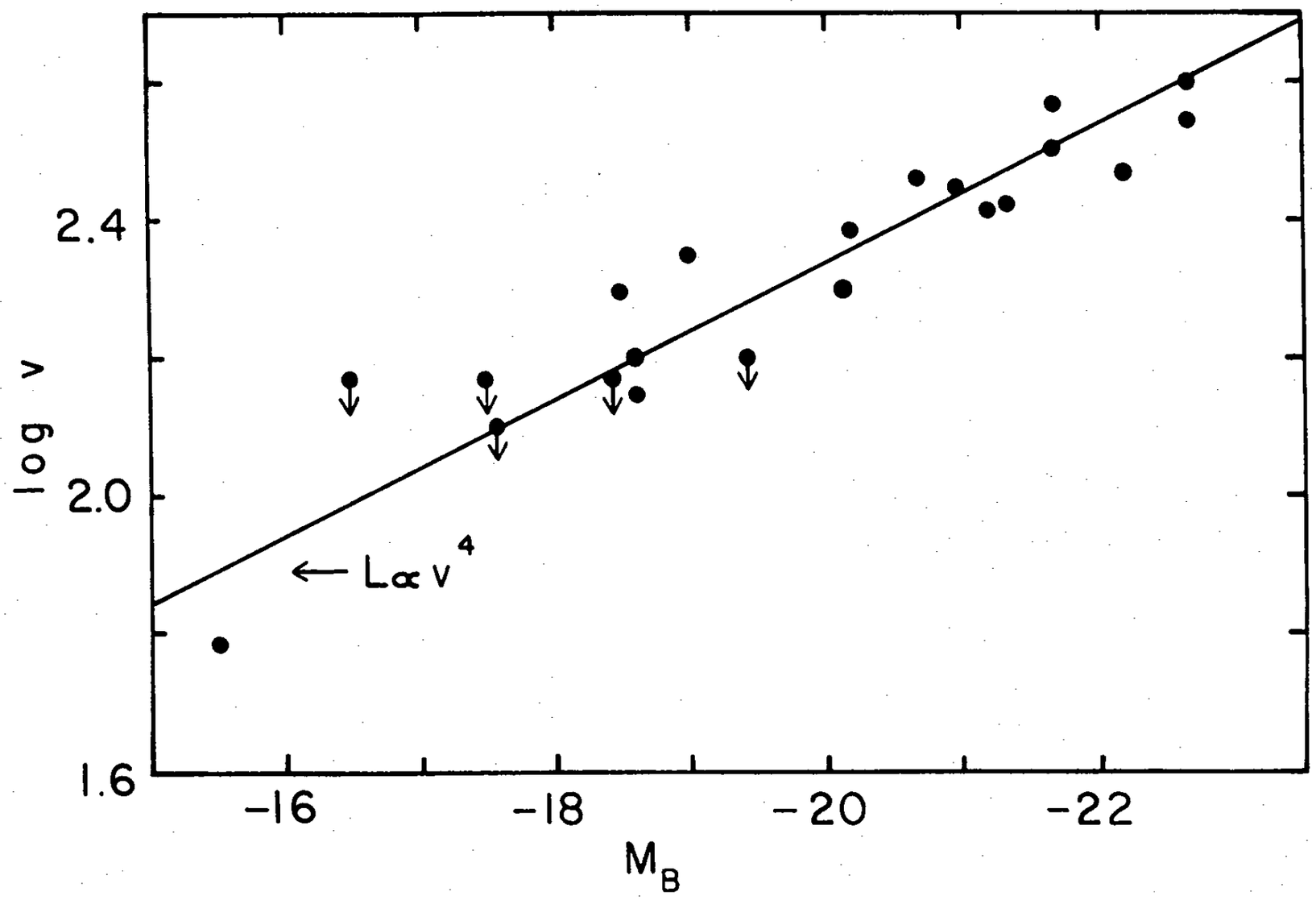

FIG. 16.—Line-of-sight velocity dispersions versus absolute magnitude from Table 1. The point with smallest velocity corresponds to M32, for which the velocity dispersion (60 km s^{-1}) was taken from Richstone and Sargent (1972).

Put it all together

There are parameter correlations between galaxy size, density

(i.e. surface brightness), and stellar velocity dispersion (or ``temperature'').

We can find a coordinate transformation to a plane that minimized the scatter in all three coordinates: Known as the Fundamental Plane.

THE ASTROPHYSICAL JOURNAL, 313:59–68, 1987 February 1

First interest was as a distance indicator.

FUNDAMENTAL PROPERTIES OF ELLIPTICAL GALAXIES[1]

S. DJORGOVSKI[2]
Harvard-Smithsonian Center for Astrophysics and Department of Astronomy, University of California, Berkeley

AND

MARC DAVIS
Department of Astronomy, University of California, Berkeley, and Department of Physics, University of California, Berkeley
Received 1986 May 30; accepted 1986 July 18

ABSTRACT

The global properties of elliptical galaxies, such as luminosity, radius, projected velocity dispersion, projected luminosity, etc., form a two-dimensional family. This "fundamental plane" of elliptical galaxies can be defined in observable terms by the velocity dispersion and mean surface brightness. Its thickness is given at present by the present measurement error bars, and there are no significant indications of nonlinearity (deviation from power laws which define the surface), or higher dimensionality. This is indicative of a strong regularity in the process of galaxy formation. The equations of the plane can be used as new, substantially improved distance indicators for elliptical galaxies. However, all morphological parameters which describe the *shape* of the light distribution (ellipticity, ellipticity gradient, isophotal twist rate, slope of the surface brightness profile), and reflect dynamical anisotropies of stars, are completely independent of this fundamental plane, and thus, the elliptical galaxies are actually a "$2+N$" parameter family. The M/L ratios correlate only with the velocity dispersions and show a small intrinsic scatter, perhaps only $\sim 30\%$, in a luminosity range spanning some four orders of magnitude; this suggests a constant fraction of the dark matter contribution in elliptical galaxies.

Subject headings: cosmology — galaxies: internal motions — galaxies: photometry — galaxies: structure

Mon. Not. R. Astron. Soc. **280,** 167–185 (1996)

The Fundamental Plane for cluster E and S0 galaxies

Inger Jørgensen,[1,2,4★†] Marijn Franx[3,4★] and Per Kjærgaard[1★]

[1] *Copenhagen University Observatory, Øster Voldgade 3, DK-1350 Copenhagen, Denmark*
[2] *McDonald Observatory, The University of Texas at Austin, RLM 15.308, Austin, TX 78712, USA (Postal address for IJ)*
[3] *Kapteyn Institute, PO Box 800, 9700 AV Groningen, The Netherlands (Postal address for MF)*
[4] *Center for Astrophysics, 60 Garden Street, Cambridge, MA 02138, USA*

Accepted 1995 November 16. Received 1995 October 30; in original form 1995 July 17

ABSTRACT

We have analysed the shape of the Fundamental Plane (FP) for a sample of 226 E and S0 galaxies in 10 clusters of galaxies. We find that the distribution of galaxies is well approximated by a plane of the form

$$\log r_e = 1.24 \log \sigma - 0.82 \log \langle I \rangle_e + \gamma$$

for photometry obtained in Gunn *r*. This result is in good agreement with previous determinations. The FP has a scatter of 0.084 in $\log r_e$. For galaxies with velocity dispersion larger than 100 km s^{-1} the scatter is 0.073. If the FP is used for distance determinations this scatter is equivalent to 17 per cent uncertainties on distances to single galaxies.

We find that the slope of the FP is not significantly different from cluster to cluster. Selection effects and measurement errors can introduce biases in the derived slope. The residuals of the FP correlate weakly with the velocity dispersion and the surface brightness. Some of the coefficients used in the literature give rather strong correlations between the residuals and absolute magnitudes. This implies that galaxies need to be selected in a homogeneous way to avoid biases of derived distances on the level of 5–10 per cent or smaller.

The FP has significant intrinsic scatter. No other structural parameters like ellipticity or isophotal shape can reduce the scatter significantly. This is in contradiction to simple models, which predict that the presence of discs in E and S0 galaxies can introduce scatter in the FP. It remains unknown what the source of scatter is. It is therefore unknown whether this source produces systematic errors in distance determinations.

The Mg_2–σ relation for the cluster galaxies differs slightly from cluster to cluster. Galaxies in clusters with lower velocity dispersions have systematically lower Mg_2. The effect can be caused by both age and metallicity variations. With the current stellar population models, the best agreement with our results regarding the FP is if the offsets are mainly caused by differences in metallicity.

Most of the distances that we derive from the FP imply small peculiar motions (< 1000 km s^{-1}). The zero point of the FP must therefore be quite stable. Only for one cluster, located 28° from the direction towards the 'Great Attractor', do we find a peculiar motion of 1300 km s^{-1}. This motion is reduced to 890 km s^{-1} if we use the FP corrected for the offset of the Mg_2–σ relation. This confirms earlier suggestions that the residuals from the Mg_2–σ relation can be used to flag galaxies with deviant populations, and possibly to correct the distance determinations for the deviations.

Note that the FP was derived originally as a distance measurement device

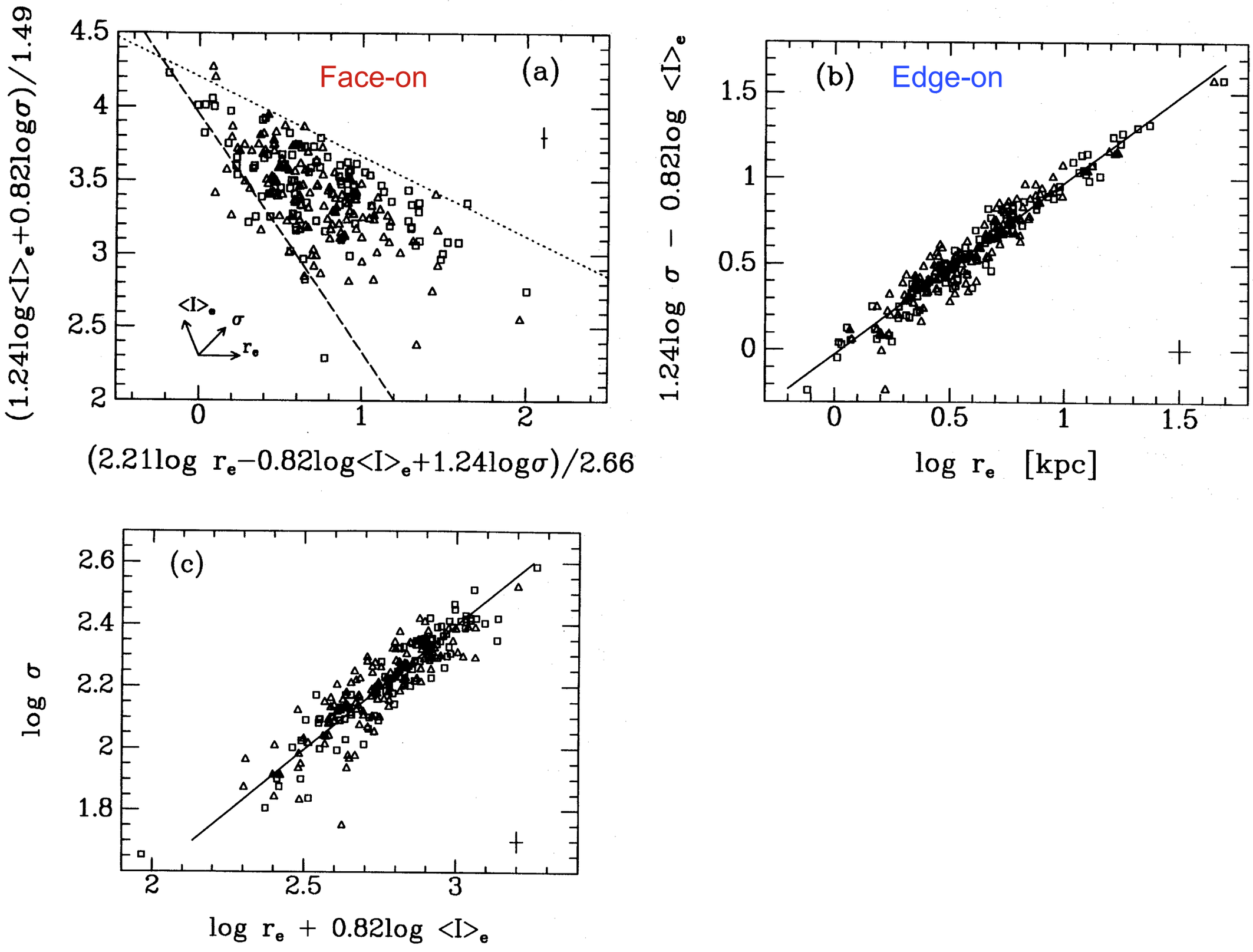

Figure 1. (a) The FP in Gunn *r* as derived in equation (1) shown face-on for all galaxies in the sample. The arrows in the lower left corner of the panel show in which directions the measured parameters increase. The dashed line shows the selection effect due to

Origin of the FP (following Faber 1987)

1. Definition of surface brightness: $\mathbf{\langle I_e \rangle = L_{tot} / (2 \pi R_e^2)}$**. R_e is the effective radius.**

2. By the virial theorem: $2T + W = 0$

$m \sigma^2 - GMm/r = 0 \dashrightarrow \sigma^2 = GM/r$

$\mathbf{M = c R_e \sigma_e^2}$ where c is a structural constant that accounts for possible differences between R_e and R_{tot} depending on the shape (same for σ^*)

3. Taking $\mathbf{L_{tot} = \langle I_e \rangle (2 \pi R_e^2)}$ and inserting into $\mathbf{(M/L)\, L = c R_e \sigma_e^2}$ we find:

$\mathbf{R_e = (c / 2 \pi) \sigma_e^2 \langle I_e \rangle^{-1} (M/L)^{-1}}$

$\mathbf{or: \log R_e = Log [(c / 2 \pi) (M/L)^{-1}] + 2 Log \sigma_e - Log \langle I_e \rangle}$

$\mathbf{or: \log R_e = Log [(c / 2 \pi) (M/L)^{-1}] + 2 Log \sigma_e - 0.4 \langle \mu_e \rangle}$

This looks just like the FP, but the exponents are slightly different:

$\mathbf{\log R_e \alpha 1.4 Log \sigma_e - 0.4 \langle \mu_e \rangle}$

4. There are two ways to make the exponents match. Either we make c a function of L (or M) or we make (M/L) a function of L. Or both. Specifically, with a bit of algebra, you find that:

$(M/L) \alpha L^p$ where $0.2 < p < 0.25$

Fundamental Plane

Elliptical galaxies obey tight scaling relations between their sizes, shapes, and stellar velocity dispersions. In this three-dimensional space, galaxies occupy a plane. This tells us that elliptical galaxies have very similar stellar and dark matter structures.

Dissipationless merging moves galaxies along the FP, while gas-rich merging, feedback, etc, move galaxies in different ways.

The FP is basically the virial theorem, but there is a tilt. Either $M/L \alpha L^{0.2}$ or there is some structural non-homology, such that the orbital structure of ellipticals is correlated with mass or σ^*.

Recent observations seem to support a model in which M/L increases with L due both to older stellar populations AND increasing DM content in the most massive elliptical galaxies. Theoretical papers suggest that such a trend results from increased dissipational merging in lower-mass galaxies.

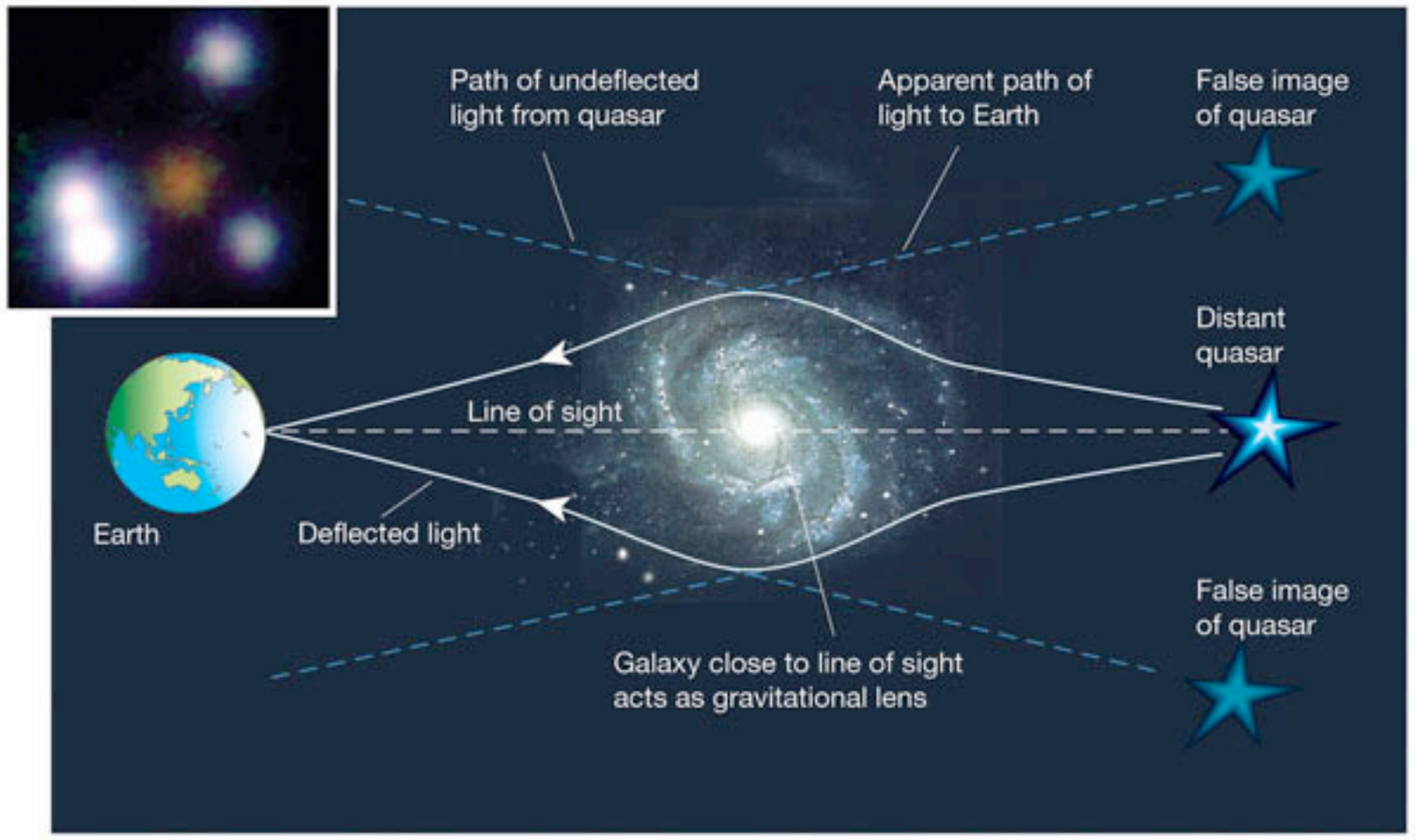
Path of undeflected light from quasar
Apparent path of light to Earth
False image of quasar
Distant quasar
Line of sight
Earth
Deflected light
False image of quasar
Galaxy close to line of sight acts as gravitational lens

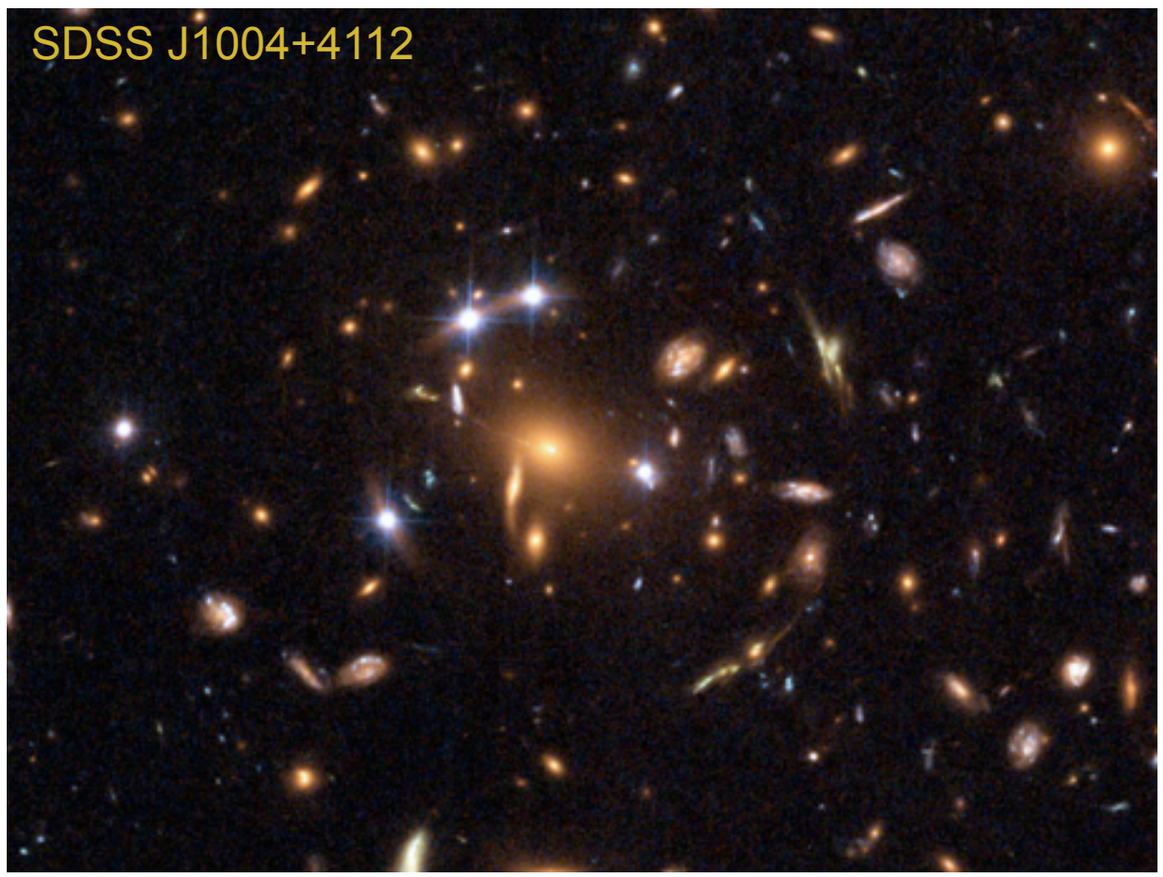
SDSS J1004+4112

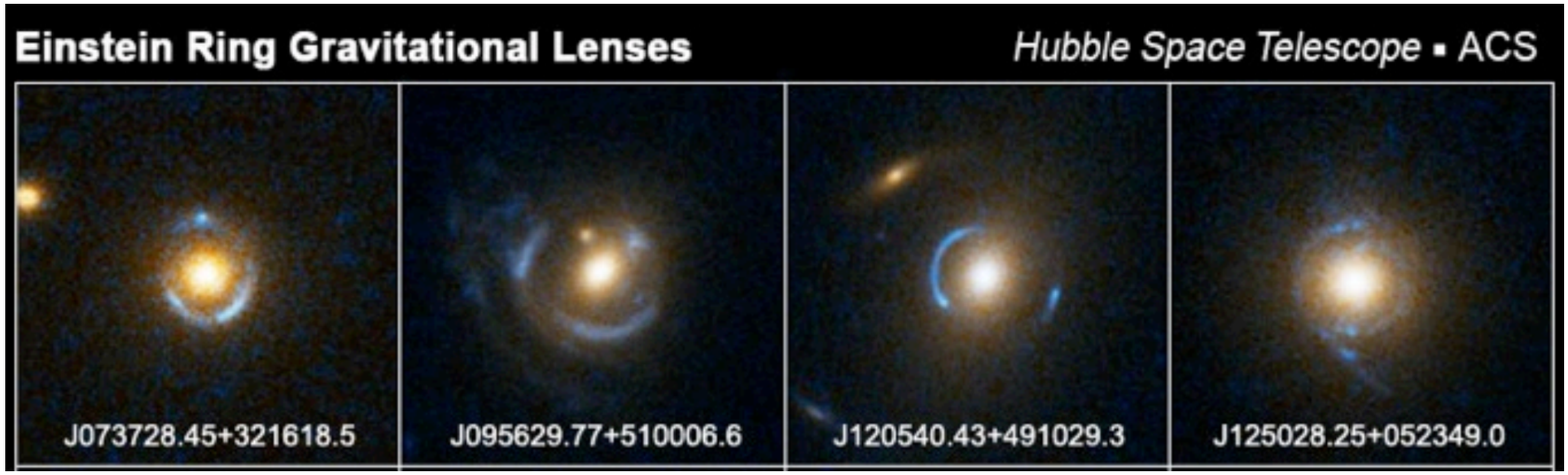

SLACS

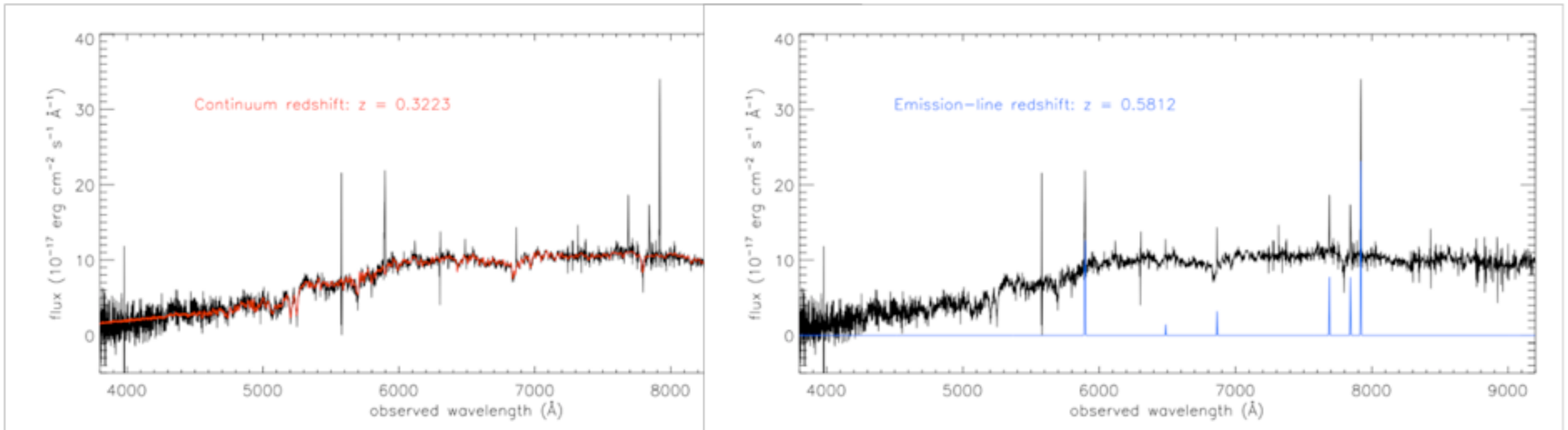

Selection of SDSS spectra with a red galaxy at one redshift and emission lines at a higher redshift. These are guaranteed to be strong lenses. The lensing of the background galaxy provides an enclosed mass for the foreground galaxy.
see Bolton et al. 2006 for a description of the survey.

Adam Bolton et al.

THE ASTROPHYSICAL JOURNAL, 724:511–525, 2010 November 20

THE SLOAN LENS ACS SURVEY. X. STELLAR, DYNAMICAL, AND TOTAL MASS CORRELATIONS OF MASSIVE EARLY-TYPE GALAXIES

M. W. AUGER[1], T. TREU[1,8], A. S. BOLTON[2], R. GAVAZZI[3], L. V. E. KOOPMANS[4], P. J. MARSHALL[1,5], L. A. MOUSTAKAS[6], AND S. BURLES[7]

[1] Department of Physics, University of California, Santa Barbara, CA 93106, USA; mauger@physics.ucsb.edu
[2] Department of Physics and Astronomy, University of Utah, Salt Lake City, UT 84112, USA
[3] Institut d'Astrophysique de Paris, UMR7095 CNRS & Univ. Pierre et Marie Curie, 98bis Bvd Arago, F-75014 Paris, France
[4] Kapteyn Astronomical Institute, University of Groningen, P.O. Box 800, 9700AV Groningen, The Netherlands
[5] Kavli Institute for Particle Astrophysics and Cosmology, Stanford University, Stanford, CA 94305, USA
[6] Jet Propulsion Laboratory, California Institute of Technology, 4800 Oak Grove Drive, M/S 169-237, Pasadena, CA 91109, USA
[7] D. E. Shaw & Co., L.P., 20400 Stevens Creek Boulevard, Suite 850, Cupertino, CA 95014, USA
Received 2010 June 8; accepted 2010 September 17; published 2010 November 3

ABSTRACT

We use stellar masses, surface photometry, strong-lensing masses, and stellar velocity dispersions ($\sigma_{e/2}$) to investigate empirical correlations for the definitive sample of 73 early-type galaxies (ETGs) that are strong gravitational lenses from the SLACS survey. The traditional correlations (fundamental plane (FP) and its projections) are consistent with those found for non-lens galaxies, supporting the thesis that SLACS lens galaxies are representative of massive ETGs (dimensional mass $M_{\rm dim} = 10^{11}$–$10^{12}\ M_{\odot}$). The addition of high-precision strong-lensing estimates of the total mass allows us to gain further insights into their internal structure: (1) the average slope of the total mass-density profile ($\rho_{\rm tot} \propto r^{-\gamma'}$) is $\langle\gamma'\rangle = 2.078 \pm 0.027$ with an intrinsic scatter of 0.16 ± 0.02; (2) γ' correlates with effective radius (r_e) and central mass density, in the sense that denser galaxies have steeper profiles; (3) the dark matter (DM) fraction within $r_e/2$ is a monotonically increasing function of galaxy mass and size (due to a mass-dependent central cold DM distribution or due to baryonic DM—stellar remnants or low-mass stars—if the initial mass function is non-universal and its normalization increases with mass); (4) the dimensional mass $M_{\rm dim} \equiv 5r_e\sigma^2_{e/2}/G$ is proportional to the total (lensing) mass $M_{r_e/2}$, and both increase more rapidly than stellar mass M_* ($M_* \propto M^{0.8}_{r_e/2}$); (5) the mass plane (MP), obtained by replacing surface brightness with surface mass density in the FP, is found to be tighter and closer to the virial relation than the FP and the M_*P, indicating that the scatter of those relations is dominated by stellar population effects; (6) we construct the fundamental hyper-plane by adding stellar masses to the MP and find the M_* coefficient to be consistent with zero and no residual intrinsic scatter. Our results demonstrate that the dynamical structure of ETGs is not scale invariant and that it is fully specified by $M_{r_e/2}$, r_e, and $\sigma_{e/2}$. Although the basic trends can be explained qualitatively in terms of varying star formation efficiency as a function of halo mass and as the result of dry and wet mergers, reproducing quantitatively the observed correlations and their tightness may be a significant challenge for galaxy formation models.

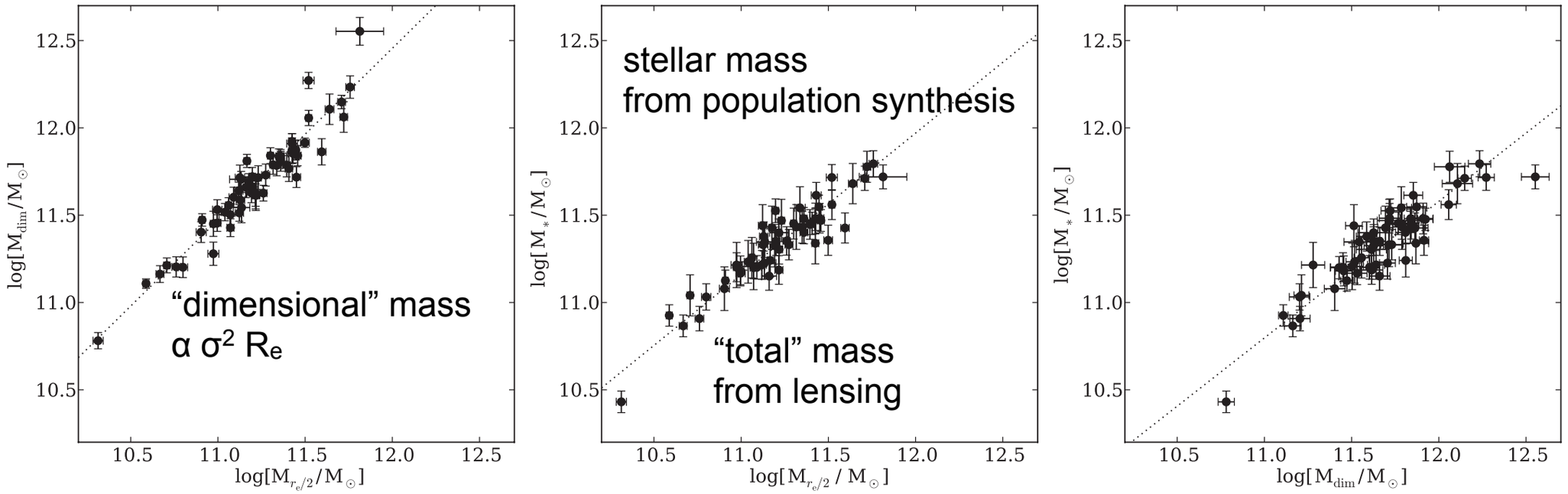

Figure 3. Bivariate correlations between dimensional ($M_{\rm dim}$), total ($M_{r_e/2}$), and stellar mass (M_*). The best-fitting linear relations are shown as dotted lines. Their coefficients are given in Table 3. Note the linear relation between dimensional and total mass, and the nonlinearity of the other two relations. These are consistent with a constant virial coefficient and an increase with mass of the dark matter content and/or stellar initial mass function normalization.

4. Tight correlations are found between dimensional mass $M_{\rm dim} = \frac{5\sigma^2 r_e}{G}$, stellar ($M_*$) and total mass ($M_{\rm tot}$). The relationship between total mass and dimensional mass is found to be consistent with linear with very little scatter, implying that the virial coefficient of ETGs is constant over this mass range. The correlation between total (dynamical) mass and stellar mass is nonlinear ($M_* \propto M_{r_e/2}^{0.8}$) consistent with the hypothesis that the central CDM content and/or the normalization of the stellar IMF changes with mass.
5. Assuming a universal IMF the stellar mass-to-light ratio is nearly constant over the range in masses probed by the SLACS ETGs. In contrast, the total mass-to-light ratio correlates strongly with lens properties; the most significant correlations are with the central velocity dispersion and central total mass. As a result, the DM fraction within $r_e/2$ is a monotonically increasing function of galaxy mass and size. If the universal IMF assumption is relaxed, the trend could be explained at least in part by an increasing IMF normalization with galaxy mass.

The Astrophysical Journal, 729:129 (21pp), 2011 March 10 doi:10.1088/0004-637X/729/2/129

GALAXY KINEMATICS WITH VIRUS-P: THE DARK MATTER HALO OF M87

Jeremy D. Murphy, Karl Gebhardt, and Joshua J. Adams
Department of Astronomy, University of Texas at Austin, 1 University Station C1400, Austin, TX 78712, USA; murphy@astro.as.utexas.edu
Received 2010 October 11; accepted 2011 January 2; published 2011 February 17

ABSTRACT

We present two-dimensional stellar kinematics of M87 out to $R = 238''$ taken with the integral field spectrograph VIRUS-P. We run a large set of axisymmetric, orbit-based dynamical models and find clear evidence for a massive dark matter halo. While a logarithmic parameterization for the dark matter halo is preferred, we do not constrain the dark matter scale radius for a Navarro–Frenk–White (NFW) profile and therefore cannot rule it out. Our best-fit logarithmic models return an enclosed dark matter fraction of $17.2^{+5.0}_{-5.0}$% within one effective radius ($R_e \cong 100''$), rising to $49.4^{+7.2}_{-8.8}$% within 2 R_e. Existing SAURON data ($R \leqslant 13''$), and globular cluster (GC) kinematic data covering $145'' \leqslant R \leqslant 554''$ complete the kinematic coverage to $R = 47$ kpc ($\sim 5\ R_e$). At this radial distance, the logarithmic dark halo comprises $85.3^{+2.5}_{-2.4}$% of the total enclosed mass of $5.7^{+1.3}_{-0.9} \times 10^{12}\ M_\odot$ making M87 one of the most massive galaxies in the local universe. Our best-fit logarithmic dynamical models return a stellar mass-to-light ratio (M/L) of $9.1^{+0.2}_{-0.2}$ (V band), a dark halo circular velocity of 800^{+75}_{-25} km s^{-1}, and a dark halo scale radius of 36^{+7}_{-3} kpc. The stellar M/L, assuming an NFW dark halo, is well constrained to $8.20^{+0.05}_{-0.10}$ (V band). The stars in M87 are found to be radially anisotropic out to $R \cong 0.5\ R_e$, then isotropic or slightly tangentially anisotropic to our last stellar data point at $R = 2.4\ R_e$ where the anisotropy of the stars and GCs are in excellent agreement. The GCs then become radially anisotropic in the last two modeling bins at $R = 3.4\ R_e$ and $R = 4.8\ R_e$. As one of the most massive galaxies in the local universe, constraints on both the mass distribution of M87 and anisotropy of its kinematic components strongly inform our theories of early-type galaxy formation and evolution in dense environments.

Key words: dark matter – galaxies: elliptical and lenticular, cD – galaxies: kinematics and dynamics

Online-only material: color figures

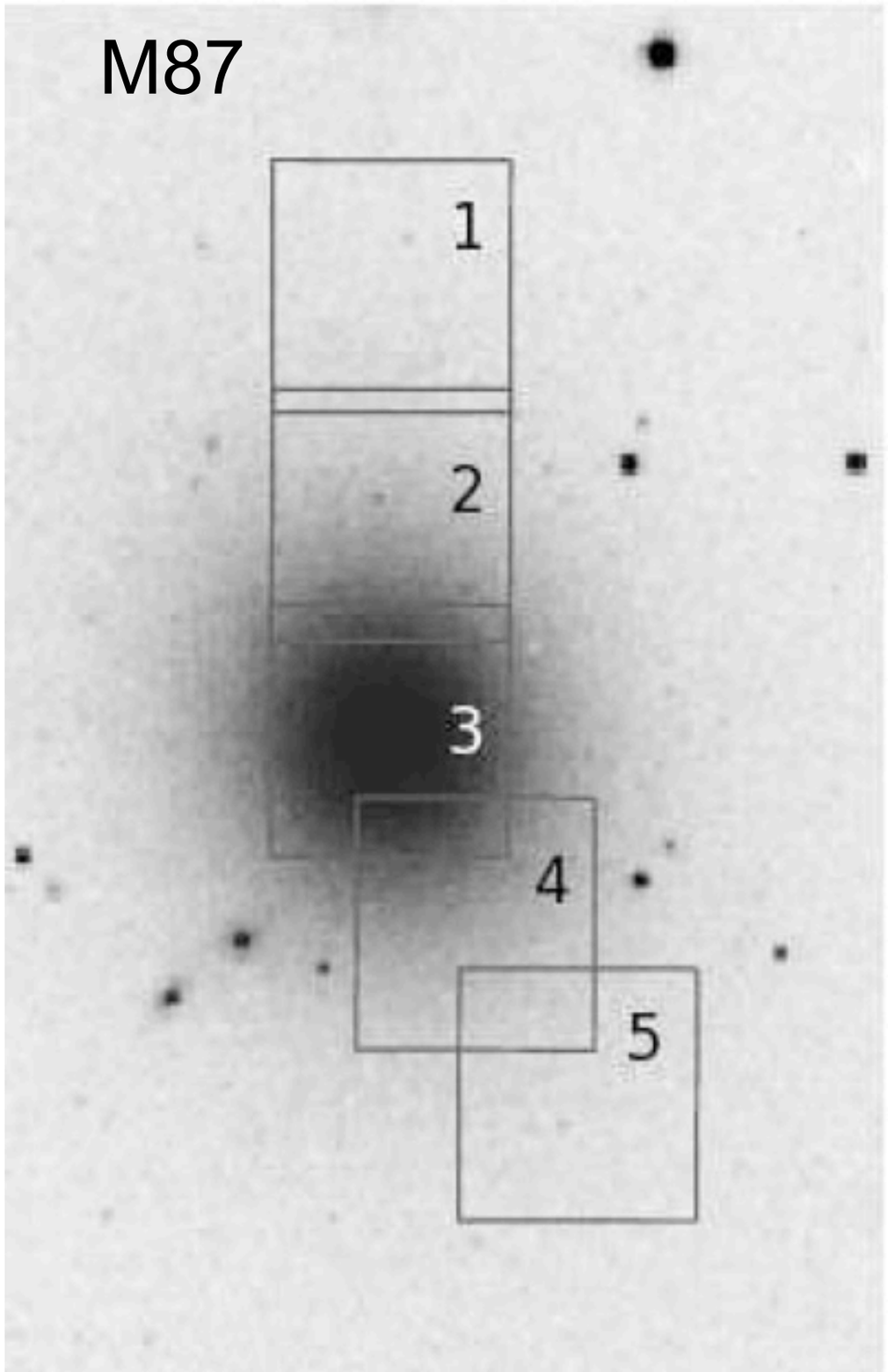
M87
1
2
3
4
5

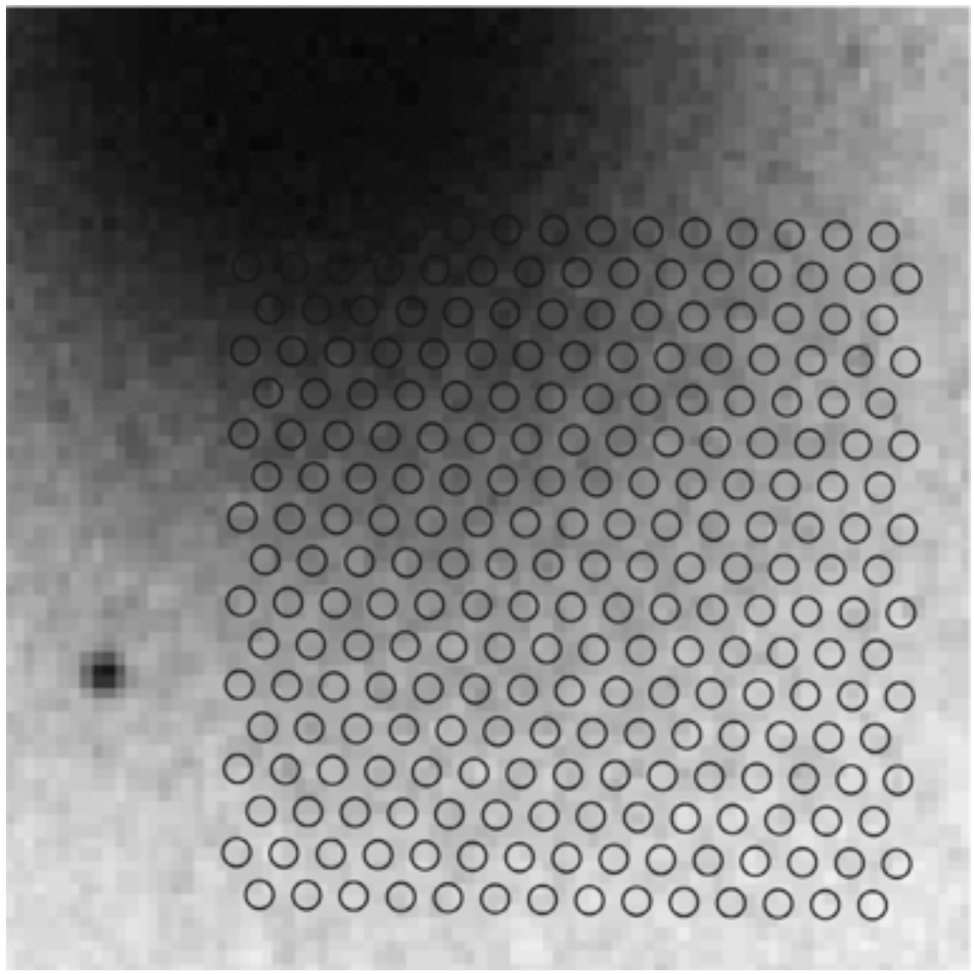

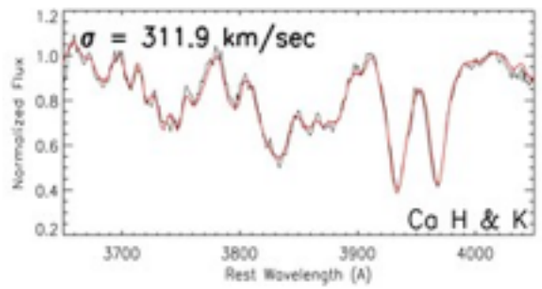
σ = 311.9 km/sec
Ca H & K
Normalized Flux
Rest Wavelength (A)

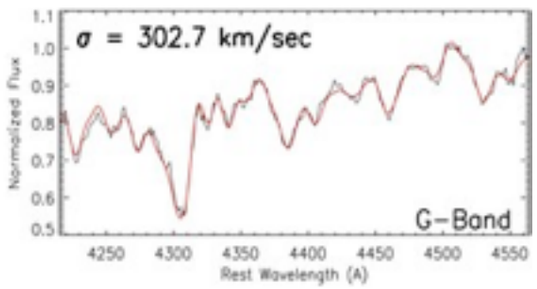
σ = 302.7 km/sec
G-Band
Normalized Flux
Rest Wavelength (A)

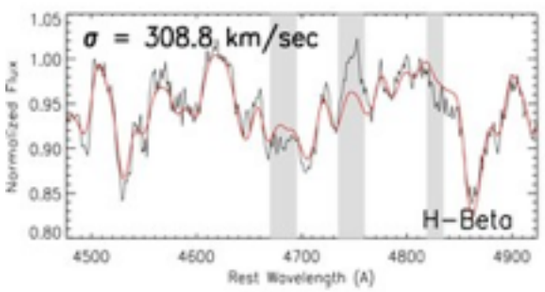
σ = 308.8 km/sec
H-Beta
Normalized Flux
Rest Wavelength (A)

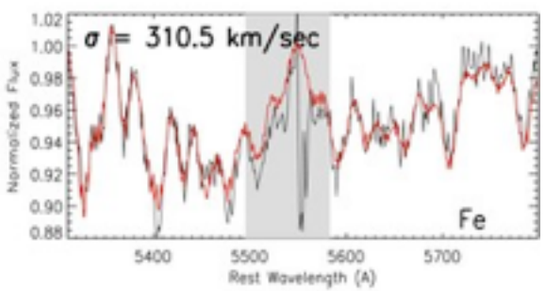
σ = 310.5 km/sec
Fe
Normalized Flux
Rest Wavelength (A)

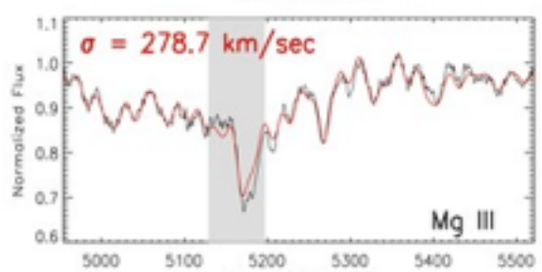
σ = 278.7 km/sec
Mg III
Normalized Flux

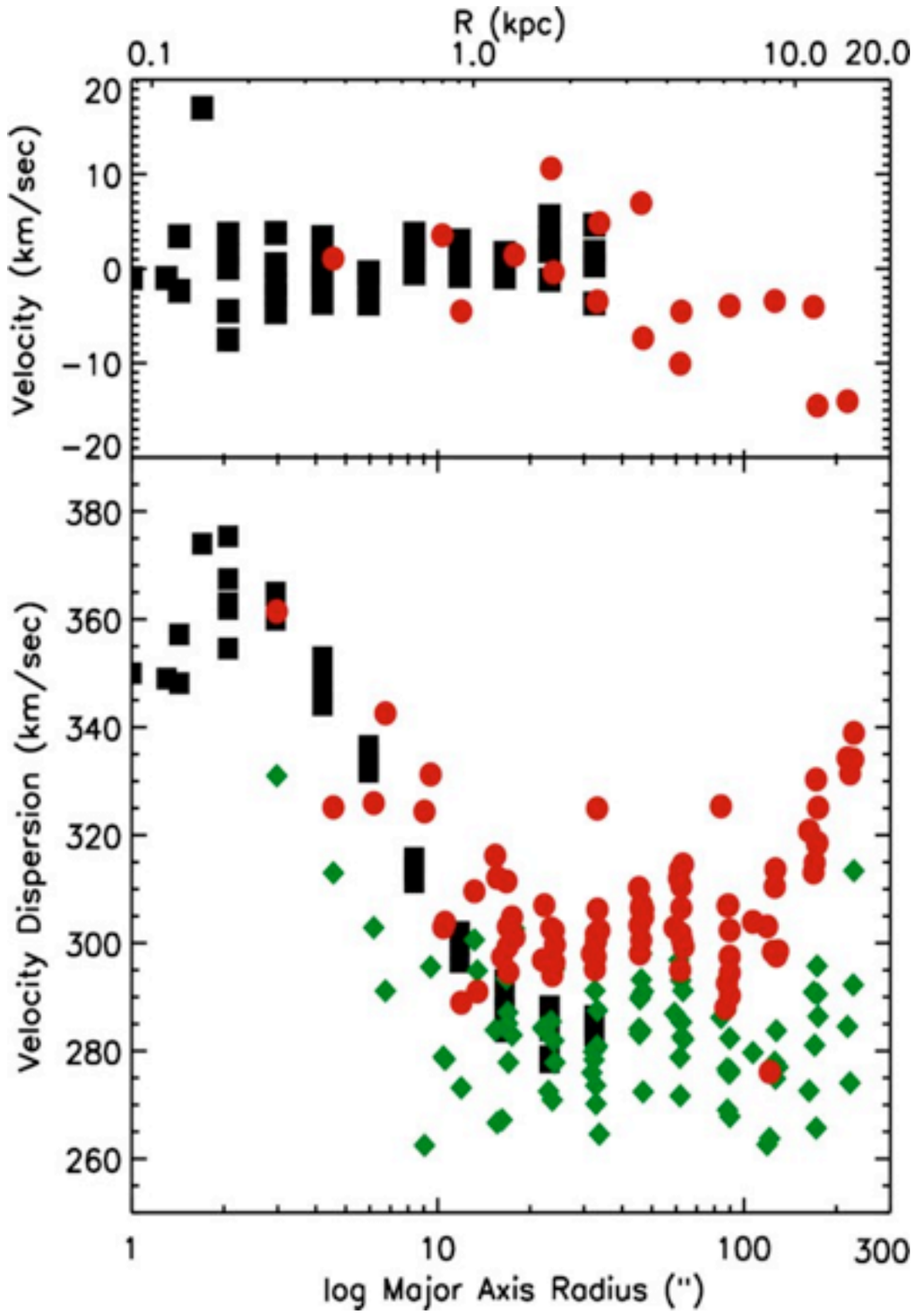

Model of galaxy+ dark halo

Total mass in stars + dark halo

Dynamical Modeling

The SAURON project – IV. The mass-to-light ratio, the virial mass estimator and the Fundamental Plane of elliptical and lenticular galaxies

Michele Cappellari,[1⋆] R. Bacon,[2] M. Bureau,[3] M. C. Damen,[1] Roger L. Davies,[3] P. T. de Zeeuw,[1] Eric Emsellem,[2] Jesús Falcón-Barroso,[1] Davor Krajnović,[3] Harald Kuntschner,[4] Richard M. McDermid,[1] Reynier F. Peletier,[5] Marc Sarzi,[3] Remco C. E. van den Bosch[1] and Glenn van de Ven[1]

[1] *Leiden Observatory, Postbus 9513, 2300 RA Leiden, the Netherlands*
[2] *Centre de Recherche Astrophysique de Lyon, 9 Avenue Charles André, 69230 Saint Genis Laval, France*
[3] *Denys Wilkinson Building, University of Oxford, Keble Road, Oxford OX1 3RH*
[4] *Space Telescope European Coordinating Facility, European Southern Observatory, Karl-Schwarzschild-Str 2, 85748 Garching, Germany*
[5] *Kapteyn Astronomical Institute, Postbus 800, 9700 AV Groningen, the Netherlands*

Accepted 2005 November 18. Received 2005 November 12; in original form 2005 April 28

Mon. Not. R. Astron. Soc. **366,** 1126–1150 (2006)

ABSTRACT

We investigate the well-known correlations between the dynamical mass-to-light ratio (M/L) and other global observables of elliptical (E) and lenticular (S0) galaxies. We construct two-integral Jeans and three-integral Schwarzschild dynamical models for a sample of 25 E/S0 galaxies with SAURON integral-field stellar kinematics to about one effective (half-light) radius R_e. They have well-calibrated I-band *Hubble Space Telescope* WFPC2 and large-field ground-based photometry, accurate surface brightness fluctuation distances, and their observed kinematics is consistent with an axisymmetric intrinsic shape. All these factors result in an unprecedented accuracy in the M/L measurements. We find a tight correlation of the form $(M/L) = (3.80 \pm 0.14) \times (\sigma_e/200\,\mathrm{km\,s^{-1}})^{0.84\pm0.07}$ between the M/L (in the I band) measured from the dynamical models and the luminosity-weighted second moment σ_e of the LOSVD within R_e. The observed rms scatter in M/L for our sample is 18 per cent, while the inferred intrinsic scatter is ∼13 per cent. The (M/L)–σ_e relation can be included in the remarkable series of tight correlations between σ_e and other galaxy global observables. The comparison of the observed correlations with the predictions of the Fundamental Plane (FP), and with simple virial estimates, shows that the 'tilt' of the FP of early-type galaxies, describing the deviation of the FP from the virial relation, is almost exclusively due to a real M/L variation, while structural and orbital non-homology have a negligible effect. When the photometric parameters are determined in the 'classic' way, using growth curves, and the σ_e is measured in a large aperture, the virial mass appears to be a reliable estimator of the mass in the central regions of galaxies, and can be safely used where more 'expensive' models are not feasible (e.g. in high-redshift studies). In this case the best-fitting virial relation has the form $(M/L)_{vir} = (5.0 \pm 0.1) \times R_e\sigma_e^2/(LG)$, in reasonable agreement with simple theoretical predictions. We find no difference between the M/L of the galaxies in clusters and in the field. The comparison of the dynamical M/L with the $(M/L)_{pop}$ inferred from the analysis of the stellar population, indicates a median dark matter fraction in early-type galaxies of ∼30 per cent of the total mass inside one R_e, in broad agreement with previous studies, and it also shows that the stellar initial mass function varies little among different galaxies. Our results suggest a variation in M/L at constant $(M/L)_{pop}$, which seems to be linked to the galaxy dynamics. We speculate that fast-rotating galaxies have lower dark matter fractions than the slow-rotating and generally more-massive ones. If correct, this would suggest a connection between the galaxy assembly history and the dark matter halo structure. The tightness of our correlation provides some evidence against cuspy nuclear dark matter profiles in galaxies.

Stellar motions

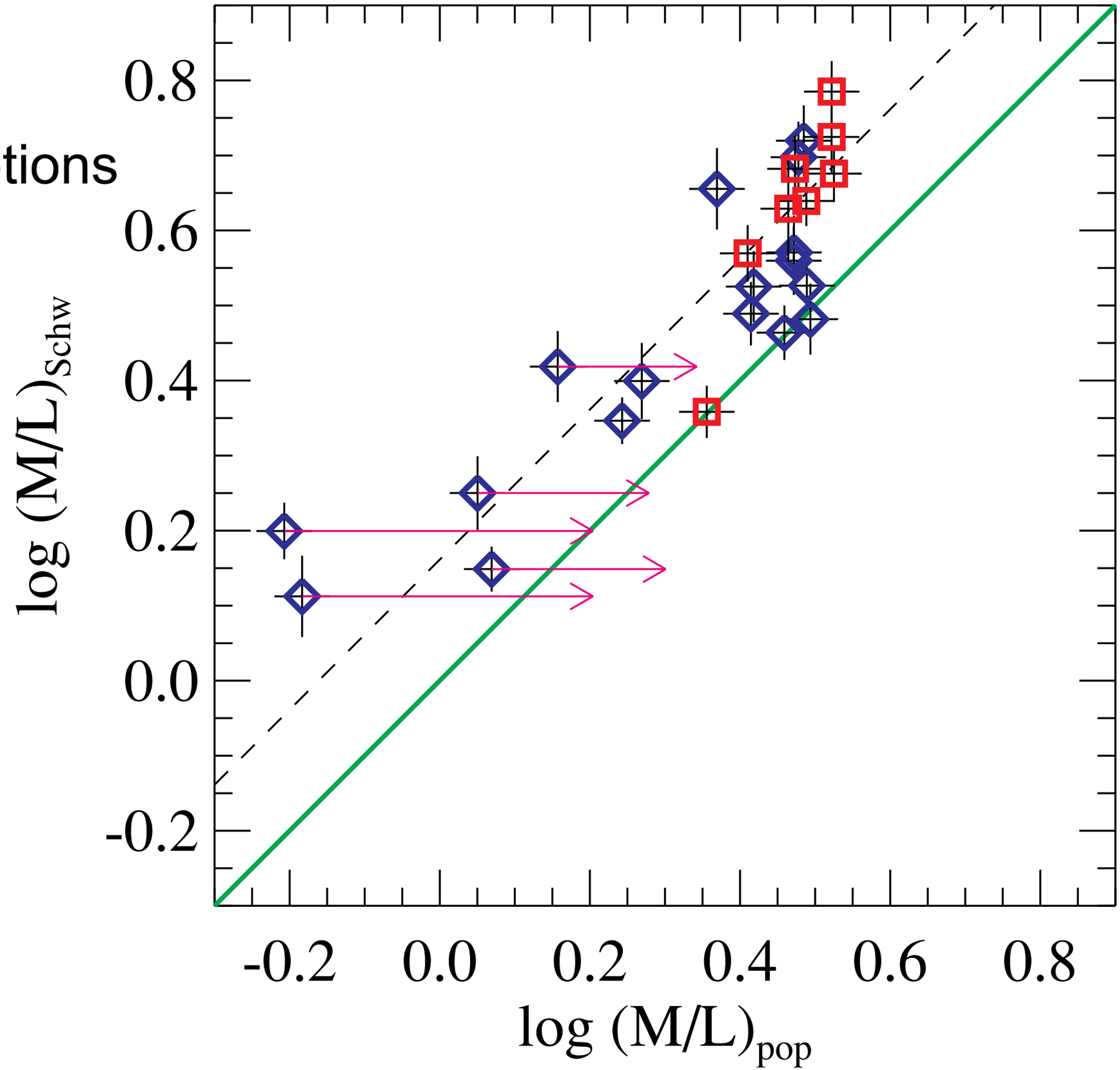

Stellar populations

Stellar Population Trends

Elliptical galaxies formed their stars early

More massive systems are more metal-enriched

More massive systems formed their stars faster

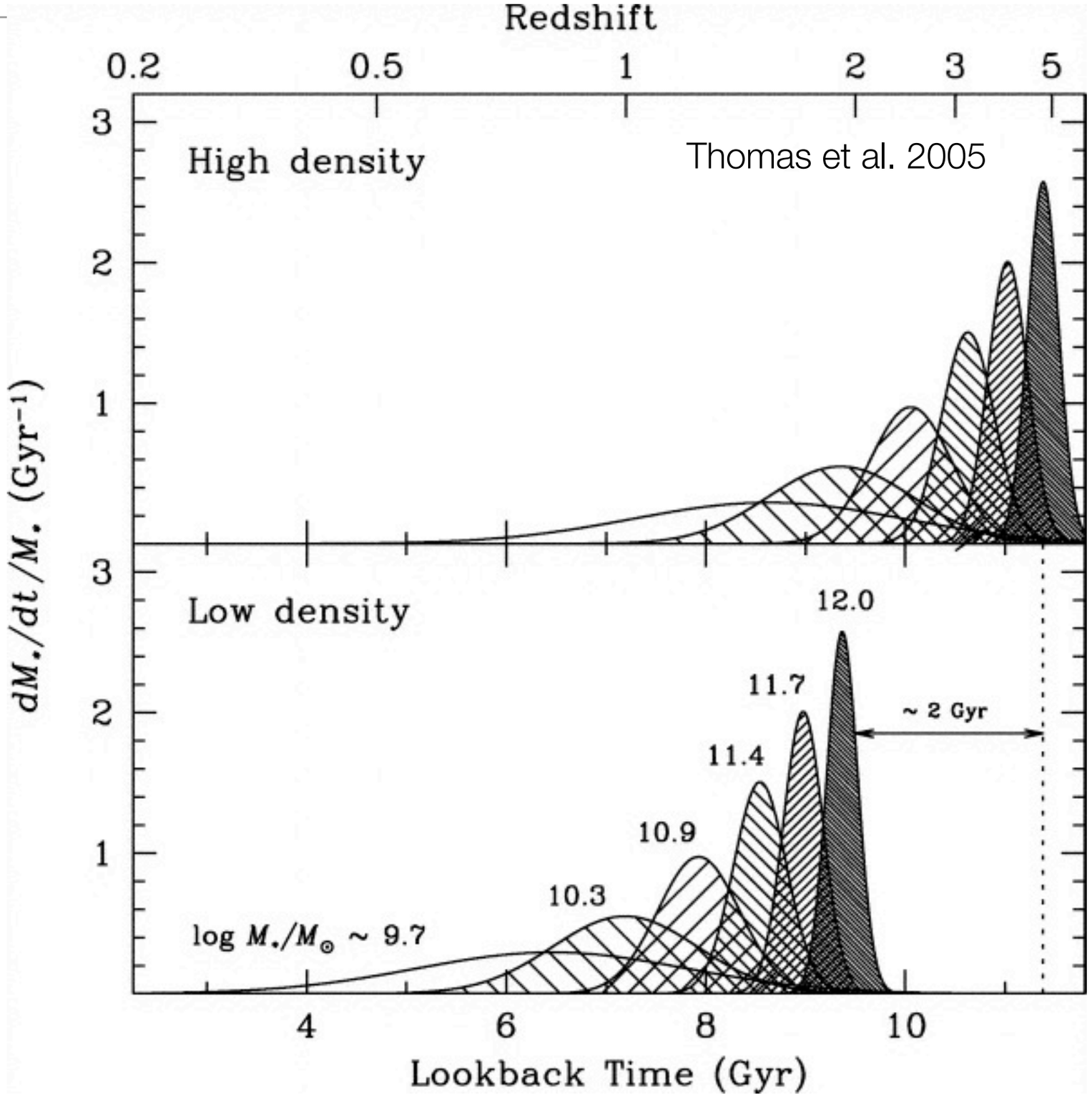

How were elliptical galaxies formed?

Ellipticals are a family of dynamically hot stellar systems that fall on the Fundamental Plane.

They obey tight scaling relations between metallicity and velocity dispersion, and their stars were formed earlier and faster at higher mass

Basic idea is that elliptical galaxies are formed through merging (which scrambles orbits of disks). It is thought that more massive galaxies formed very fast at early times, but then suffered more gas-free merging at late times, which may lead to the correlation between n (Sersic index) and mass, as well as the variations in M/L that cause a tilt in the fundamental plane.

Another challenge -- keeping the galaxies red and not too massive at late times (see black holes later)

THE ASTROPHYSICAL JOURNAL, 411:153–169, 1993 July 1

DYNAMICALLY HOT GALAXIES. II. GLOBAL STELLAR POPULATIONS

RALF BENDER
Landessternwarte Königstuhl, D6900 Heidelberg, Germany
DAVID BURSTEIN
Department of Physics and Astronomy, Arizona State University, Tempe, AZ 85287-1504
AND
S. M. FABER
UCO/Lick Observatory, University of California, Santa Cruz, CA 95064
Received 1992 August 31; accepted 1992 December 31

ABSTRACT

The global relationship between the stellar populations and structural properties of hot galaxies is studied using the same sample of objects analyzed in Bender, Burstein, and Faber. Two measures of global stellar population are used: the Mg_2 index at the center of a galaxy and $(B-V)_0$ color measured over a much larger volume. The sample of galaxies studied includes luminous ellipticals that span a wide range in luminosity, compact ellipticals, dwarf ellipticals, and the bulges of S0 galaxies. The degree of anisotropy of internal stellar motions is known for most of these objects.

The total sample spans a range of over four orders of magnitude in mass and surface brightness, and the various subclasses populate the fundamental plane in very different ways. Despite this, all galaxies follow the *same mean* relationship between Mg_2 and velocity dispersion σ_0. The relative tightness of this relation is impressive: galaxies show a mean scatter of only 0.025 mag in Mg_2, versus a full range of nearly 0.35 mag in Mg_2. At least some of the scatter is intrinsic, but the residuals do not correlate with any of the structural properties studied (e.g., velocity anisotropy; effective radius, surface brightness or mass). The residuals also do not show any relation with the positions of the objects within *or* perpendicular to the fundamental plane. The only properties that do correlate are the morphological and kinematical peculiarities of a handful of disturbed ellipticals, as shown both in this paper and in the study of Schweizer et al. The observed scatter sets an upper limit of 15% on the rms variation of both age and metallicity at fixed σ_0 for bright ellipticals.

The Mg_2–$(B-V)_0$ relation is also examined and found to be tight and consistent for all dynamically hot galaxies. Several S0 galaxies have much bluer *global* colors compared to *central* Mg_2 than do other hot galaxies, but these exceptions are likely due to contamination of the global color by young disk light. The generally tight relation between *central* Mg_2 and *global* $(B-V)_0$ means that variations in the internal color and line-strength gradients from galaxy to galaxy must be small.

The Mg_2–σ_0 relationship can be reformulated as a function of the mass of the galaxy $\boldsymbol{M}$ and the *average* volume density of baryonic matter ρ as defined by the stars. This new relation can be expressed as $Mg_2 = (\boldsymbol{M}^2\rho)^{0.033}$. Though ρ is used here to denote average volume density, this relation might also be interpreted as a correlation between the local stellar population and local volume density *within* each dynamically hot galaxy. This prediction will be tested against observed color and line strength gradients in the next paper of this series.

High-mass galaxies retain metals due to deep potential wells

Stellar populations

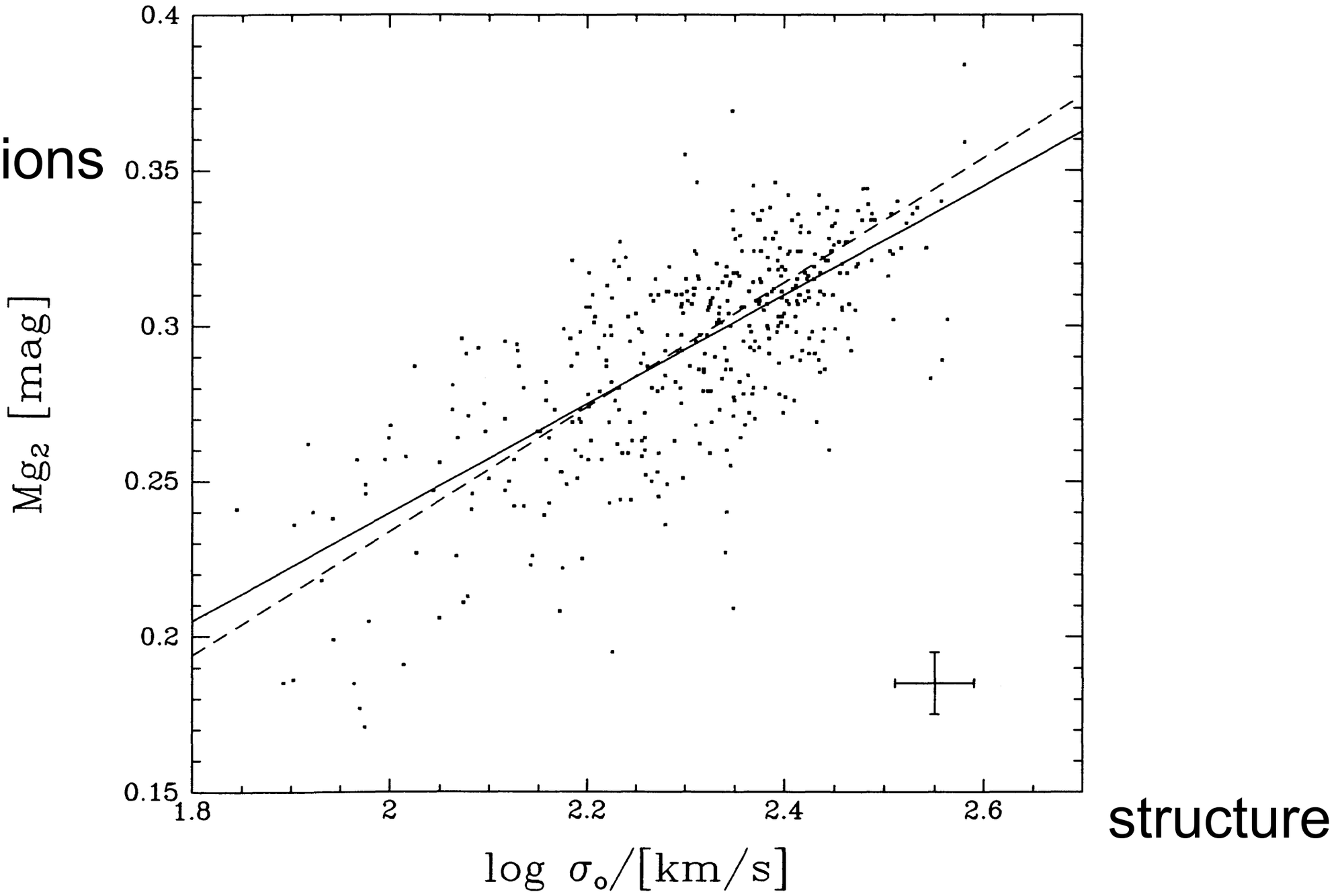

structure

FIG. 2.—Nuclear Mg_2 absorption line index plotted against log σ_0 (central velocity dispersion) for the 7 Samurai sample of elliptical galaxies (Faber et al. 1989). The full line drawn is the fit given by Burstein et al. (1988b), the dashed line is the relation adopted in this paper (see Fig. 3). Either relation is compatible with the 7 Samurai data. A typical error bar is shown.

Measurements of the metal content and abundance ratios in galaxies.

Main result:

Strong correlation with $\sigma_\star$

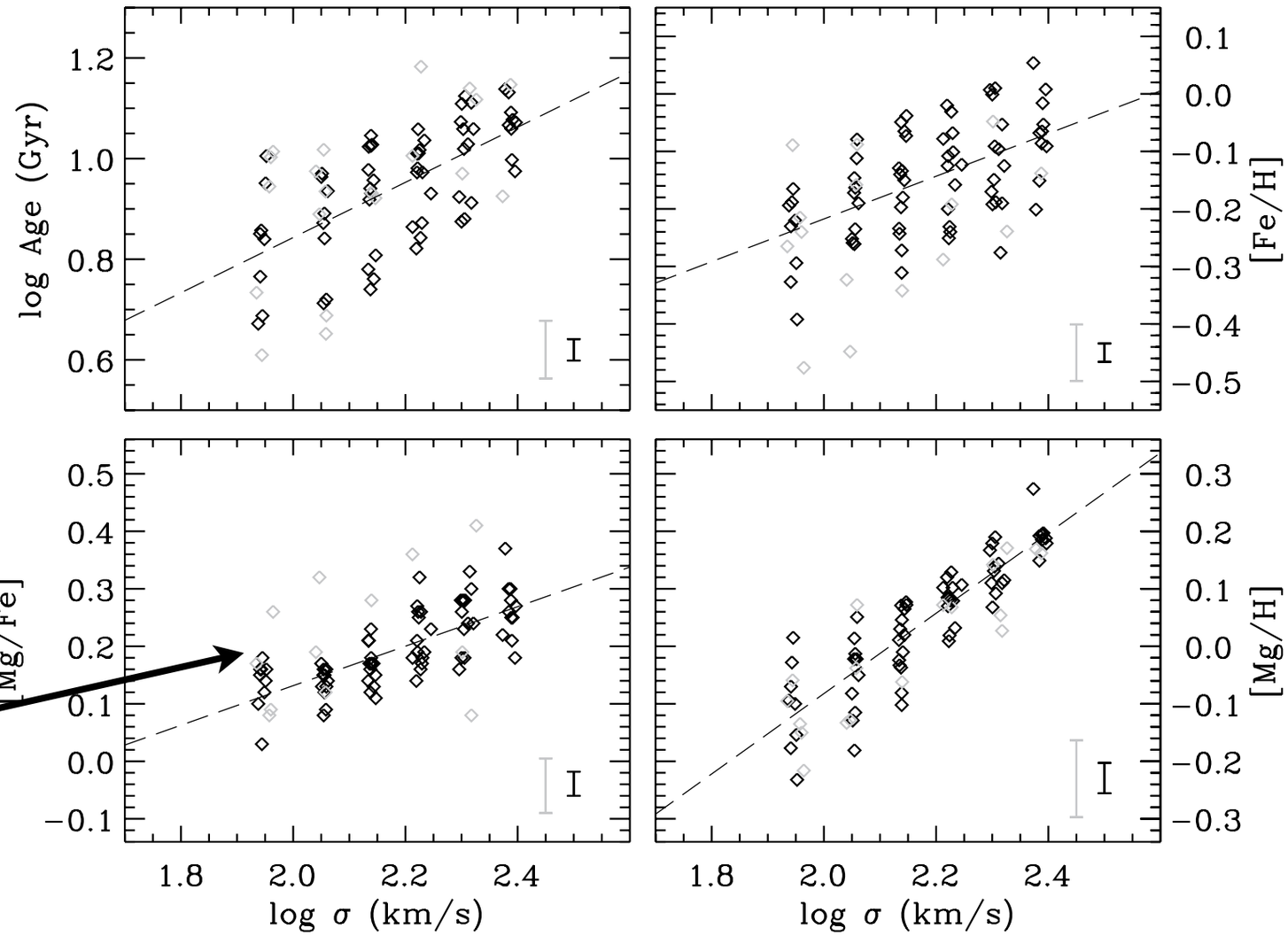

Figure 4. Stellar population modeling results, showing mean luminosity-weighted stellar age, [Fe/H], [Mg/Fe], and [Mg/H] as a function of galaxy σ. The black (gray) points and error bars indicate high (low) S/N measurements and their associated median errors. The dashed lines show linear least-squares fits of the stellar population properties as a function of σ, based on the high S/N (black) data only. Mean stellar age, [Fe/H], [Mg/Fe], and [Mg/H] all increase with increasing σ. Age and [Fe/H] both show substantial scatter at fixed σ, with total spread 4–5 times the expected spread due to measurements errors, indicating genuine underlying population variations at fixed σ. [Mg/H] and [Mg/Fe] show less scatter, only ~ 2 times that expected due to measurement errors. The [Mg/H]–σ relation is particularly strong and tight, nearly consistent with measurement errors, particularly at the high-σ end.

Graves et al. 2009

The E–E Dichotomy: There are two kinds of elliptical galaxies

(Davies + 1983; Bender 1988; Bender + 1989; Nieto + 1991; Kormendy + 1994; Lauer + 1995; Kormendy & Bender 1996; Gebhardt + 1996; Tremblay & Merritt 1996; Faber + 1997; Ravindranath + 2001; Rest + 2001; Lauer + 2007; many SAURON papers)

Normal and low luminosity Es
- are coreless,
- rotate rapidly,
- are nearly isotropic oblate spheroids,
- are substantially flattened (E3),
- have disky-distorted isophotes.

Giant ellipticals ($M_V < -21.5$)
- have cuspy cores,
- are essentially non-rotating,
- are anisotropic and triaxial,
- are less flattened (E1.5),
- have boxy-distorted isophotes.

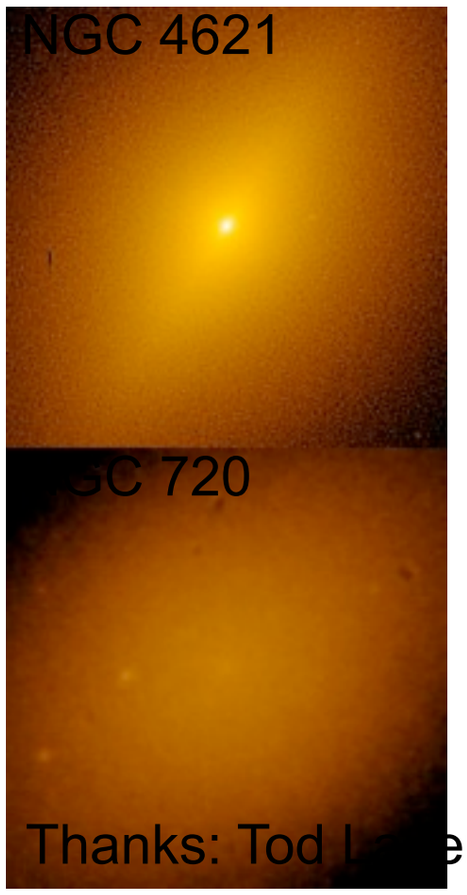

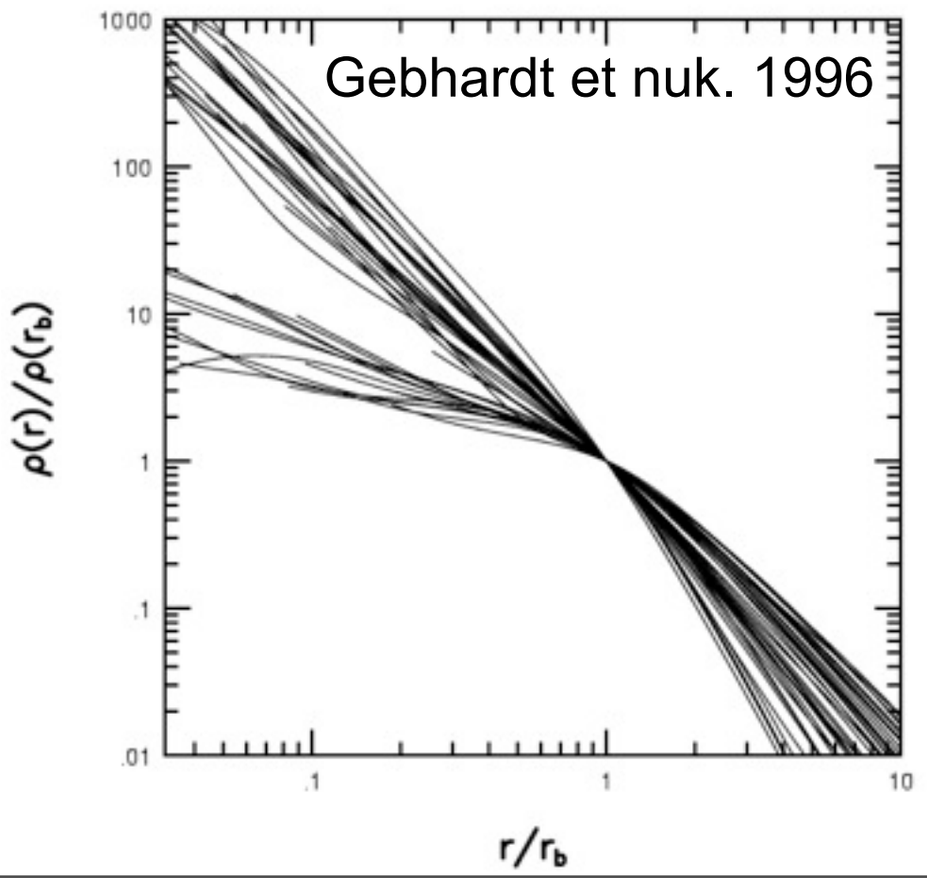

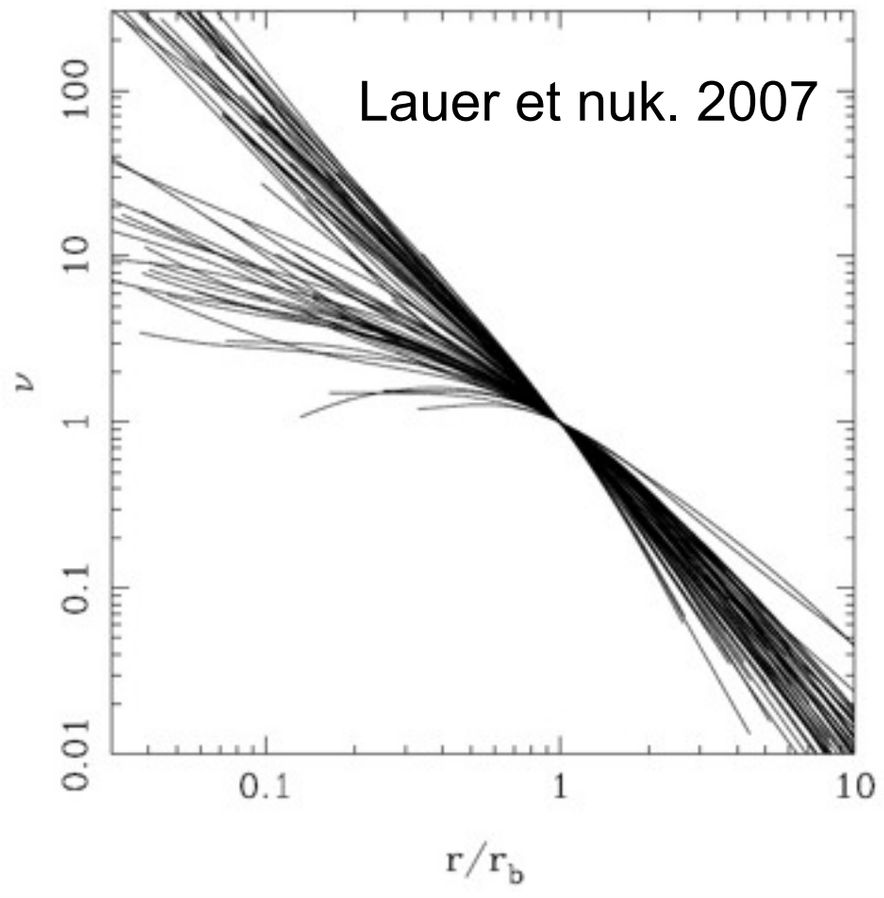

The E–E Dichotomy: There are two kinds of elliptical galaxies

Normal and low luminosity Es
rotate rapidly,
are nearly isotropic oblate spheroids,
are substantially flattened (E3),
are coreless & have extra light near
the center above the inward
extrapolation of the outer Sérsic profile,
have disky-distorted isophotes,
have n ≤ 4, independent of L,
contain younger, ~ Solar-comp. stars.

Interpretation:
the last mergers were dissipative.

BH binary scouring was overwhelmed by dissipative starburst.
[α/Fe] is consistent with prolonged merger history.

Giant ellipticals
are essentially non-rotating,
are anisotropic and triaxial,
are less flattened (E1.5),
have cuspy cores,
have boxy-distorted isophotes,
have n > 4, independent of L,
contain old, α-enhanced stars.

Interpretation:
last mergers were dissipationless, followed by BH binary scouring.

[α/Fe] $\Rightarrow$ star formation finished in first billion years; subsequent dissipationless mergers are OK.

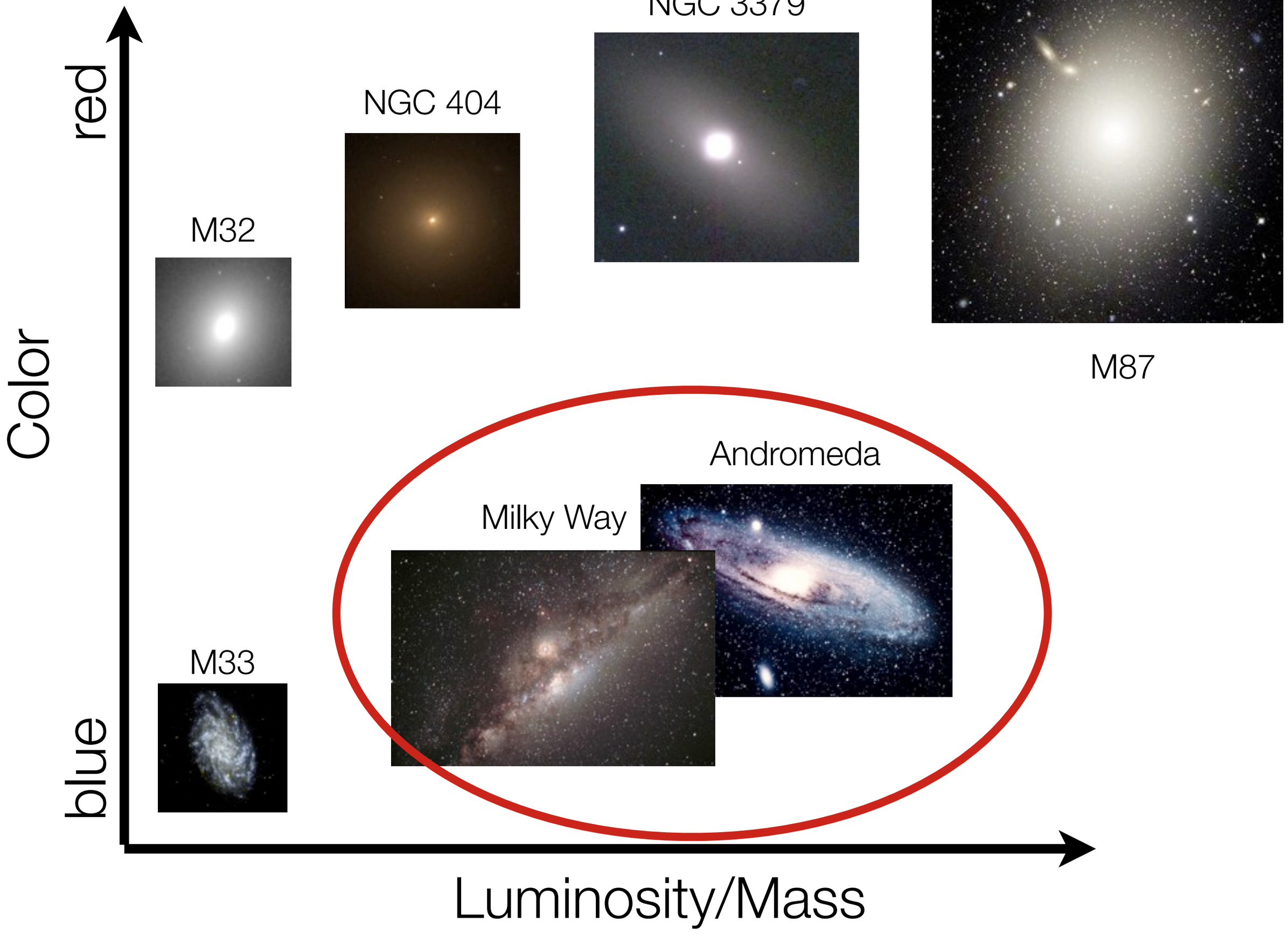
NGC 3379
NGC 404
M32
M87
Andromeda
Milky Way
M33
red
blue
Color
Luminosity/Mass

A New Method of Determining Distances to Galaxies

R. Brent Tully[1]* and J. Richard Fisher[2]

[1] Observatoire de Marseille, France
[2] National Radio Astronomy Observatory**, P.O. Box 2, Green Bank, W. Va. 24944, USA

Received July 15, 1975, revised April 26, 1976 Astron. Astrophys. 54, 661—673 (1977)

Summary. A good correlation between a distance-independent observable, global galaxian H I profile widths, and absolute magnitudes or diameters of galaxies offers a new extragalactic distance tool, as well as potentially being fundamental to an understanding of galactic structure. The relationships are calibrated with members of the Local Group, the M81 group, and the M101 group and have been used to derive distances to the Virgo cluster ($\mu_0 = 30^m.6 \pm 0^m.2$) and the Ursa Major cluster ($\mu_0 = 30^m.5 \pm 0^m.35$). A preliminary estimate of the Hubble constant is $H_0 = 80$ km/s/Mpc.

Interesting to note: Original papers focused exclusively on Sc and later galaxies.

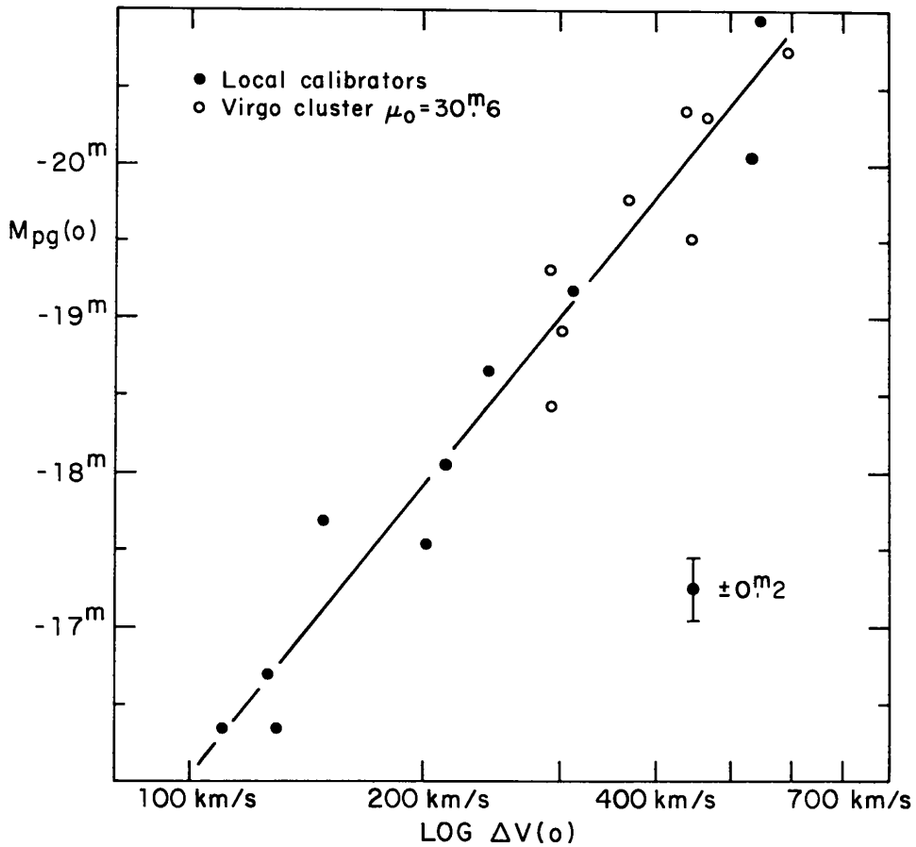

Fig. 5 (a) Absolute magnitude – global profile width relation produced by overlaying Figure 3 on Figure 1, adjusting Figure 3 vertically to arrive at a best visual fit with a distance modulus of $\mu_0 = 30^m.6 \pm 0^m.2$

Finds a correlation between the maximum rotation and the galaxy luminosity.

1. V_{max}: First measurements based on single-dish radio observations:

To derive rotation velocity from observed W_{20}, need to remove width due to random motions W_{rand}~3.6 σ and correct for inclination:

$$V_{max} = (W_{20}-W_{rand})/\sin(i)$$

2. Luminosity: Need to correct for dust...thus NIR magnitudes are best.

Below we will discuss the baryonic Tully-Fisher relation, which relates total baryonic matter (at least gas and stars) to rotation velocity.

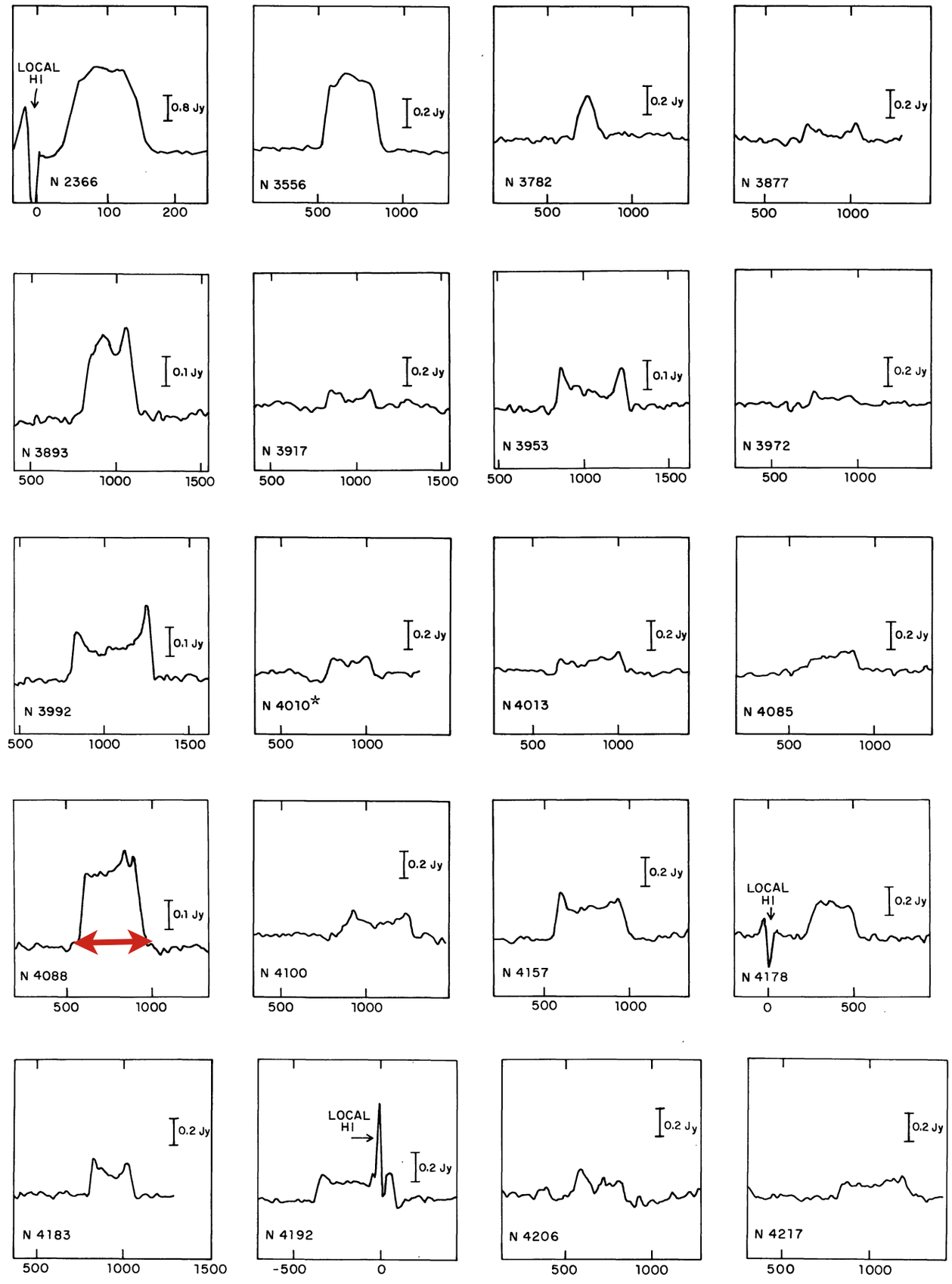

Fig. A1. Spectra of H I emission from galaxies listed in this paper. Horizontal scales are in km/s with respect to the sun, and the resolution is 22 km/s HPW except for NGC 2366, 4236, 5204 and 5585 where it is 5.5 km/s. *The spectrum of NGC 4010 is confused slightly by H I radiation from NGC 3949 in the reference spectrum

Width at 20% of the profile

Tully-Fisher Slope

The scaling of v_{max} with luminosity is easy to derive, if we assume a constant M/L.

Start with the virial theorem:

$2T + W = 0$

$m\ v^2 - GMm/r = 0$

$v^2 = GM/r$

If M/L = constant then M α L.

If I_0 is ~ constant then L α r^2.

Then: v^2 α $L/\sqrt{L}$ --> v^2 α $\sqrt{L}$

$L \alpha v^4$

Very analogous to the Faber-Jackson relation: L α σ^4 in elliptical galaxies.

Note that the scatter is very tight: 20% in v_{max} at a fixed luminosity. Also note that a constant total M/L implies a tight coupling between baryonic and dark matter.

The Baryonic Tully-Fisher Relation

In theory, there may be a relation between the total galaxy mass (stars+gas) and the dark matter halo mass.

v_c probes the dark halo mass.

At the lowest galaxy masses, gas dominates over stars. Large deviations are seen from the TF relation of massive galaxies. These go away if the gas+stars are included.

$M_{baryonic} = M_{stars} + M_{gas}$

$$M_{\rm stars} = \Upsilon^I_* \, 10^{-0.4[M_V-(V-I)-4.02]}$$

Depend on IMF and stellar population modeling

$$M_{\rm gas} = 1.4 M_{HI} = 1.4 \cdot 2.36 \cdot 10^5 D^2 \int S \, dv$$

THE BARYONIC TULLY-FISHER RELATION

S. S. McGaugh,[1] J. M. Schombert,[2] G. D. Bothun,[2] and W. J. G. de Blok[3,4]

Received 1999 December 14; accepted 2000 March 1; published 2000 March 21

ABSTRACT

We explore the Tully-Fisher relation over five decades in stellar mass in galaxies with circular velocities ranging over $30 \lesssim V_c \lesssim 300$ km s^{-1}. We find a clear break in the optical Tully-Fisher relation: field galaxies with $V_c \lesssim 90$ km s^{-1} fall below the relation defined by brighter galaxies. These faint galaxies, however, are very rich in gas; adding in the gas mass and plotting the baryonic disk mass $M_d = M_* + M_{gas}$ in place of luminosity restores the single linear relation. The Tully-Fisher relation thus appears fundamentally to be a relation between rotation velocity and total baryonic mass of the form $M_d \propto V_c^4$.

Let us suppose that, for whatever fundamental reason, there does exist a universal relationship between total mass and rotation velocity of the form $M_{\rm tot} \propto V_c^b$. The empirical Tully-Fisher relation then follows if luminosity traces mass:

$$L = \Upsilon_*^{-1} f_* f_d f_b M_{\rm tot}, \qquad (1)$$

where f_b is the baryon fraction of the universe, f_d is the fraction of the baryons associated with a particular galaxy halo which reside in the disk, f_* is the fraction of disk baryons in the form of stars, and Υ_* is the mass-to-light ratio of the stars. Each of the pieces that intervenes between L and $M_{\rm tot}$ must be a nearly universal constant shared by all disks in order to maintain the strict proportionality that the Tully-Fisher relation requires. Cast in this form, the traditional luminosity–line width relation is a subset of a more fundamental relation between *baryonic mass* and *rotational velocity*. In this context, one would expect

We have now addressed another piece of this puzzle. In addition to the near constancy of Υ_*, we have explicitly corrected for the stellar fraction f_*. Equation (1) now reduces to

$$M_d = f_d f_b M_{\rm tot}. \qquad (3)$$

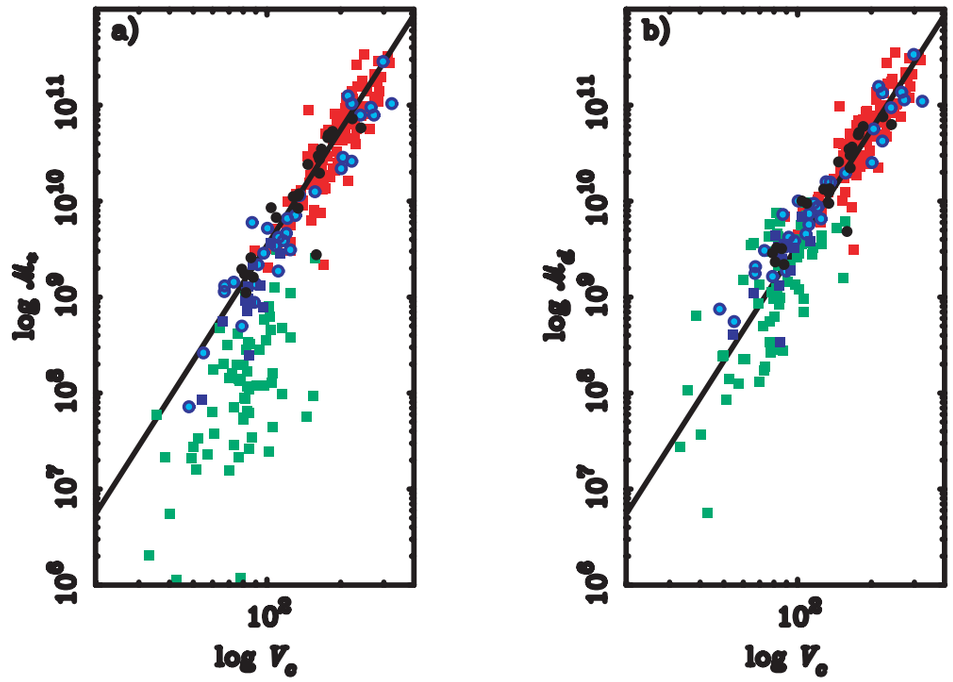

FIG. 1.—Tully-Fisher relation plotted as (*a*) stellar mass and (*b*) baryonic disk mass against rotation velocity. The squares represent galaxies where the circular velocity is estimated from the line width by $V_c = \frac{1}{2}W_{20}$, while the circles have $V_c = V_{\rm flat}$ from resolved rotation curves. The data employed include the *H*-band data of Bothun et al. (1985; *red*), the *K*′-band data of Verheijen (1997; *black*), and the *I*-band data of Pildis et al. (1997) with velocities as reported by Eder & Schombert (2000; *green*). Also shown are the *B*-band data of McGaugh & de Blok (1998; *light blue*) and of Matthews et al. (1998; *dark blue*). The stellar mass is computed from the luminosity by assuming a constant mass-to-light ratio ($M_* = \Upsilon_* L$), so (*a*) is directly analogous to the usual luminosity–line width diagram. We assume mass-to-light ratios for the stellar populations of late-type galaxies of $\Upsilon_*^B = 1.4$, $\Upsilon_*^I = 1.7$, $\Upsilon_*^H = 1.0$, and $\Upsilon_*^{K'} = 0.8\ M_\odot/L_\odot$ (see text). In (*b*), we plot the total baryonic disk mass $M_d = M_* + M_{\rm gas}$ with $M_{\rm gas} = 1.4 M_{\rm H\,I}$. In (*a*), a clear break is apparent. Galaxies with $V_c \lesssim 90$ km s^{-1} fall systematically below the Tully-Fisher relation defined by brighter galaxies. In (*b*), the deficit in mass apparent in (*a*) has been restored by including the gas mass. The solid line is an unweighted fit to the red-band data in (*b*) with a correlation coefficient of 0.92 and a slope indistinguishable from 4.

Constraints on Galaxy Formation

Tully-Fisher establishes a tight correlation between baryonic matter (L) and dark matter halo mass (v_{max}).

In detail, matching the scatter, slope, and zeropoint of the Tully-Fisher relation can test our models of structure formation.

THE ASTROPHYSICAL JOURNAL, 392:L47–L50, 1992 June 20

ELONGATED DISKS AND THE SCATTER IN THE TULLY-FISHER RELATION

MARIJN FRANX
Harvard-Smithsonian Center for Astrophysics, 60 Garden Street, Cambridge, MA 02318
AND
TIM DE ZEEUW
Sterrewacht, Huygens Laboratorium, Postbus 9513, 2300 RA Leiden, The Netherlands
Received 1991 December 24; accepted 1992 April 9

ABSTRACT

It is often speculated that the dark halos of spiral galaxies are triaxial or prolate, with the long axis pointing in the plane of the disk. This would produce a potential that is elongated in the plane of the disk. We explore the signatures produced by such deviations from axisymmetry. We find observable effects in the photometry and kinematics of the stars and gas in the disk, if substructure like bars and spiral arms can be ignored. These effects include ellipticity gradients and position angle twists in disks, velocity gradients along the apparent minor axis of the disk, differences between kinematically determined inclinations and photometrically determined inclinations, and systematic residuals in circular orbit fits to the velocity field.

Noncircular gas motions produce significant scatter in the Tully-Fisher relation, amounting to 0.46 mag if the ellipticity of the potential in the plane of the disk is 0.10. Thus, small deviations from axisymmetry are sufficient to produce all or most of the observed scatter in the Tully-Fisher relation. The ellipticity of the potential in the plane of the disk must be less than 0.10 and most likely lies in the range 0–0.06. This range corresponds to an ellipticity of the density distribution of the halo between 0 and 0.16, if halos are the dominant mass component. The constraint on the shape of the dark halo is less tight in "maximum disk" models for spiral galaxies, since in these models the disk material significantly circularizes the total potential.

These results imply that use of detailed kinematic information may reduce the observed scatter in the Tully-Fisher relation by 0.1 mag or more.

The Astrophysical Journal, 654:27–52, 2007 January 1

A REVISED MODEL FOR THE FORMATION OF DISK GALAXIES: LOW SPIN AND DARK HALO EXPANSION

Aaron A. Dutton
Department of Physics, Swiss Federal Institute of Technology (ETH Zurich), Zurich, Switzerland

Frank C. van den Bosch
Max-Planck-Institut für Astronomie, Heidelberg, Germany

Avishai Dekel
Racah Institute of Physics, Hebrew University, Jerusalem, Israel

AND

Stéphane Courteau
Department of Physics, Engineering Physics and Astronomy, Queen's University, Kingston, ON, Canada
Received 2006 April 26; accepted 2006 September 13

ABSTRACT

We use observed rotation velocity–luminosity (*VL*) and size-luminosity (*RL*) relations to single out a specific scenario for disk galaxy formation in the ΛCDM cosmology. Our model involves four independent lognormal random variables: dark halo concentration c, disk spin $\lambda_{\rm gal}$, disk mass fraction $m_{\rm gal}$, and stellar mass-to-light ratio Υ_I. A simultaneous match of the *VL* and *RL* zero points with adiabatic contraction requires low-c halos, but this model has $V_{2.2} \sim 1.8 V_{\rm vir}$ (where $V_{2.2}$ and $V_{\rm vir}$ are the circular velocity at 2.2 disk scale lengths and the virial radius, respectively), which will be unable to match the luminosity function (LF). Similarly models without adiabatic contraction but standard c also predict high values of $V_{2.2}/V_{\rm vir}$. Models in which disk formation induces an *expansion* rather than the commonly assumed contraction of the dark matter halos have $V_{2.2} \sim 1.2 V_{\rm vir}$, which allows a simultaneous fit of the LF. This may result from nonspherical, clumpy gas accretion, where dynamical friction transfers energy from the gas to the dark matter. This model requires low $\lambda_{\rm gal}$ and $m_{\rm gal}$ values, contrary to naive expectations. However, the low $\lambda_{\rm gal}$ is consistent with the notion that disk galaxies predominantly survive in halos with a quiet merger history, while a low $m_{\rm gal}$ is also indicated by galaxy-galaxy lensing. The smaller than expected scatter in the *RL* relation and the lack of correlation between the residuals of the *VL* and *RL* relations, respectively, imply that the scatter in $\lambda_{\rm gal}$ and in c needs to be smaller than predicted for ΛCDM halos, again consistent with the idea that disk galaxies preferentially reside in halos with a quiet merger history.

Observational Constraints

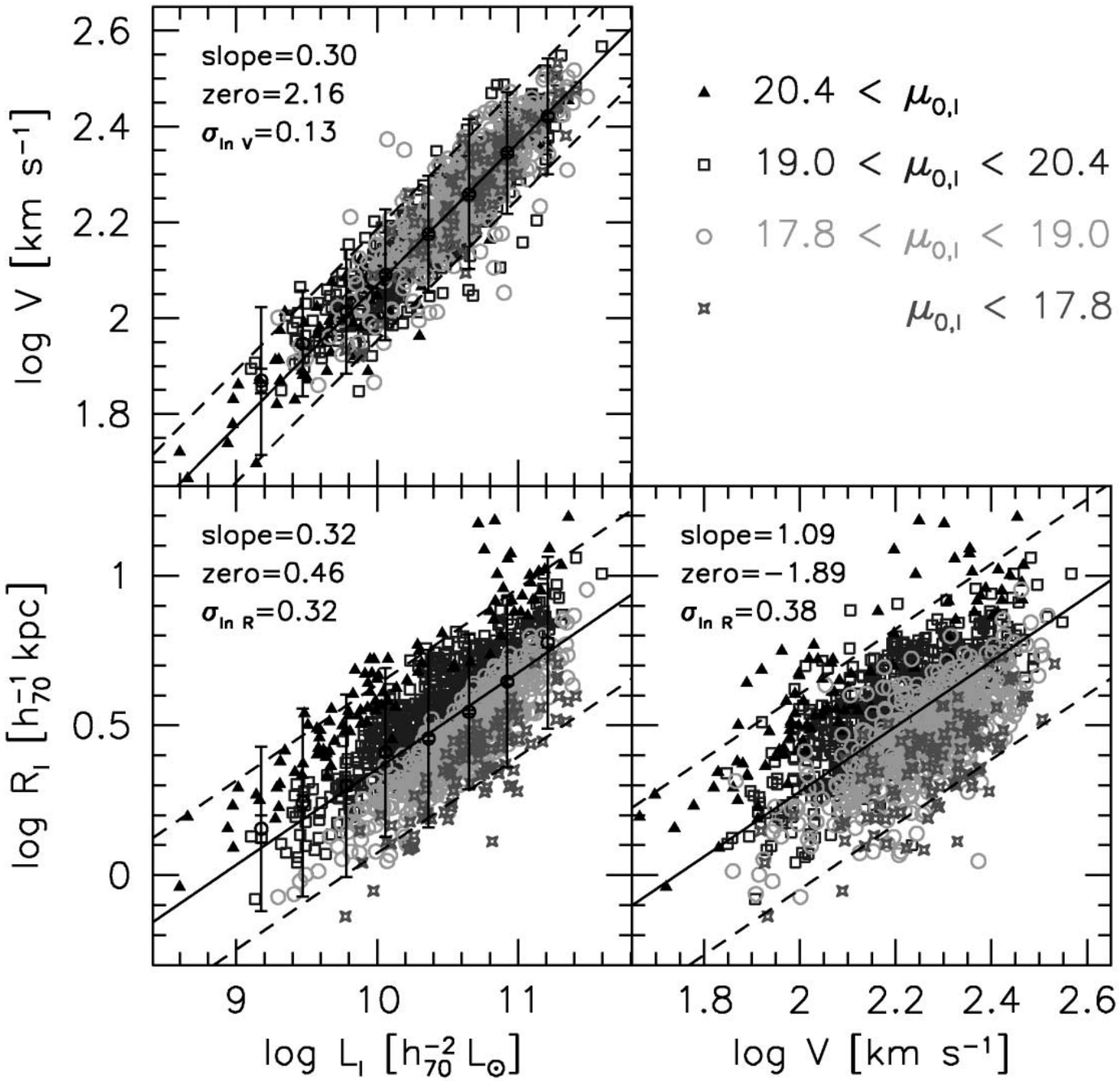

FIG. 1.—Observed *I*-band *VLR* scaling relations using data from Courteau et al. (2006). Biweighted orthogonal least-squares fits are given by the solid black lines, with 2 σ deviations given by the dashed lines. The open black circles with error bars show the mean and 2 σ scatter of the *VL* and *RL* relations binned at 0.3 dex intervals in L_I. The gray scale and point types correspond to extrapolated disk central surface brightness, $\mu_{0,I}$, as indicated in the top right panel. [*See the electronic edition of the Journal for a color version of this figure.*]

Model is constrained by RL (radius-luminosity) and VL (Tully-Fisher) relations, as well as the spiral galaxy luminosity function.

“Real Bulges” -- Elliptical galaxies with disks

Pseudob

- Two types
  luminous c
- Exponentia
- Rotationall
- Ongoing st
- bars, ovals
- These bulg
  (Kormendy

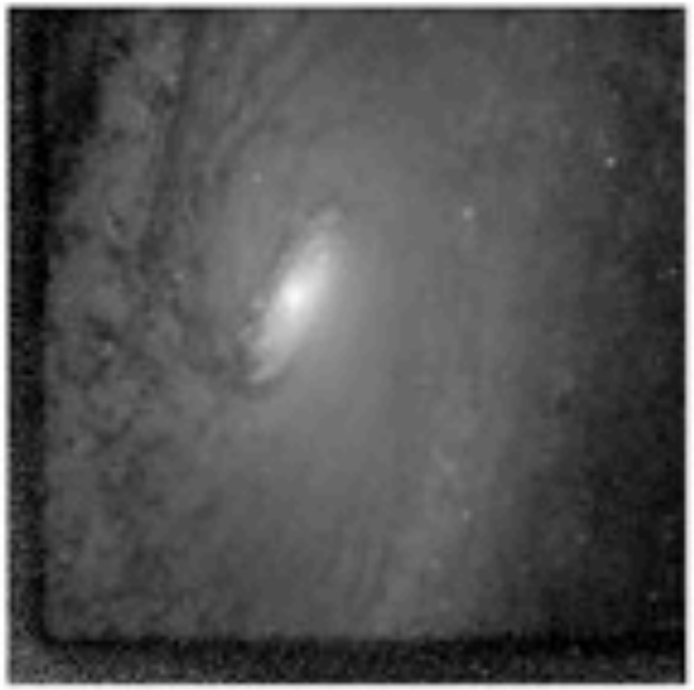

N1353 PC2 F606W p

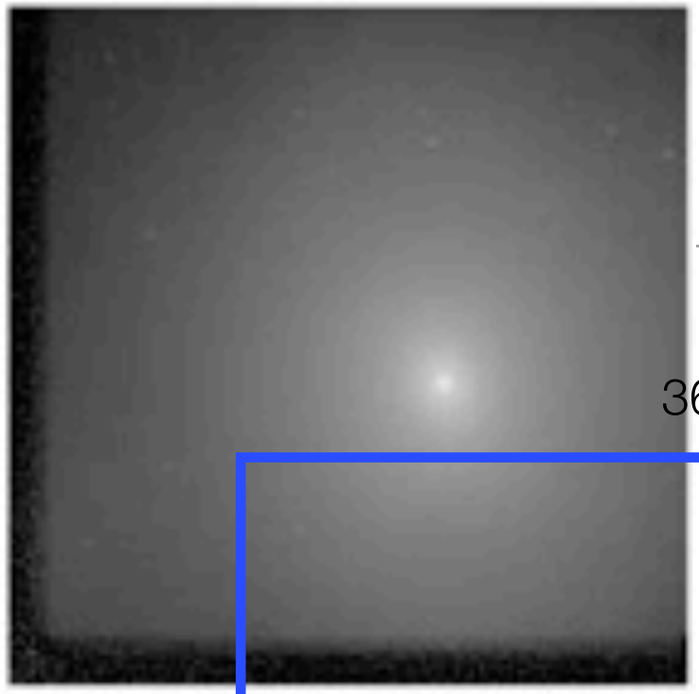

N1398 PC2 F606W c

N1566 PC2 F555W p

N2775 PC2 F606W c

36”

Fisher et al. 2009

How were spiral galaxies formed?

Disks form naturally as gas with angular momentum collapses in halos. Getting the angular momentum right to match the observed Tully-Fisher relation is not trivial.

Classical bulges are built via merging, as elliptical galaxies above.

Later-type spirals build up their central ‘bulges’ via secular processes such as bars. Star formation is ongoing in these systems.

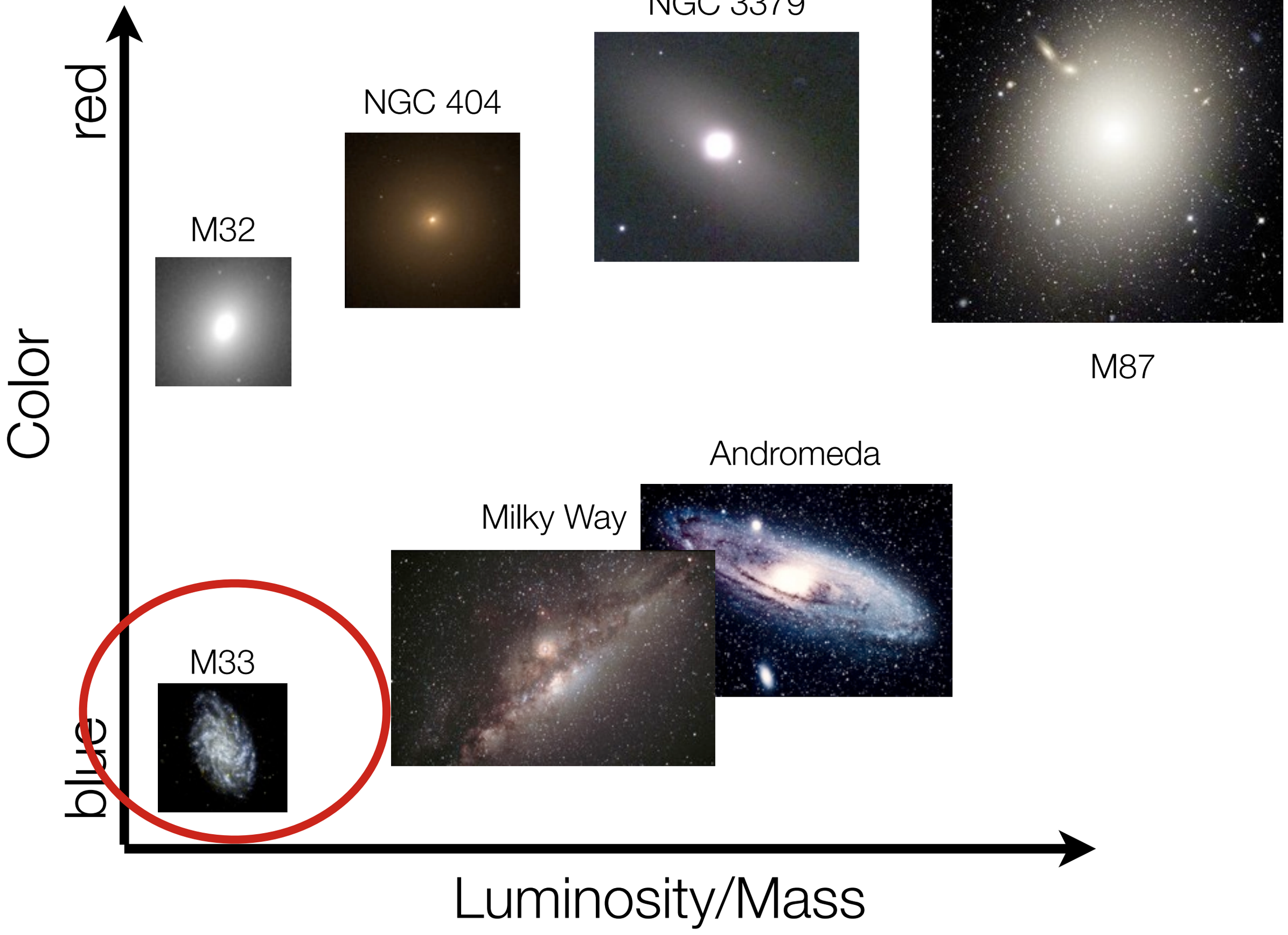
red
Color
blue
M32
NGC 404
NGC 3379
M87
Andromeda
Milky Way
M33
Luminosity/Mass

Bulgeless Galaxies: Nuclear Star Clusters

~75% of latest-type spirals contain nuclear star clusters

Structurally similar to globular clusters but with mixed stellar populations

Mass of NC correlates with mass of galaxy

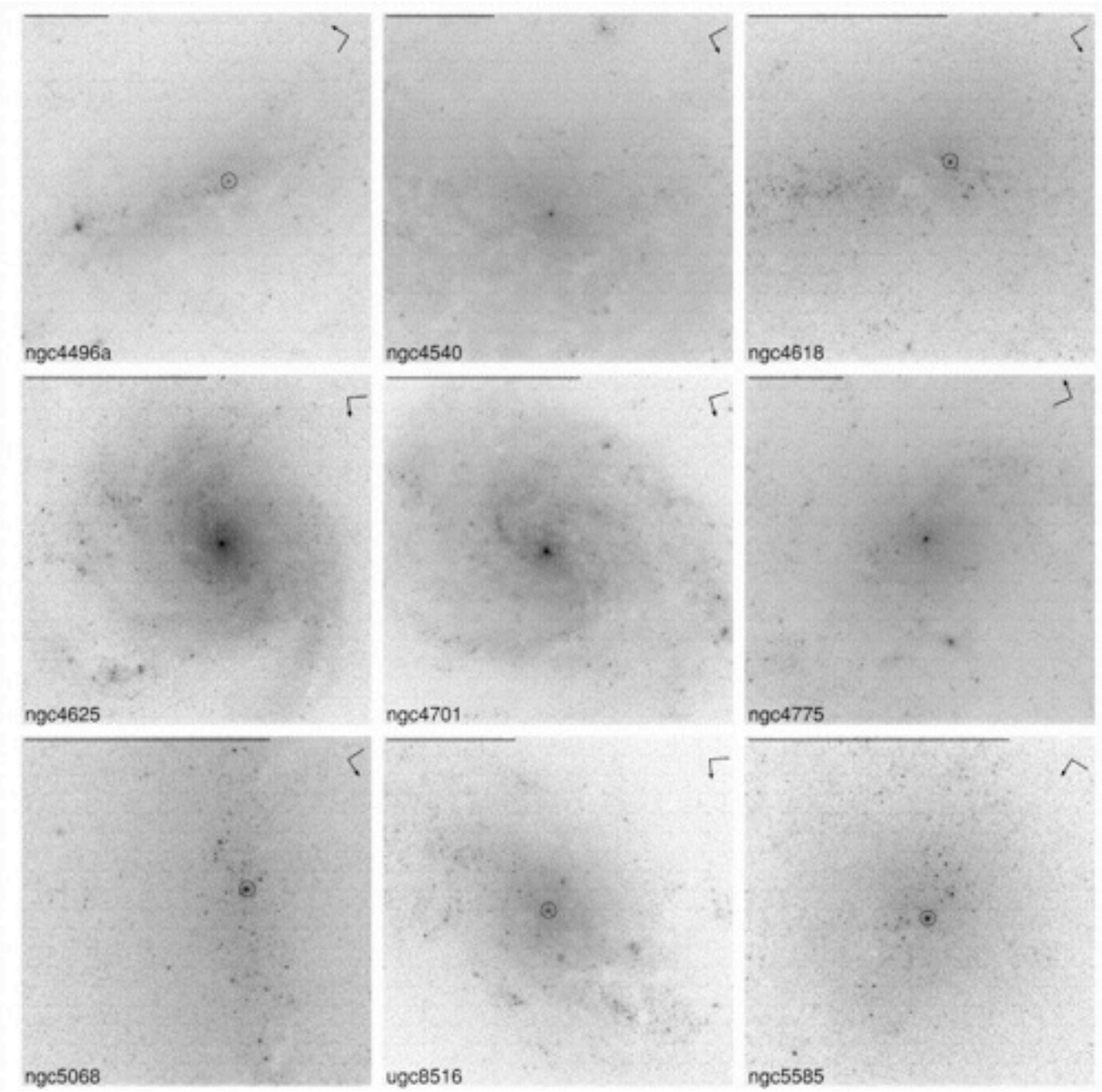

Boker et al. 2002

Bulgeless Galaxies: How does nature make them?

Pure disk galaxies present two primary challenges

1. To reproduce the Tully-Fisher relation - dump gas into a halo and get the right scaling (slope and zeropoint) between v_{max} and galaxy luminosity

complications include ‘adiabatic contraction, inflow/outflow, mass-dependent stellar populations

2. To keep the galaxy bulgeless in a hierarchical Universe